Renormalization Group Flows for Superfluid ^{3}He under Confinement

by

Adil Abdul-Jabbar Attar

A thesis submitted in partial fulfillment of the requirements for the degree of

Master of Science

Department of Physics
University of Alberta

Abstract

We theoretically investigate the effect of fluctuations in the order parameter on the phase transition of ^{3}He under nanoscale confinement of one spatial dimension realized in recent experiments. We derive a new quasi two-dimensional free energy that relies on a 3×2 complex matrix instead of the 3×3 complex matrix order parameter found in the three-dimensional system. We minimize the quasi two-dimensional free energy and present two energetically degenerate phases that are predicted: the A-phase and the planar phase.

Beyond the mean-field approximation, we calculate the RG flow in the three-dimensional, two-dimensional, and quasi two-dimensional limits. We derive the perturbative flow equations for all quartic coupling constants with non-trivial kinetic factor. We find that the B-phase is energetically favoured in the three-dimensional system in agreement with experiment. In contrast, in the quasi two-dimensional limit, weak-coupling perturbative renormalization group predicts the planar phase to be energetically favoured. However, strong-coupling corrections favour the A-phase observed in experiment.

We derived FRG flow equations for the 3D, 2D and quasi-2D cases with non-trivial kinetic factor. In the quasi-2D limit, we found that the A-phase was favoured over the planar phase for certain levels of confinement. These confinement scales were also confirmed to have a prominent Fermi liquid to A-phase transition in experiment. Due to the unstable fixed point, we find that under confinement there is a fluctuation-induced first-order transition to the A-phase.

Preface

This thesis is the original work of Adil Attar under the supervision of Professor Igor Boettcher.

Results presented in Chapters 3 have been published as Canon Sun, Adil Attar, and Igor Boettcher, "Superfluid phase transition of nanoscale-confined helium-3", Phys. Rev. B **108**, 144503 (2023).

Acknowledgements

I would like to thank Igor Boettcher for supervising my master's degree and for providing excellent support and guidance. I want to thank my parents for their endless support throughout my education and my life. I would also like to thank my wife, Nameerah Wajahat, for her support.

I would like to thank Albion Arifi, Pramodh Senarath Yapa, Canon Sun, Anffany Chen, Alex Shook and many others for their inspiring discussions surrounding this research. Additionally, I would like to thank Canon Sun for his help in editing this thesis.

I would like to thank Daniel R. Aldrich for his continuing contributions to the University of Alberta, and for his work within the graduate student community. More specifically, I would like to acknowledge the work that he put into creating the LaTeX template that this thesis was created in, and the ongoing support that he provides to the students at the University of Alberta.

Table of Contents

List of Tables

List of Figures

List of Symbols

Constants

k_B	Boltzmann's constant.	$1.380649 \times 10^{-23}\, J/K$

Latin

A	^{3}He order parameter.
F_{eff}	Effective Free Energy of ^{3}He.
F_{GL}	Ginzburg-Landau Free Energy of ^{3}He.

Greek

α	Quadratic coupling constant in the Ginzburg-Landau free energy of ^{3}He.
β_i	Quartic coupling constant in the Ginzburg-Landau free energy of ^{3}He.
Δ_A	Prefactor multiplying ^{3}He-A order parameter matrix.
Δ_B	Prefactor multiplying ^{3}He-B order parameter matrix.
Γ	Effective free energy.
γ	kinetic coupling constant in the Ginzburg-Landau free energy of ^{3}He.
Λ	Ultraviolet momentum cutoff.
$\mathcal{G}$	Propagator
Ω	Used to denote angular or spherical coordinates.

Abbreviations

BCS Bardeen-Cooper-Schrieffer theory of superconductivity.

FRG Functional Renormalization Group.

GL Ginzburg-Landau.

RG Renormalization Group..

Chapter 1

Introduction

1.1 Motivation

One of the greatest wonders of physics is how randomly and chaotically moving particles can come together to form something as ordered and sophisticated as a block of cheese. Order emerges in matter at sufficiently low temperatures when its tendency towards chaos is overtaken by its desire to minimize its energy. Describing the order in matter is challenging and requires identifying the important degrees of freedom and relevant scale. The concept of scale dependence is especially important for understanding the emergence of order. It encapsulates the idea that fundamentally different physics can emerge from the same units of matter, depending on the length or energy scale. In astrophysics, at different length scales, matter organizes itself into vastly different structures, such as planets, solar systems and galaxies. In particle physics, each energy scale requires a different field theory to describe it. In condensed matter physics, the notion of scale plays an immensely important role in understanding the phases of matter.

Phases of matter are characterized by long-range order, which involves a physical property being present macroscopically in a material. The phases of matter observed at room temperature are those that survive the thermal fluctuations of their environment. In extremely cold temperatures, these thermal fluctuations begin to disappear and reveal the true quantum nature of matter. The long-distance or infrared (IR)

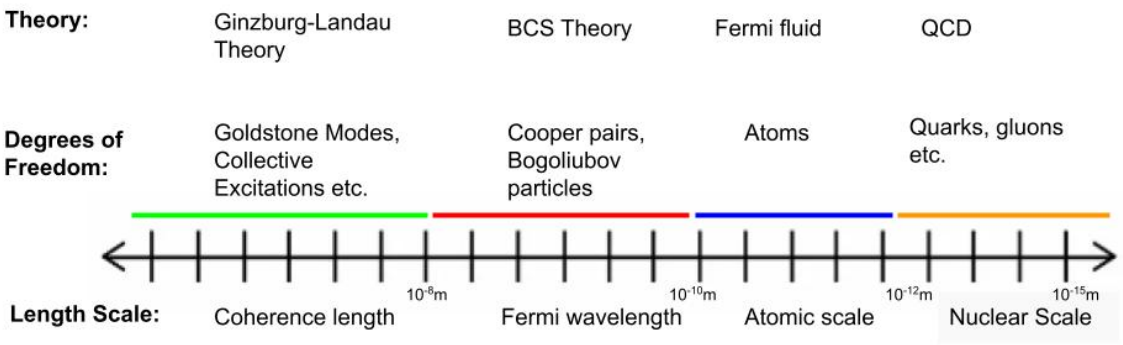

Figure 1.1: **Relevant length scales.** We show the scale dependence of physics in ^{3}He. The bottom row corresponds to the various physical length scales. Above the scale, we see the relevant degrees of freedom at each length scale, with their region of validity highlighted. The top row shows the theory that describes the physics best at each length scale.

energy scale describes the physics of these phases, as opposed to the ultraviolet (UV) scale that our field theories may describe. Though the physics of a system varies greatly with scale, all these physical theories at various scales can be related by the Renormalization Group (RG). RG provides a framework to indicate which degrees of freedom become important at any given scale. In experiments, we only have access to a particular energy scale, which often is at a different scale than the theory being tested. For example, the long-wavelength degrees of freedom often determine the behaviour of cold temperature systems in condensed matter systems; however, the physics of these long-wavelength modes are not obvious from the microscopic Hamiltonian of the system. RG provides a powerful tool that allows us to reconcile what we calculate in theory and what we observe in experiments by allowing us to include or remove irrelevant degrees of freedom into our theory.

We aim to use RG to analyze and describe phase transitions in superfluid ^{3}He. When ^{3}He is cooled below 2.7 mK at atmospheric pressure, it undergoes a phase transition from a normal Fermi liquid state to a superfluid state [1], which corresponds to the transition from blue to red in ref. fig. 1.1. This phase transition is rather unique and complex, even compared to other superfluids. Unlike superfluid ^{4}He,

superfluid ^{3}He is fermionic and thus cannot condense into a single quantum state due to the Pauli exclusion principle. Instead, it forms Cooper pairs, where a pair of ^{3}He atoms couple to effectively form a boson-like particle, which allows it to condense into a single quantum state. These Cooper pairs form a p-wave spin-triplet state, which gives superfluid ^{3}He an incredibly rich and complex phase behaviour [2]. These Cooper pairs are described by Bardeen-Schrieffer-Cooper (BCS) theory and they are the relevant degrees of freedom in the red region in fig. 1.1. We can apply the Hubbard-Stratonovich transformation to our BCS theory and obtain the Ginzburg-Landau theory of ^{3}He to describe the physics at a length scale larger than thermal fluctuations. To understand the phase transitions in superfluid ^{3}He, we must consider an even lower energy theory, which requires us to perform RG on the Ginzburg-Landau theory. Consequently, the RG analysis of superfluid ^{3}He is quite challenging, but it is also crucial for the theoretical understanding of the low-energy physics of ^{3}He.

Alongside its importance in theoretical physics, ^{3}He has garnered much interest in experimental physics. The quantum behaviours present in superfluid ^{3}He, such as its dissipationless flow, have given rise to many promising technologies, including cryogenics for quantum computers, quantum sensors, and other quantum devices [3, 4]. The first wave of interest in superfluid ^{3}He occurred in the 1970s when much of the theory was developed. With the advent of nanotechnology, new excitement has emerged over the last decade [1]. ^{3}He is now being studied extensively in different, confined geometries, which vastly restrict the ^{3}He in one or more dimensions. In the Davis lab at the University of Alberta, the phase diagram of ^{3}He has been studied under nanoscale uniaxial confinement, where it has displayed a drastic shift from the unconfined case [5, 6]. In one direction, the system is confined to approximately the size of a Cooper pair, which is given by its coherence length ξ_0. This means Cooper pairs have restricted mobility in one dimension, making them effectively two-dimensional. For this reason, we will refer to the uniaxially confined system as quasi-

2D and the unconfined system as 3D. This experiment involved oscillating ^{3}He in and out of a cavity with a resonator that was uniaxially confined to $500 - 1000$ nm in the z direction, as illustrated in fig. 1.2a. This resonator is connected to the circuit illustrated in fig. 1.2b, used to indirectly measure the phase of the ^{3}He-A at various pressures and temperatures and varying degrees of confinement. Under these conditions, a magnification of the ^{3}He-A phase in the pressure-temperature phase diagram is observed. Because this effect is so large, it should be observed in the RG analysis. Understanding the RG analysis of the phases of superfluid ^{3}He in the quasi-2D regime will contribute greatly to our theoretical understanding of this experiment and can help extract measurable observables for future experiments.

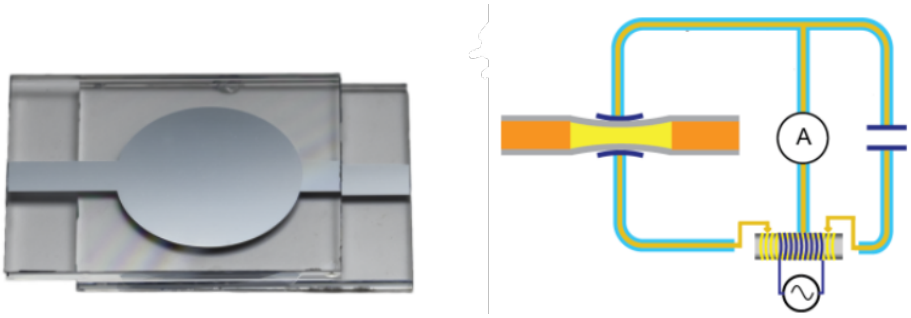

(a) (b)

Figure 1.2: **Experimental setup for confinement of ^{3}He.** Illustrations of the nanoscale confinement experiments in ref. [6] a) A resonator that confines ^{3}He uniaxially. It oscillates in its confined dimension through the application of an AC current. b) Circuit diagram of the experimental system, where resonance frequency is measured, which also determines the superfluid fraction. Figures taken from [6].

1.2 Ginzburg-Landau Theory of ^{3}He

Though the Ginzburg-Landau theory (GL theory) originally was a phenomenological theory to describe the superconductor phase transition, it was found to be applicable in many different phase transitions, including superfluid ^{3}He. GL theory centers around a quantity known as the order parameter, which summarises the degrees of freedom relevant to a phase transition. In a ferromagnetic system, the order parameter

is the net magnetization, and in liquid-gas transitions, the order parameter is the difference between the liquid and gas densities [7]. The order parameter is generally a field that can take on various forms depending on the complexity of the transition. Some order parameters, like the net magnetization, form a real vector field. In the case of superfluid ^{3}He, 18 real parameters are needed to describe the transition, so a more complicated complex matrix-valued field describes the order parameter, which can be written as

$$\mathrm{A} = \begin{pmatrix} \mathrm{A}_{xx} & \mathrm{A}_{xy} & \mathrm{A}_{xz} \\ \mathrm{A}_{yx} & \mathrm{A}_{yy} & \mathrm{A}_{yz} \\ \mathrm{A}_{zx} & \mathrm{A}_{zy} & \mathrm{A}_{zz} \end{pmatrix}.$$

The components $\mathrm{A}_{\mu j}$ of A are labelled by the spin μ and orbital angular momentum j degrees of freedom, respectively. A nonzero $\mathrm{A}_{\mu j}$ signifies the condensation of Cooper pairs in the p_j orbital with zero spin in the μ direction. Since superfluid ^{3}He forms a spin-triplet p-wave superfluid, it has spin $S = 1$ and total orbital angular momentum $L = 1$, allowing for nine combinations of these two degrees of freedom.

Symmetry plays a vital role in GL theory. In a phase transition, there is a state with a larger symmetry group, known as the disordered phase and a phase with a smaller symmetry group, known as the ordered phase. The transition between these two phases involves a spontaneous breaking of symmetry. For example, in a ferromagnet, the order parameter (the net magnetization) points in a fixed direction, breaking the rotational symmetry. A phase transition occurs when the order parameter, which is zero in the disordered state, becomes non-zero in the ordered state. It is called a continuous or second-order phase transition if the order parameter changes continuously. If there is a discontinuity in the order parameter, then this is called a discontinuous or first-order transition. Second-order transitions occur when large-scale fluctuations of the order parameter become very large near a critical temperature and cause spontaneous symmetry breaking. Another way to describe a first-order transition is the presence of latent heat. Fluctuation-induced first-order transitions occur when fluc-

tuations cause symmetry breaking. When the jump in the order parameter is much smaller than the thermal fluctuations at the phase transition, this is known as a weak first-order transition. These phase transitions can potentially be mistaken for second-order phase transitions in low-resolution experiments.

The symmetry group of ^{3}He is given by

$$G = \mathrm{SO}(3)_L \times \mathrm{SO}(3)_S \times \mathrm{U}(1), \tag{1.1}$$

where the action of the group on the order parameter is given by

$$\mathrm{A} \to e^{i\phi} R \mathrm{A} S^T, \tag{1.2}$$

where $e^{i\phi} \in \mathrm{U}(1)$ is a phase factor, $R \in \mathrm{SO}(3)_S$ is a 3-dimensional rotation matrix that acts on the spin index, and $S \in \mathrm{SO}(3)_L$ is a 3-dimensional rotation matrix that rotates the angular index. The Ginzburg-Landau free energy functional, F_{GL}, is a phenomenological free energy that contains all possible terms that respect the symmetry of the system. Generally, terms up to the fourth order in the order parameter are sufficient to describe a second-order phase transition. From this symmetry group, we can derive all terms up to the fourth order in A that respect

$$F[\mathrm{A}] = F[e^{i\phi} R \mathrm{A} S^T] \tag{1.3}$$

for all $A \in \mathbb{C}^{3\times 3}$. The GL free energy is given by

$$\begin{aligned} F_{GL}[\mathrm{A}] = \int^{\Lambda} d^3 r \, \big\{ & \alpha \mathrm{tr}(\mathrm{A}\mathrm{A}^\dagger) + \beta_1 |\mathrm{tr}(\mathrm{A}\mathrm{A}^T)|^2 + \beta_2 [\mathrm{tr}(\mathrm{A}\mathrm{A}^\dagger)]^2 \\ & + \beta_3 \mathrm{tr}(\mathrm{A}\mathrm{A}^T \mathrm{A}^* \mathrm{A}^\dagger) + \beta_4 \mathrm{tr}(\mathrm{A}\mathrm{A}^\dagger \mathrm{A}\mathrm{A}^\dagger) + \beta_5 \mathrm{tr}(\mathrm{A}\mathrm{A}^\dagger \mathrm{A}^* \mathrm{A}^T) \\ & + K(\gamma - 1) \partial_i \mathrm{A}^*_{\mu i} \partial_j \mathrm{A}_{\mu j} + K \partial_i \mathrm{A}^*_{\mu j} \partial_i \mathrm{A}_{\mu j} \big\}, \end{aligned} \tag{1.4}$$

where Λ is the ultraviolet cut-off, which ensures we do not integrate outside the validity of our assumption of bosonic particles. This is because the Cooper pairs behave as individual ^{3}He atoms above this Λ. Some choices for Λ include the Fermi wavevector k_F, the inverse coherence length ξ_0^{-1}, and the average thermal fluctuation $\sqrt{T_c}$.

As we stated before, BCS theory can be related to GL theory, through a method known as mean-field theory, which assumes the order parameter is given by minimizing there are no fluctuations in the order parameter. The phenomenological coupling constants in eq. (1.4) can be determined using mean-field theory at weak coupling. Near the critical temperature T_c and at low pressures, weak-coupling theory determines the values of the GL coupling constants as

$$\alpha(T,P) = N(0)\left(1 - T/T_c(P)\right)/3, \tag{1.5}$$

$$\beta_0(P) = \frac{7\zeta(3)}{240\pi^2}\frac{N(0)}{\left(k_B T_c(P)\right)^2}, \tag{1.6}$$

$$\beta_i(P) = n_i\beta_0(P), \quad n_i = (-1,2,2,2,-2), \tag{1.7}$$

$$K(P) \equiv \alpha(T,P)\xi_{GL}^2, \tag{1.8}$$

$$\xi_{GL}(T,P) = \frac{\xi_0}{\sqrt{1 - T/T_c}}\left(\frac{7\zeta(3)}{20}\right)^{1/2}, \tag{1.9}$$

$$\xi_0(P) = \frac{\hbar v_F}{2\pi k_B T_c(P)}, \tag{1.10}$$

$$\gamma = 3, \tag{1.11}$$

where N(0) is the single-spin density of states at the Fermi energy in the normal Fermi fluid state, v_F is the Fermi velocity, ξ_{GL} is the Ginzburg-Landau coherence length, and ξ_0 is the coherence length at $T = 0$. These are determined by performing a Hubbard-Stratonovich transformation using the microscopic Hamiltonian of superfluid ^{3}He. Strong coupling corrections must be considered at nonzero pressures to accurately describe the values of the quartic coupling constants β_i. The deviation of these coupling constants $\Delta\beta_i^{SC}(P)$ from the weak-coupling values β_i^{WC} was experimentally determined in ref. [8] and [9], and this is shown in fig. 1.3. The strong coupling $\beta_i(T,P)$ are given by

$$\beta_i(T,P) = \beta_i^{WC}\left(P, T_c(P)\right) + \frac{T}{T_c}\Delta\beta_i^{SC}(P). \tag{1.12}$$

The order parameter takes on the value that minimizes F_{GL}[A]. For 3D case, this minimum either corresponds to ^{3}He-A or ^{3}He-B, depending on the values of the β_i's.

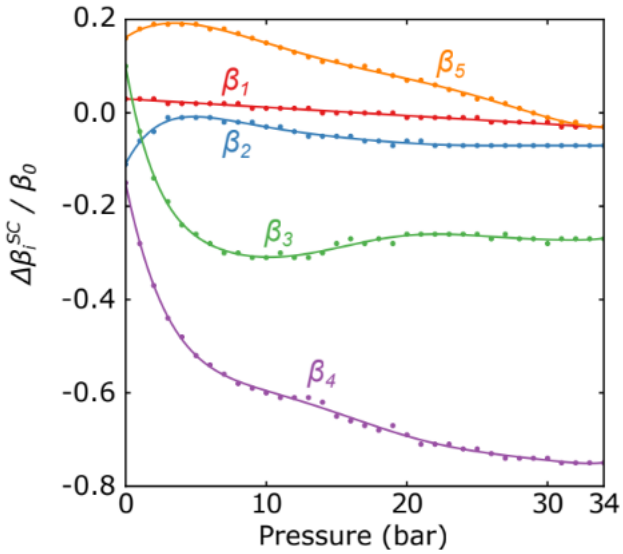

Figure 1.3: **Experimentally determined strong-coupling corrections.** Strong coupling corrections to β_i determined from [8][9]. The figure was taken from [5].

The change of the five quartic coupling constants $\beta_1 \ldots \beta_5$ with scale, confinement length, temperature, and pressure plays an essential role in studying the phases of ^{3}He. To understand how these coupling constants are affected by fluctuations in the order parameter, we must understand the renormalization group.

1.3 Renormalization Group Flows

The Renormalization Group was first developed as a consistent way to remove the infinities in quantum field theories. The term 'group' was added to its name because it was developed when Group Theory was very popular. However, the renormalization group is only semigroup, as there is no group inverse. Additionally, its algebraic structure does not play an important role in physics. RG was discovered to be a much more general tool than originally thought, and it was shown to have importance in all areas of physics. The quintessential purpose of RG is to relate physics at various scales. This makes it an excellent tool for exploring the long-distance physics of phase transitions.

The Renormalization group (RG) flow of our Ginzburg-Landau free energy allows

us to examine the low-energy effective theory of our free energy. Our free energy F_{GL} is the function of an order parameter ϕ and some coupling constants g_i. In ^{3}He, these would be the quadratic constant α, and the quartic coupling constants β_i. We imagine our system being put in a box with height L, so the fluctuations in the system cannot have a wavelength larger than L. We then expand our box by replacing $L \to bL$, where $b > 1$ is known as our RG parameter. We are interested in the IR regime, which corresponds to taking $b \to \infty$, or the box becoming infinitely large. Though the value of F_{GL} is given by its minimization up to first order in the coupling constants, there are fluctuation-induced corrections that need to be considered. In fact, these corrections can show that phases that look stable to first order, are indeed unstable. In perturbative RG, these corrections will take the form of n-loop corrections to the free energy, while in Functional RG, the corrections will be an infinite series of diagrams that is often uncontrolled. These corrections can be written as a function of b, and the system can be rescaled to its original size. If we add the corrections to the original free energy, we will see that we can replace the coupling constants g_i with *renormalized* coupling constants $\tilde{g}_i(b)$ to absorb the correction into the form of the original free energy. Generally, we cannot solve for $\tilde{g}_i(b)$ directly, but rather we derive a series of flow equations of b in the form

$$\frac{dg_i}{d\ln b} = B_{g_i}(g_1, g_2, \dots),$$

where each B_{g_i} is known as a beta function, not to be confused with our β_i quartic coupling constants and the mathematical special functions also referred to by the same name. To check the stability of a phase with fluctuations, we simply minimize F_{GL} with the IR renormalized couplings $\tilde{g}_i(\infty)$. A second-order phase transition will show itself as a fixed point of the RG flow. This is because second-order phase transitions involve a diverging coherence length, which causes the system to become self-similar. Self-similarity causes the free energy to remain the same when the length is rescaled by the RG parameter b. This fixed point can only be considered physical if it is stable

under perturbations.

1.4 Phases of Superfluid ^{3}He

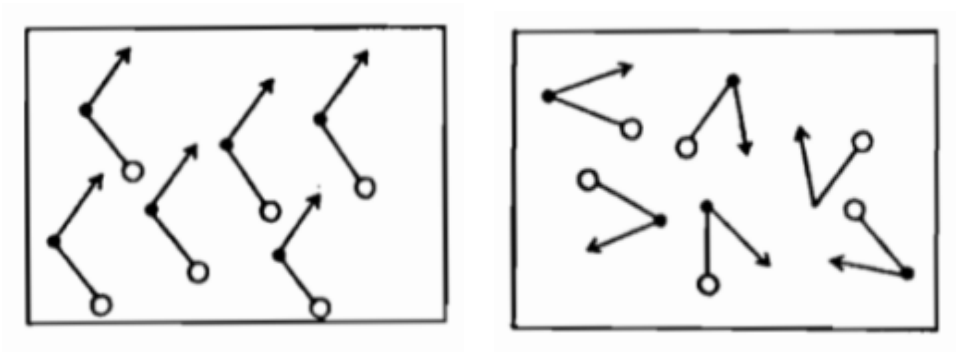

(a) (b)

Figure 1.4: **Representation of spin and orbital angular momentum degrees of freedom in ^{3}He.** Arrows represent spin, while circles represent orbital angular momentum. a) Spin and orbital angular momentum configuration in ^{3}He-A. Angular momentum is fixed macroscopically, while spin is fixed at an angle from the angular momentum vector. b) Spin and orbital angular momentum configuration in ^{3}He-B. Angular momentum and spin have a fixed angle between them. Figures taken from [1].

The rich symmetries of ^{3}He and its complicated order parameter allow for dozens of possible phases; however, very few are thermodynamically stable. 3D superfluid ^{3}He takes on two phases as seen in fig. 1.5; ^{3}He-A and ^{3}He-B, which are also known as the A and B phases. ^{3}He-B is a quasi-isotropic phase where the spin and angular momentum degrees of freedom attain a joint rotational symmetry rather than their original independent rotational symmetry, as seen in fig. 1.4b. ^{3}He-A is an anisotropic phase involving the angular momentum degrees of freedom aligning macroscopically and all the spins aligning microscopically as well, as seen in fig. 1.4a.

As seen in Figure 1.5, ^{3}He-B dominates the phase diagram,[1] whereas ^{3}He-A is only thermodynamically favourable in the high-pressure regime within a limited temperature range. However, this changes under confinement. We can see in fig. 1.6 that under confinement ^{3}He-A begins to dominate ^{3}He-B, which prevents the phase tran-

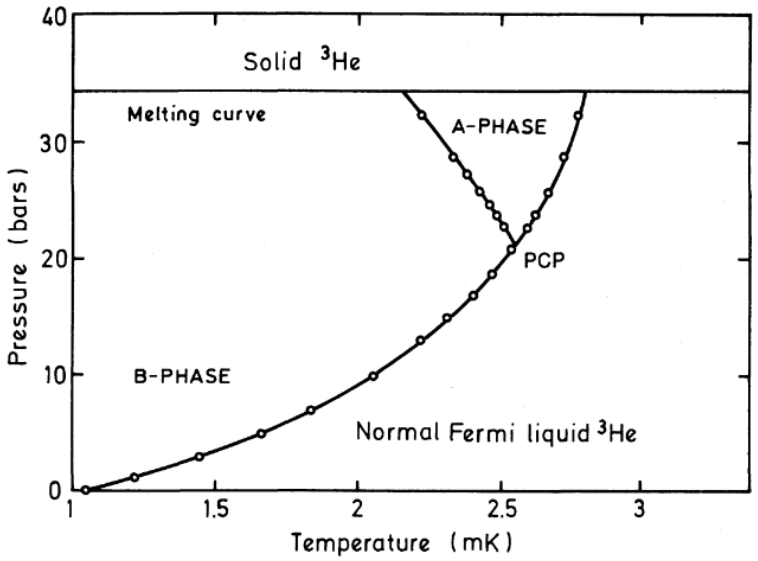

Figure 1.5: **Experimental phase diagram of ^{3}He.** Phase diagram of ^{3}He in terms of pressure (P) measured in bars, and temperature (T) measured in mK. Figure taken from [1]

.

sition directly from the normal Fermi liquid phase to ^{3}He-B. A new phase appears between the A and B phases, which also appears to become wider with increased confinement. The phase of ^{3}He is determined by which phase has the lower free energy. The criterion that decides that ^{3}He-A is energetically favourable is given by the inequality

$$C_{AB} = \beta_1 + \frac{1}{3}(\beta_3 - 2\beta_{45}) > 0 \tag{1.13}$$

Where we use the notation $\beta_{ij\ldots} = \beta_i + \beta_j + \ldots$. The shift in the boundary between the A and B phases in the quasi-2D regime can be considered a shift in these β_i coupling constants, causing a change to C_{AB}.

1.5 Thesis Objectives

In light of these new experiments, we aim to further the theoretical description of superfluid ^{3}He in the quasi-2D regime. Some progress has been made in understanding this effect. Directly minimizing the GL equations, using the Euler-Lagrange equa-

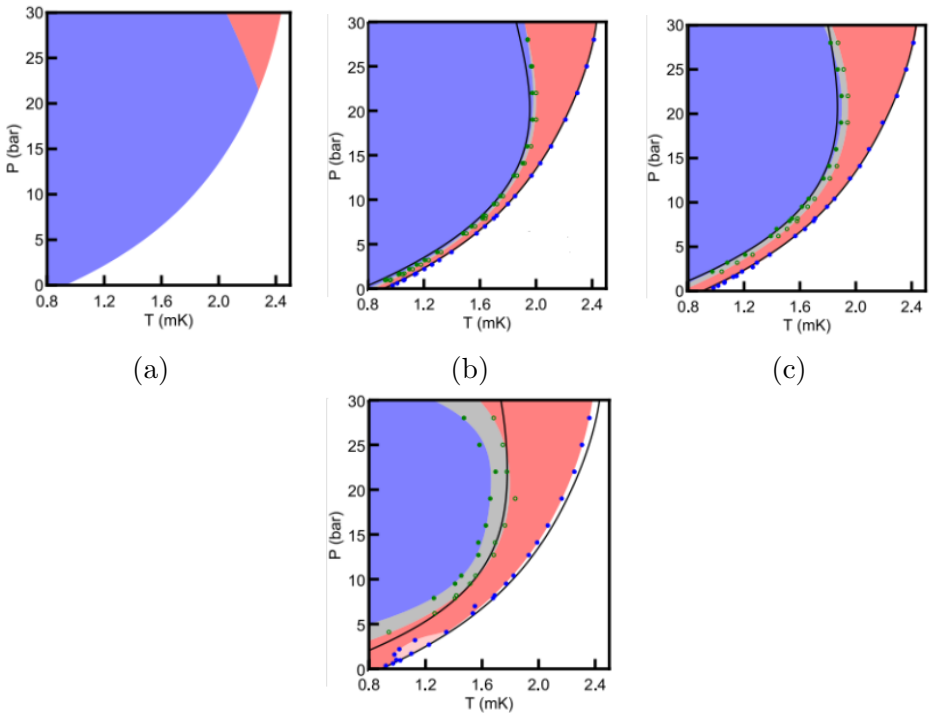

Figure 1.6: **Phase diagram of ^{3}He under confinement.** The phase diagram of ^{3}He in terms of pressure (P) measured in bars, and temperature (T) measured in mK (a) Bulk phase diagram shown for reference, with the ^{3}He-A in red and ^{3}He-B in blue. Phase diagrams for confinements of (b) 1067 nm, (c) 805 nm, and (d) 636 nm. Under confinement, a new phase appears, which is colored grey. This figure is taken from [6].

tions, has shown the amplification of ^{3}He-A [10, 11]. Many attempts have been made to theoretically understand the "stripe phase" which appears between ^{3}He-A and ^{3}He-B [12–14]. Adding a cubic symmetry-breaking term manually in the GL theory appears to reproduce the newly observed phase [12].

However, we have several reasons to believe that the dominance of the A-phase under confinement can be explained purely by fluctuations of the order parameter without considering additional interactions. Additionally, we hypothesize that we can see this by adding fluctuations to weak-coupling theory. In fig. 1.6, we see that under sufficient confinement, the A-phase appears at low pressures. The low-pressure physics of ^{3}He is described by weak-coupling theory. Another reason for our hypothe-

sis is that experimental evidence suggests a second-order phase transition occurs from the Fermi liquid to the A-phase [6, 10], and second-order phase transitions are usually driven by fluctuations. In fact, fluctuations are known to play a more pronounced role in lower dimensional systems and often lead to the formation of new phases [15, 16].

In order to prove this hypothesis, we will take the following steps. Firstly, we aim to understand confinement from a very different angle; we would like to understand the statistical field theory of ^{3}He under confinement. We first undertake the challenge of properly describing ^{3}He under confinement. We derive a 2D GL free energy from a confined symmetry group. In ref. [17], the GL theory of a system with a similar symmetry group was explored in the context of p-wave superconductors. We will see what happens in the quasi-2D regime by quantizing the angular momentum in the confined dimension, similar to a particle in a box. We apply the quantization procedure in ref. [18], which calculates the quasi-2D case for a simpler system, namely a one-component bosonic superfluid. Further, we will explore the effect of different boundary conditions on the result. After developing appropriate mathematical models describing confinement, we will study the RG flows in different cases. We employ techniques for computing RG flow of matrix order parameters from [19], using the trace-log formula derived in ref. [20].

We hypothesize that under confinement, the fixed point that corresponds to the ^{3}He-B shifts to produce the fixed point corresponding ^{3}He-A. We will attempt to do this using both the Wilsonian Renormalization Group and the Functional Renormalization Group. FRG will allow us to probe further into non-perturbative and non-universal behaviours in ^{3}He. In ref. [21], FRG is applied to the 3D superfluid ^{3}He system, and ^{3}He-A is found to be stable if strong coupling corrections are used.

1.6 Thesis Outline

Since our thesis revolves around the understanding of the GL theory of phase transitions, we will dedicate Chapter 2 to its introduction and exploration. We will begin by applying GL theory to a toy model, then proceed to explore the order parameter, phases, propagator, and Goldstone modes in the 3D system. Next, we will derive a new GL theory of ^{3}He with reduced symmetry and describe its properties. In Chapter 4, we will introduce the perturbative Renormalization Group and show its calculation on a toy model. Next, we will review the application of this to 3D ^{3}He and discuss the main results. Next, we will apply RG to our confined 2D ^{3}He system by observing the phases under various degrees of confinement. This is where we expect to see the A-phase dominate over the B-phase at sufficient confinement. We will need to extend our work by using more powerful RG methods. In Chapter 4, we will do this by introducing functional renormalization and applying it to a U(1) toy model. We will see the FRG result in 3D and compare it to our new calculations of FRG under confinement. In Appendix A, we derive several properties of path integrals, including the trace-log formula. In Appendix B, we derive the formulas for the derivatives of various functions of the propagator. In Appendix C, we discuss our flow equations and their derivations. Finally, in Appendix D, we have listed some notation and conventions that may be helpful to the reader.

Chapter 2

Ginzburg-Landau Theory

2.1 Introduction to Ginzburg-Landau Theory

Let us denote the order parameter of an arbitrary system by $\Delta(\mathbf{r})$, and let G be the symmetry group of the system. We can calculate physical observables relating to the phase transition exactly by calculating the partition function. For a given GL free energy, the partition function $\mathcal{Z}$ given by the path integral

$$\mathcal{Z} = \int \mathcal{D}[\Delta] \exp\left(-\beta F_{GL}[\Delta]\right). \tag{2.1}$$

As an alternative to the partition function, we can also define the effective free energy F_{eff} as

$$\exp\left(-\beta F_{\text{eff}}\right). = \int \mathcal{D}[\Delta] \exp\left(-\beta F_{GL}[\Delta]\right). \tag{2.2}$$

Evaluating such path integrals is a near-impossible task, so we must take approximations. We have employed the saddle-point approximation to solve such path integrals in Appendix A. We find that the effective free energy can be expanded as

$$F_{\text{eff}} = F_{GL}[\bar{\Delta}] + \frac{1}{2}\int_{\mathbf{q}} \operatorname{tr} \ln \mathcal{G}^{-1}(\bar{\Delta}, q) + h.o.c., \tag{2.3}$$

where $\bar{\Delta}$ corresponds to the location of the global minimum of F_{GL}. $\mathcal{G}$ is the propagator, which encodes the behaviour of collective modes, which form the fluctuations of the order parameter. The first term in the expansion corresponds to mean-field theory, which assumes that the order parameter minimizes F_{GL}. In an infinite domain,

this reduces to solving a system of polynomial equations of the form

$$\left.\frac{\delta F_{GL}[\Delta]}{\delta \Delta_a}\right|_{\Delta=\bar{\Delta}} = 0, \tag{2.4}$$

Here we assume that Δ_a is the 'a-th' component of Δ. We will always work in an infinite domain in our work and thus use eq. (2.4) for our minimization. The second term in eq. (2.3) represents the correction to the free energy due to "fluctuations" in the order parameter.

2.1.1 Symmetries

Symmetries play an essential role in our study of phase transitions. Mainly, they help us construct a suitable free energy for our system and allow us to investigate symmetry breaking during the phase transition. Every term of $F_{GL}[\Delta]$ needs to be invariant under the symmetry group of the system G such that $F_{GL}[\Delta]$ contains all terms invariant under G such that

$$F_{GL}(g \cdot \Delta) = F_{GL}(\Delta) \tag{2.5}$$

for every group element $g \in G$. This g can be, for example, a negative sign, a complex phase, or more complicated like some matrix multiplication. In the context of condensed matter systems, the broken symmetry is usually a rotational symmetry about some axis. Rotations about one axis correspond to the group SO(2), which is equivalent to the unitary group U(1), and rotations in three dimensions are represented by the non-Abelian group SO(3).

Generally, F_{GL} can contain infinitely many terms that satisfy eq. (2.5), but only a few of these terms are important for understanding the phase transition. A sample free energy may look like

$$F_{GL} \sim \int d^d\mathbf{x} \left[(\partial_{\mathbf{x}}\Delta(\mathbf{x}))^2 + \alpha\Delta(\mathbf{x})^2 + \lambda\Delta(\mathbf{x})^4\right], \tag{2.6}$$

which involves derivative terms known as the kinetic terms, quadratic terms in the order parameter known as the mass term, and finally, quartic terms in the order

parameter known as the interaction terms. Here α and λ are coefficients known as coupling constants. The values of the coupling constants are very important for the phase transitions, and they can usually be measured in experiment.

Let X be the set global minima of F_{GL}. Then H, the residual symmetry group, is defined to be the largest group such that

$$h \cdot \bar{\Delta} = \bar{\Delta} \tag{2.7}$$

for all $h \in H$. H is the symmetry group of an order parameter $\bar{\Delta}$ that minimize F_{GL}. We can see that $H \subseteq G$. This reduction of the symmetry group from G to H following A phase transition is known as 'spontaneous symmetry breaking'. Broken symmetries are the hallmarks of phase transitions and are essential to understanding them. A broken symmetry refers to when the ground state of a system is no longer invariant under the full group of symmetries G, as it was before the transition. Certain symmetries are 'broken' such that the system is still invariant under a subgroup H of G after the transition. The coset R is defined by

$$R = G/H, \tag{2.8}$$

and it describes the transformations that physically change the new ground state and encodes information about fluctuations and, in particular, Goldstone modes. This can be thought 'space of fluctuations'. Generally, R will be a manifold and not necessarily a group. We are guaranteed a group structure on R when H is a normal subgroup of G.

2.1.2 Example

The idea of GL theory is to describe phase transitions purely with the energetics of a system in the form of the Ginzburg-Landau free energy functional and understand the symmetries of this free energy. The first key observation that GL theory attempts to explain is that during a phase transition, the order parameter spontaneously becomes

non-zero below a critical temperature T_c. The second key observation is that symmetry is broken below T_c; the ground state possesses only a subset of the symmetry of the free energy. We now use Landau's model for the superconducting transition as a simple model to demonstrate GL Theory.

Landau's key insight was that he ingeniously expanded the free energy of a superconductor in terms of its macroscopic wavefunction $\phi(r)$, such that the density of superconducting states $n_s(r)$ were given by $n_s = \phi^*\phi$. Landau then expanded the system in terms that respected the U(1) symmetry of ϕ given by

$$\phi \to e^{i\varphi}\phi.$$

From the U(1) symmetry, we can write down all the relevant invariant low-order terms under this group. Then GL free energy functional is given by

$$F_{GL}[\phi] = F_0 + \int d^d\mathbf{x} \left(|\partial\phi(\mathbf{x})|^2 + \alpha|\phi(\mathbf{x})|^2 + \frac{\lambda}{2}|\phi|^4(\mathbf{x}) \right). \tag{2.9}$$

The minimum of the free energy decides the value of the order parameter. If we try to minimize this free energy, we realize that ϕ must be a constant field to minimize the $|\partial\phi(\mathbf{x})|^2$ term. A simple calculation tells us that the minimizing order parameter is

$$\phi_{min} = \begin{cases} 0 & \alpha > 0 \\ \sqrt{-\frac{\alpha}{\lambda}}e^{i\varphi_0} & \alpha < 0 \end{cases}. \tag{2.10}$$

We can see that when α changes sign, suddenly the Cooper pair density is non-zero as seen in Figure 2.1, which indicates a phase transition occurred. The order parameter now has 'picked' a phase φ_0, so the $U(1)$ symmetry is broken with no residual symmetry remaining.

We can see that the coupling constant α changing signs causes the phase transition, leading to spontaneous symmetry breaking. Since $\alpha = 0$ happens exactly at the phase transition, it must also correspond to corresponds to $T = T_c$. Now that we have seen a simple case of phase transitions, we are now ready for the more complicated case of superfluid ^{3}He.

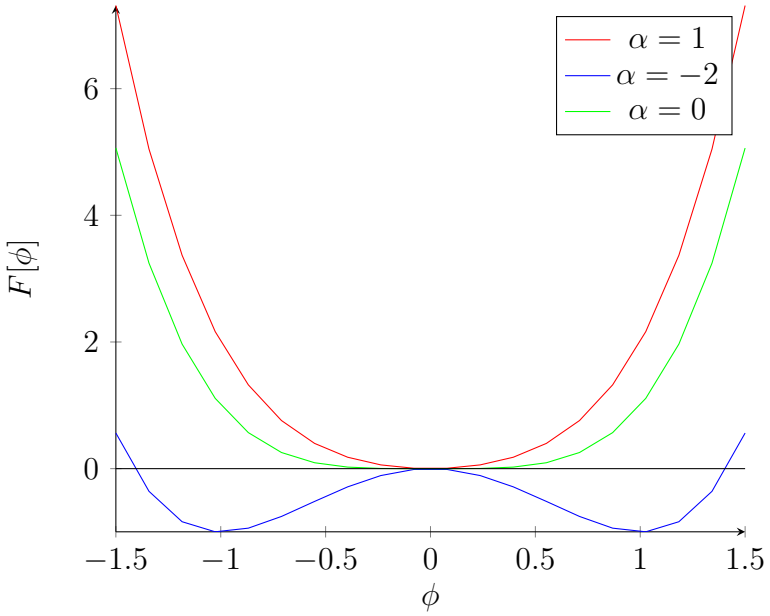

Figure 2.1: **Spontaneous symmetry breaking in the ground state of the free energy.** Spontaneous symmetry breaking in the ground state of the free energy for $\lambda = 2$. As the value of α becomes negative, the global minimum suddenly shifts away from zero and breaks the symmetry of the system.

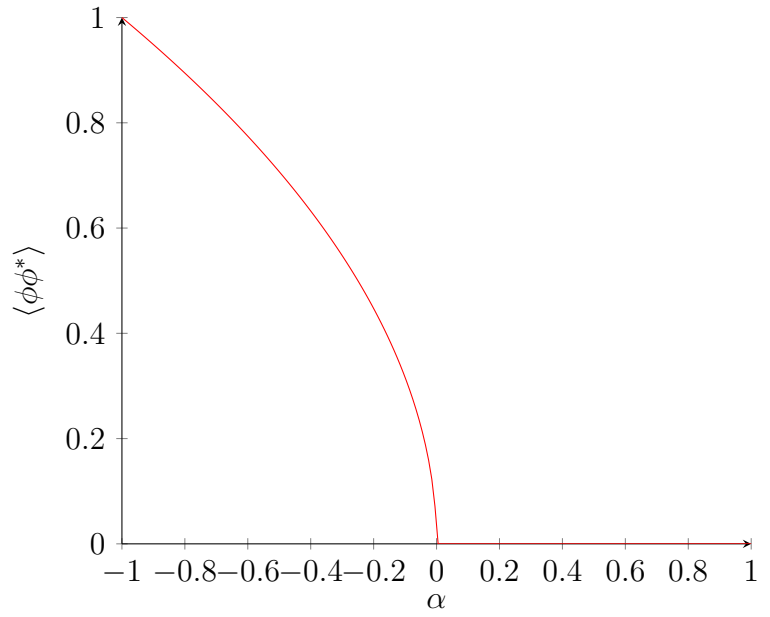

Figure 2.2: **Spontaneous breaking of symmetry of the order parameter in the U(1) model.** Spontaneous symmetry breaking in the ground state of the free energy. As α is made negative, the expectation value of the order parameter becomes non-zero continuously, signifying a second-order phase transition

2.2 Ginzburg-Landau Theory of ^{3}He

Superfluid ^{3}He has a 3 by 3 matrix order parameter, which is the main reason for its complexity. The cooper pairs in superfluid ^{3}He have spin quantum number $S = 1$ and angular moment $L = 1$, so the order parameter forms a 3 by 3 second-rank matrix, with components given by each combination of angular momentum and spin degree of freedom. The most general form of the ^{3}He order parameter is

$$\mathrm{A} = \begin{pmatrix} \mathrm{A}_{1,1} & \mathrm{A}_{1,2} & \mathrm{A}_{1,3} \\ \mathrm{A}_{2,1} & \mathrm{A}_{2,2} & \mathrm{A}_{2,3} \\ \mathrm{A}_{3,1} & \mathrm{A}_{3,2} & \mathrm{A}_{3,3} \end{pmatrix}, \tag{2.11}$$

where each entry in the matrix is a complex-valued function with spatial dependence. We will write this in index notation as $\mathrm{A}_{\mu i}$, where μ is the spin index and i is the angular momentum index. The free energy for superfluid helium in terms of this order parameter is given by

$$\begin{aligned} F[\mathrm{A}] = \int d^3\mathbf{r} \big\{ & \alpha \mathrm{tr}(\mathrm{A}\mathrm{A}^\dagger) + \beta_1 |\mathrm{tr}(\mathrm{A}\mathrm{A}^T)|^2 + \beta_2 [\mathrm{tr}(\mathrm{A}\mathrm{A}^\dagger)]^2 \\ & + \beta_3 \mathrm{tr}(\mathrm{A}\mathrm{A}^T\mathrm{A}^*\mathrm{A}^\dagger) + \beta_4 \mathrm{tr}(\mathrm{A}\mathrm{A}^\dagger\mathrm{A}\mathrm{A}^\dagger) + \beta_5 \mathrm{tr}(\mathrm{A}\mathrm{A}^\dagger\mathrm{A}^*\mathrm{A}^T) \\ & + K(\gamma - 1)\partial_i \mathrm{A}^*_{\mu i} \partial_j \mathrm{A}_{\mu j} + K \partial_i \mathrm{A}^*_{\mu j} \partial_i \mathrm{A}_{\mu j} \big\}. \end{aligned} \tag{2.12}$$

Here, $\alpha, \beta_1 \ldots \beta_5, K, \gamma$ are all coupling constants, and summation is implied over repeated indices. Assuming the order parameter is constant, we can integrate over momentum space

$$\begin{aligned} F[\mathrm{A}] = & K^{-\frac{3}{2}} \int d^3\mathbf{q} \big\{ \alpha \mathrm{tr}(\mathrm{A}\mathrm{A}^\dagger) + \beta_1 |\mathrm{tr}(\mathrm{A}\mathrm{A}^T)|^2 + \beta_2 [\mathrm{tr}(\mathrm{A}\mathrm{A}^\dagger)]^2 \\ & + \beta_3 \mathrm{tr}(\mathrm{A}\mathrm{A}^T\mathrm{A}^*\mathrm{A}^\dagger) + \beta_4 \mathrm{tr}(\mathrm{A}\mathrm{A}^\dagger\mathrm{A}\mathrm{A}^\dagger) + \beta_5 \mathrm{tr}(\mathrm{A}\mathrm{A}^\dagger\mathrm{A}^*\mathrm{A}^T) \\ & + (\gamma - 1) q_i \mathrm{A}^*_{\mu i} q_j \mathrm{A}_{\mu j} + q_i \mathrm{A}^*_{\mu j} q_i \mathrm{A}_{\mu j} \big\}. \end{aligned} \tag{2.13}$$

Here, we have rescaled our momentum $\mathbf{q}$ to $\sqrt{K}\mathbf{q}$ and factored it outside the free energy. This allows us to ignore K dependence as an overall factor in the free energy, which we will ignore. The symmetry group of ^{3}He is

$$G = SO(3)_S \times SO(3)_L \times U(1)_\phi. \tag{2.14}$$

The group acts on the order parameter as follows:

$$\mathrm{A} \to e^{i\phi} R \mathrm{A} S^T \tag{2.15}$$

Where $S \in \mathrm{SO}(3)_L$ corresponds to a rotation of space. $R \in \mathrm{SO}(3)_S$, which corresponds to a rotation of spin. Finally, $e^{i\phi} \in U(1)$ corresponds to the gauge symmetry.

The breaking of the $U(1)$ gauge symmetry is what leads to superfluidity and long-range order, so the $U(1)$ is broken in all the possible superfluid phases of ^{3}He. The components of the order parameter of ^{3}He-B can be most generally written as

$$\mathrm{A}_{\mu j} = \Delta_{\mathrm{B}} e^{i\phi} R_{\mu j}(\theta, \hat{\boldsymbol{n}}), \tag{2.16}$$

where $R_{\mu j}(\theta, \hat{\boldsymbol{n}}) \in$SO(3) is an arbitrary rotation matrix about the axis $\hat{\boldsymbol{n}}$, with angle θ. ϕ is a phase, and Δ_A is a gap parameter that is chosen by minimizing the free energy. The order parameter is left invariant when rotations of spin R^S that gets undone by a rotation of the angular momentum $R^L = \left(R^S\right)^T$. Therefore, the spin and angular momentum have a symmetry where they can be rotated together. Symmetries such as this one where two different symmetries combine to make the same symmetry transformation known as relative symmetries. The symmetry group is thus given by

$$H_B = \mathrm{SO}(3)_{\mathrm{L+S}}. \tag{2.17}$$

Here, the '$L + S$' signifies that a rotation in spin angular momentum space is no different from a rotation in orbital angular momentum space. For convenience, we can write the B phase order parameter as

$$\mathrm{A}_B = \Delta_B \begin{pmatrix} 1 & 0 & 0 \\ 0 & 1 & 0 \\ 0 & 0 & 1 \end{pmatrix}, \tag{2.18}$$

where we have fixed $\phi = 0$, and the rotation matrix is the identity matrix. We can determine the parameter Δ_B, by minimizing the free energy with respect to it. Then, the free energy is

$$F[\mathrm{A}_B] = 3\alpha\Delta_B^2 + 3(3\beta_{12} + \beta_{345})\Delta_B^4, \tag{2.19}$$

which has the critical points satisfying

$$\frac{F[\mathrm{A}_B]}{d\Delta_B} = 0 \implies \Delta_B = \sqrt{\frac{-\alpha}{2(3\beta_{12}+\beta_{345})}}, \tag{2.20}$$

for $\alpha < 0$ where we are allowing the coupling constants to be fully general. The free energy takes the value

$$F[\mathrm{A}_B] = -\frac{3\alpha^2}{4(3\beta_{12}+\beta_{345})} \tag{2.21}$$

in the B phase.

The A phase has a relative symmetry between rotations of angular momentum about the z-axis and applying an overall phase. The spins have a rotational symmetry about a fixed axis. Finally, there is a discrete $\mathbb{Z}_2$ symmetry. The symmetry group is given by

$$H_A = U(1)_{L_z-\phi} \times U(1)_S \times \mathbb{Z}_2. \tag{2.22}$$

Note that discrete symmetries do not contribute to the Goldstone modes, so they have less relevance in the context of phase transitions. We can see that though we still have a $U(1)$ symmetry, the original gauge symmetry is broken, giving us long-range order and superfluidity. We choose a representative order-parameter matrix for the A phase as

$$\mathrm{A}_A = \Delta_A \begin{pmatrix} 1 & i & 0 \\ 0 & 0 & 0 \\ 0 & 0 & 0 \end{pmatrix}, \tag{2.23}$$

where Δ_A is a real parameter chosen to minimize the GL free energy. When $\alpha < 0$, then this is the minimum. The free energy is given by

$$F[\mathrm{A}_A] = 2\alpha\Delta_A^2 + 4\beta_{245}\Delta_A^4, \tag{2.24}$$

which can be minimized to give the value of Δ_A as

$$\Delta_A = \sqrt{\frac{-\alpha}{4\beta_{245}}} \tag{2.25}$$

and its minimized free energy as

$$F[\mathrm{A}_A] = \frac{-\alpha^2}{4(\beta_{245})}. \tag{2.26}$$

There are other possible phases that do not appear in experiment, but still correspond to local minimums of the GL free energy. The A_1 phase appears in ^{3}He under magnetic fields and has an order parameter of

$$A_{A_1} = \Delta_{A_1} \begin{pmatrix} 1 & i & 0 \\ -i & 1 & 0 \\ 0 & 0 & 0 \end{pmatrix}, \tag{2.27}$$

We are interested in finding out when the A phase will be favoured over the B phase. We can derive the conditions in which this occurs with the following derivation:

$$F[A_B] > F[A_A] \tag{2.28}$$

$$\implies -\frac{3\alpha^2}{4(3\beta_{12}+\beta_{345})} > -\frac{\alpha^2}{4(\beta_{245})} \implies \frac{3\alpha^2}{4(3\beta_{12}+\beta_{345})} < \frac{\alpha^2}{4(\beta_{245})} \tag{2.29}$$

$$\implies \beta_{12} + \frac{1}{3}\beta_{345} > \beta_{245} \tag{2.30}$$

$$\implies C_{AB} = \beta_1 + \frac{1}{3}(\beta_3 - 2\beta_{45}) > 0. \tag{2.31}$$

In general, finding the global minima for a matrix order parameter is a very challenging task, so it is helpful to use some techniques from group theory to simplify this problem. The order parameters we see in experiment, such as the A and B phases, still have a non-trivial residual symmetry H. This is because our symmetry group G is large enough to have many different non-trivial subgroups. In fact, all of the order-parameters corresponding to stationary points of the GL free energy have non-trivial remaining symmetry [22, 23]. It appears that order parameters with higher symmetry have a lower free energy. It is difficult to prove this rigorously, but it provides important intuition in searching for minima. Minimizing the free energy for arbitrary β_i is extremely challenging, and involves solving a set of eighteen coupled nonlinear equations, so instead we search through the different symmetry-breaking possibilities by determining all the factorizations of G. Once the residual symmetry H and the corresponding order parameter for each phase is determined, we can compare their

free energy to see which phase will be stable. In ref. [22], we can find all the stationary points of the free energy, which include

$$\text{the polar state } \mathrm{A}_{polar} = \Delta_{polar} \begin{pmatrix} 0 & 0 & 0 \\ 0 & 0 & 0 \\ 0 & 0 & 1 \end{pmatrix},$$

$$\text{the } \beta\text{-state } \mathrm{A}_{\beta} = \Delta_{\beta} \begin{pmatrix} 0 & 0 & 1 \\ 0 & 0 & i \\ 0 & 0 & 0 \end{pmatrix},$$

$$\text{the planar state } \mathrm{A}_{planar} = \Delta_{planar} \begin{pmatrix} 1 & 0 & 0 \\ 0 & 1 & 0 \\ 0 & 0 & 0 \end{pmatrix},$$

$$\text{the bipolar state } \mathrm{A}_{bipolar} = \Delta_{bipolar} \begin{pmatrix} 1 & 0 & 0 \\ 0 & i & 0 \\ 0 & 0 & 0 \end{pmatrix},$$

$$\text{and the } \alpha\text{-state } \mathrm{A}_{\alpha} = \Delta_{\alpha} \begin{pmatrix} 1 & 0 & 0 \\ 0 & e^{i\pi/3} & 0 \\ 0 & 0 & e^{2u\pi/3} \end{pmatrix}.$$

as well as the A, $\mathrm{A}_1$and B phases, which appear in experiment. These all satisfy

$$\frac{\delta \mathrm{F}[\mathrm{A}]}{\delta \mathrm{A}^*_{\mu j}} = 0, \tag{2.32}$$

for all μ and j and all values of coupling constants. Though none of these states occur in 3D, these potential phases may be relevant for the quasi-2D case.

2.3 Propagator of ^{3}He

To better understand fluctuations of our order parameter, we must better understand the propagator. The Hessian of the free energy gives the propagator and encodes the behaviour of collective modes within a given field. A has nine complex components that can be written in eighteen real components. To give our propagator a simpler

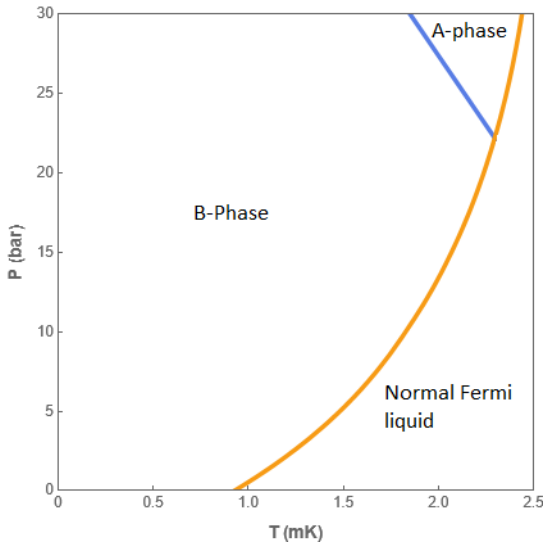

Figure 2.3: **Phase diagram of He-3.** Phase diagram of ^{3}He in 3D found using eq. (2.31) to determine the blue line separating the A and B phases, with the inequality replaced with equality, and the coupling constants including strong-coupling corrections.

form, we choose the basis given by

$$\mathrm{A}_{\mu i} = \frac{1}{\sqrt{2}}\left(\psi_{\mu i} + \bar{\psi}_{\mu i}\right) + \frac{i}{\sqrt{2}}\left(\psi_{\mu i} - \bar{\psi}_{\mu i}\right), \tag{2.33}$$

where $\psi_{\mu i}$ and $\bar{\psi}_{\mu i}$ are real numbers that are used to define the order parameter as an alternative to $A_{\mu,i}$. Let $\Psi = (\psi_{1,1}, \psi_{1,2}, \psi_{1,3}, \psi_{2,1} \ldots \psi_{3,3})$ and $\bar{\Psi} = (\bar{\psi}_{1,1}, \bar{\psi}_{1,2}, \bar{\psi}_{1,3}, \bar{\psi}_{2,1} \ldots \bar{\psi}_{3,3})$. Let $q^2 = q_x^2 + q_y^2 + q_z^2$. The inverse propagator is given by the Hessian matrix of the free energy [24]

$$\frac{\delta^2 F_{GL}}{\delta \mathrm{A}^2} = \mathcal{G}^{-1}(\Psi, \bar{\Psi}, \mathbf{q}), \tag{2.34}$$

where q is the momentum. Now we calculate the Hessian, given by

$$F^{(2)}[\Psi, \bar{\Psi}] = \frac{\delta^2 F[\Psi, \bar{\Psi}]}{\delta\Psi(\mathbf{q})\delta\Psi(\mathbf{q}')} = \delta^{(d)}(\mathbf{q} - \mathbf{q}') \begin{pmatrix} \frac{\delta^2 F[\Psi, \bar{\Psi}]}{\delta\psi^2} & \frac{\delta^2 F[\Psi, \bar{\Psi}]}{\delta\bar{\psi}\delta\psi} \\ \frac{\delta^2 F[\Psi, \bar{\Psi}]}{\delta\psi\delta\bar{\psi}} & \frac{\delta^2 F[\Psi, \bar{\Psi}]}{\delta\bar{\psi}^2}, \end{pmatrix} \tag{2.35}$$

where each block of the matrix is a 9×9 matrix, and this will be a rank 4 tensor since the order parameter is rank 2.

We can write our inverse propagator as the sum of a momentum-dependant term

$\mathcal{G}_0^{-1}(\mathbf{q})$ and a term that depends on the order parameter $\mathcal{V}(\Psi, \bar{\Psi})$ as

$$\mathcal{G}^{-1}(\Psi, \bar{\Psi}, q) = \mathcal{G}_0^{-1}(\mathbf{q}) + \mathcal{V}(\Psi, \bar{\Psi}). \tag{2.36}$$

We can define the non-interacting inverse propagator as

$$\mathcal{G}_0^{-1}{}_{\mu i,\nu j}(\boldsymbol{q}) = \delta_{\mu\nu} \left(q^2 \delta_{ij} + (\gamma - 1) q_i q_j\right) \begin{pmatrix} 1 & 0 \\ 0 & 1 \end{pmatrix}. \tag{2.37}$$

The corresponding propagator is

$$\mathcal{G}_0(\boldsymbol{q}) = \frac{\delta_{\mu\nu}}{q^2} \left(\delta_{ij} + \left(\gamma^{-1} - 1\right) \frac{q_i q_j}{q^2}\right) \begin{pmatrix} 1 & 0 \\ 0 & 1 \end{pmatrix}. \tag{2.38}$$

Finally, our interacting part of the inverse propagator is

$$
\begin{aligned}
\mathcal{V}_{\mu i,\nu j} = 8\beta_1 &\begin{pmatrix} \left(\psi_{\mu i}\psi_{\nu j} + \bar{\psi}_{\mu i}\bar{\psi}_{\nu j}\right) & \left(\psi_{\mu i}\bar{\psi}_{\nu j} - \bar{\psi}_{\mu i}\psi_{\nu j}\right) \\ \left(\bar{\psi}_{\mu i}\psi_{\nu j} - \psi_{\mu i}\bar{\psi}_{\nu j}\right) & \left(\psi_{\mu i}\psi_{\nu j} + \bar{\psi}_{\mu i}\bar{\psi}_{\nu j}\right) \end{pmatrix} \\
+4\beta_1 &\begin{pmatrix} (\|\Psi\|^2 - \|\bar{\Psi}\|^2)\delta_{ij}\delta_{\mu\nu} & 2\Psi\cdot\bar{\Psi}\delta_{ij}\delta_{\mu\nu} \\ 2\Psi\cdot\bar{\Psi}\delta_{ij}\delta_{\mu\nu} & (-\|\Psi\|^2 + \|\bar{\Psi}\|^2)\delta_{ij}\delta_{\mu\nu} \end{pmatrix} \\
+8\beta_2 &\begin{pmatrix} \psi_{\mu i}\psi_{\nu j} & \bar{\psi}_{\mu i}\psi_{\nu j} \\ \psi_{\mu i}\bar{\psi}_{\nu j} & \bar{\psi}_{\mu i}\bar{\psi}_{\nu j} \end{pmatrix} + 4\beta_2(\|\Psi\|^2 + \|\bar{\Psi}\|^2) \begin{pmatrix} \delta_{ij}\delta_{\mu\nu} & 0 \\ 0 & \delta_{ij}\delta_{\mu\nu} \end{pmatrix} \\
+4\beta_3 &\sum_{\alpha} \begin{pmatrix} \left(\psi_{\alpha i}\psi_{\alpha j} + \bar{\psi}_{\alpha i}\bar{\psi}_{\alpha j}\right) & \left(\bar{\psi}_{\alpha i}\psi_{\alpha j} - \psi_{\alpha i}\bar{\psi}_{\alpha j}\right) \\ \left(\psi_{\alpha i}\bar{\psi}_{\alpha j} - \bar{\psi}_{\alpha i}\psi_{\alpha j}\right) & \left(\psi_{\alpha i}\psi_{\alpha j} + \bar{\psi}_{\alpha i}\bar{\psi}_{\alpha j}\right) \end{pmatrix} \delta_{\mu\nu} \\
+4\beta_3 &\sum_{k} \begin{pmatrix} \left(\psi_{\mu k}\psi_{\nu k} - \bar{\psi}_{\mu k}\bar{\psi}_{\nu k}\right) & \left(\bar{\psi}_{\mu k}\psi_{\nu k} + \psi_{\mu k}\bar{\psi}_{\nu k}\right) \\ \left(\bar{\psi}_{\mu k}\psi_{\nu k} + \psi_{\mu k}\bar{\psi}_{\nu k}\right) & \left(\bar{\psi}_{\mu k}\bar{\psi}_{\nu k} - \psi_{\mu k}\psi_{\nu k}\right) \end{pmatrix} \delta_{ij} \\
+4\beta_3 &\begin{pmatrix} \left(\psi_{\mu j}\psi_{\nu i} + \bar{\psi}_{\mu j}\bar{\psi}_{\nu i}\right) & \left(\psi_{\mu j}\bar{\psi}_{\nu i} - \bar{\psi}_{\mu j}\psi_{\nu i}\right) \\ \left(\bar{\psi}_{\mu j}\psi_{\nu i} - \psi_{\mu j}\bar{\psi}_{\nu i}\right) & \left(\psi_{\mu j}\psi_{\nu i} + \bar{\psi}_{\mu j}\bar{\psi}_{\nu i}\right) \end{pmatrix} \\
+4\beta_4 &\sum_{\alpha} \begin{pmatrix} \left(\psi_{\alpha i}\psi_{\alpha j} + \bar{\psi}_{\alpha i}\bar{\psi}_{\alpha j}\right) & \left(\bar{\psi}_{\alpha i}\psi_{\alpha j} - \psi_{\alpha i}\bar{\psi}_{\alpha j}\right) \\ \left(\psi_{\alpha i}\bar{\psi}_{\alpha j} - \bar{\psi}_{\alpha i}\psi_{\alpha j}\right) & \left(\psi_{\alpha i}\psi_{\alpha j} + \bar{\psi}_{\alpha i}\bar{\psi}_{\alpha j}\right) \end{pmatrix} \delta_{\mu\nu} \\
+4\beta_4 &\sum_{k} \begin{pmatrix} \left(\psi_{\mu k}\psi_{\nu k} + \bar{\psi}_{\mu k}\bar{\psi}_{\nu k}\right) & \left(\psi_{\mu k}\bar{\psi}_{\nu k} - \bar{\psi}_{\mu k}\psi_{\nu k}\right) \\ \left(\bar{\psi}_{\mu k}\psi_{\nu k} - \psi_{\mu k}\bar{\psi}_{\nu k}\right) & \left(\bar{\psi}_{\mu k}\bar{\psi}_{\nu k} + \psi_{\mu k}\psi_{\nu k}\right) \end{pmatrix} \delta_{ij} \\
+4\beta_4 &\begin{pmatrix} \left(\psi_{\mu j}\psi_{\nu i} - \bar{\psi}_{\mu j}\bar{\psi}_{\nu i}\right) & \left(\psi_{\mu j}\bar{\psi}_{\nu i} + \bar{\psi}_{\mu j}\psi_{\nu i}\right) \\ \left(\bar{\psi}_{\mu j}\psi_{\nu i} + \psi_{\mu j}\bar{\psi}_{\nu i}\right) & \left(\bar{\psi}_{\mu j}\bar{\psi}_{\nu i} - \psi_{\mu j}\psi_{\nu i}\right) \end{pmatrix} \\
+4\beta_5 &\sum_{\alpha} \begin{pmatrix} \left(\psi_{\alpha i}\psi_{\alpha j} - \bar{\psi}_{\alpha i}\bar{\psi}_{\alpha j}\right) & \left(\bar{\psi}_{\alpha i}\psi_{\alpha j} + \psi_{\alpha i}\bar{\psi}_{\alpha j}\right) \\ \left(\psi_{\alpha i}\bar{\psi}_{\alpha j} + \bar{\psi}_{\alpha i}\psi_{\alpha j}\right) & \left(\bar{\psi}_{\alpha i}\bar{\psi}_{\alpha j} - \psi_{\alpha i}\psi_{\alpha j}\right) \end{pmatrix} \delta_{\mu\nu} \\
+4\beta_5 &\sum_{k} \begin{pmatrix} \left(\psi_{\mu k}\psi_{\nu k} + \bar{\psi}_{\mu k}\bar{\psi}_{\nu k}\right) & \left(\psi_{\mu k}\bar{\psi}_{\nu k} - \bar{\psi}_{\mu k}\psi_{\nu k}\right) \\ \left(\bar{\psi}_{\mu k}\psi_{\nu k} - \bar{\psi}_{\nu k}\psi_{\mu k}\right) & \left(\bar{\psi}_{\mu k}\bar{\psi}_{\nu k} + \psi_{\mu k}\psi_{\nu k}\right) \end{pmatrix} \delta_{ij} \\
+4\beta_5 &\begin{pmatrix} \left(\psi_{\mu j}\psi_{\nu i} + \bar{\psi}_{\mu j}\bar{\psi}_{\nu i}\right) & \left(\psi_{\mu j}\bar{\psi}_{\nu i} - \bar{\psi}_{\mu j}\psi_{\nu i}\right) \\ \left(\bar{\psi}_{\mu j}\psi_{\nu i} - \psi_{\mu j}\bar{\psi}_{\nu i}\right) & \left(\bar{\psi}_{\mu j}\bar{\psi}_{\nu i} - \psi_{\mu j}\psi_{\nu i}\right) \end{pmatrix}
\end{aligned}
\tag{2.39}
$$

We define $\|\Psi\|^2 = \sum_{\mu i} \psi_{\mu i}^2$, and $\|\bar{\Psi}\|^2 = \sum_{\mu i} \bar{\psi}_{\mu i}^2$. This equation is derived simply by taking second derivatives of the free energy. We employ symbolic algebra tools such

as Mathematica to confirm and manipulate this reliably. We can use this propagator to study fluctuations of the order parameter.

2.4 Goldstone Modes

Spontaneous symmetry breaking can give rise to long wavelength excitations in the order parameter known as Goldstone modes. They occur when the order parameter is degenerate over a manifold of states, leading to oscillations in the order parameter inside this manifold. Since the states are energetically degenerate, they require no initial energy and can have arbitrarily low wavelengths. Thermal fluctuations with energy $\epsilon \sim T$, where T is temperature, would lead to Goldstone modes with a wavelength $\lambda \sim T^{-\frac{1}{2}}$ fluctuating the order parameter.

These Goldstone modes are the primary contributors to the long wavelength fluctuations of the order parameter during phase transitions. The presence of new Goldstone modes after a phase transition can give the new phases profoundly different properties. To calculate the number of Goldstone modes that appear in each phase, we need to count the 'number' of symmetries broken. Each symmetry broken corresponds to an independent Goldstone mode. Goldstone's theorem tells us the number of Goldstone modes is given by

$$N = n(G) - n(H), \tag{2.40}$$

where N is the number of Goldstone modes, $n(G)$ is the number of generators of the system's symmetry G, and $n(H)$ is the number of generators of the residual symmetry of the system. The number of generators of a group is no different than the concept of the dimension in a manifold. In fact, if we view each Lie group as a manifold, the number of generators is the same as its dimension. For example, $U(1)$ can be seen as a one-dimensional circle as a manifold; therefore, it has only one generator. We can then see that when the product of multiple groups is taken, their number of generators is summed. We can now find the value of the number of Goldstone modes

in each phase. For ^{3}He-A we have

$$N_A = n(G) - n(H_A), \tag{2.41}$$

and for ^{3}He-B we have

$$N_B = n(G) - n(H_B), \tag{2.42}$$

where G, H_A and H_B are given in eq. (2.14), eq. (2.22) and eq. (2.17), respectively. We can see that

$$n(G) = 2 \times n\left(SO(3)\right) + n\left(U(1)\right) = 2 \times 3 + 1 = 7, \tag{2.43}$$

and

$$n(H_A) = n\left(SO(2)\right) + n\left(U(1)\right) = 1 + 1 = 2, \tag{2.44}$$

and finally

$$n(H_B) = n\left(SO(3)\right) = 3. \tag{2.45}$$

It follows that $N_A = 5$ and $N_B = 4$. We can also approach this calculation by the use of our inverse propagator. The eigenvalues of the propagator are the dispersion relations $\epsilon(q)$ of the collective modes. Since the inverse propagator is 18 dimensional, there are 18 collective modes. The Goldstone modes can be identified with having $\epsilon(q = 0) = 0$, where $\epsilon(q)$ is the inverse propagator's eigenvalue. The eigenvalue tells us about each collective mode's energy as a function of momentum. Note that the eigenvalues of a local minimum should all be greater than or equal to zero; otherwise, we have found an incorrect minimum for our free energy. We can confirm that we get the same number N_A and N_B through the use of the propagator in section 2.4, and we can see the dispersion relations of the collective modes plotted in fig. 2.4.

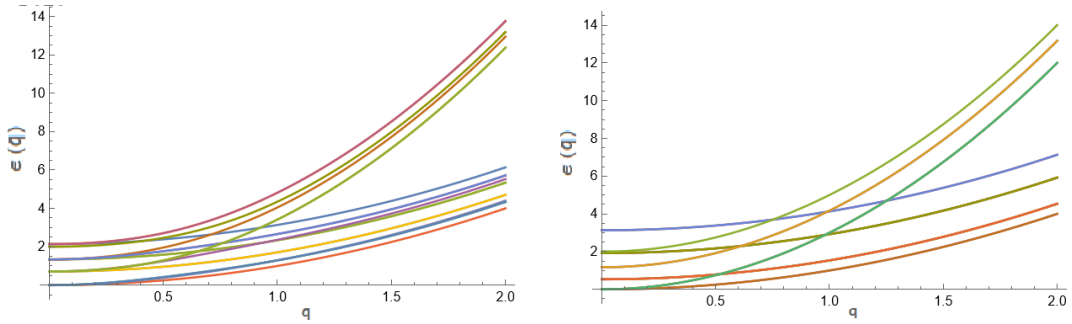

(a) (b)

Figure 2.4: **Collective modes of ^{3}He.** The eigenvalues ϵ of the propagator as a function of momentum q, with $\gamma = 1$. The colouring scheme is to help distinguish between various eigenvalues. The weak-coupling values were used for the coupling constants. a) The collective modes of the A phase. b) The collective modes of the B phase.

Phase	Eigenvalue $\epsilon(q=0)$	Degeneracy
^{3}He-A	0	5
	$\frac{2(\beta_1+\beta_3)}{\beta_{245}}$	2
	$\frac{(\beta_3-\beta_4-\beta_5)}{\beta_{245}}$	4
	$\frac{-2\beta_4}{\beta_{245}}$	2
	$\frac{-(\beta_4+\beta_5)}{\beta_{245}}$	4
	2	1
^{3}He-B	0	4
	$-\frac{6\beta_1}{3\beta_{12}+\beta_{345}}$	5
	$-\frac{2(3\beta_1+\beta_2-\beta_4+\beta_5)}{3\beta_{12}+\beta_{345}}$	3
	$\frac{2(\beta_3+\beta_4+\beta_5)}{3\beta_{12}+\beta_{345}}$	5
	2	1

Table 2.1: The eigenvalues at $q = 0$ of the 18 possible modes in both ^{3}He-B and ^{3}He-B. We set $\alpha = -1$ for convenience. The degeneracy is the number of modes that share the same $\epsilon(q = 0)$. We find 5 Goldstone modes in ^{3}He-A and 4 for ^{3}He-B as expected.

2.5 2D Ginzburg-Landau Theory

We can apply the principles of GL theory to derive a quasi-two-dimensional theory of He-3. When confined to the quasi-2D regime, our 3D symmetry group reduces to a confined quasi-2D symmetry group given by

$$G_{2D} = SO(2)_{L_z} \times SO(3)_S \times U(1). \tag{2.46}$$

Here, we assume the confinement is enough to restrict the Cooper pairs' motion in the direction of their confinement, leading the $SO(3)_L$ symmetry to become $SO(2)_{L_z}$. The quasi-2D symmetry group allows us to introduce new terms in our Ginzburg-Landau Theory that are not included in the 3D free energy. For example, we could try to consider terms like $\alpha_1 \left(\mathrm{A}_{21}\mathrm{A}^*_{12} + \mathrm{A}_{23}\mathrm{A}^*_{11}\right)$ or $\beta_6 \mathrm{A}_{11}\mathrm{A}_{31}\mathrm{A}_{32}\mathrm{A}_{33}$, but we have to check if they are invariant terms. We would ideally like to find every single possible term that is invariant under our new symmetry that is second or fourth order. We will start by examining second-order terms.

Since we have a $U(1)$ symmetry A and A^* must appear equally like in $\mathrm{A}_{11}\mathrm{A}^*_{12}$. We also know that the spin symmetry is still the same as in the 3D case, which tells us the spin indices of the two order parameter components multiplied must be the same as it is in the 2D case. Under these considerations, we can see the most general second-order invariant to be the linear combination of quadratic terms, which can be written as

$$M^L_{ab}\mathrm{A}_{\alpha a}\mathrm{A}^*_{\alpha b}. \tag{2.47}$$

Here, we sum over repeated indices. M^L_{ab} can be thought of as coefficients that scale each quadratic term. Next, we must check which conditions M^L needs to obey for eq. (2.47) to be invariant under our symmetries.

In the 3D case, we need the term to be invariant under the action of any element $R \in SO(3)_L$. If eq. (2.47) is invariant then

$$M^L_{ab}R_{ac}A_{\alpha c}R_{bd}\mathrm{A}^*_{\alpha d} = M^L_{ab}\mathrm{A}_{\alpha a}\mathrm{A}^*_{\alpha b} \tag{2.48}$$

must hold true. We can relabel indices, remove the order parameter components common to both sides and write this in the matrix form

$$R^T M^L R = M^L. \tag{2.49}$$

Therefore M^L must be a matrix that is invariant under all rotations, which is only true for scalar multiples of the identity matrix. We can now substitute back in $M^L = \alpha \cdot \mathbb{I}$ into eq. (2.47) and get

$$M^L_{ab} \mathrm{A}_{\alpha a} \mathrm{A}^*_{\alpha b} = \alpha \delta_{ab} \mathrm{A}_{\alpha a} \mathrm{A}^*_{\alpha b} = \alpha \sum_{\mu i} \mathrm{A}_{\mu i} \mathrm{A}^*_{\mu i} = \alpha \mathrm{tr}(A A^\dagger). \tag{2.50}$$

Here, α is an arbitrary real constant, and δ_{ab} is the usual Kronecker delta. This gives us back the expected second-order invariant in our 3D free energy. What we have proven is that eq. (2.50) is the only quadratic form that is invariant under the 3D symmetry group G.

When restricted to the confined symmetry, M^L has more freedom. Let us apply an $SO(2)_{L_z}$ transformation T to our quadratic form in A, and enforce that the form remains invariant. Elements of $SO(2)_{L_z}$ are rotations about the z-axis. They have the form

$$T = \begin{pmatrix} \sin\theta & -\cos\theta & 0 \\ \cos\theta & \sin\theta & 0 \\ 0 & 0 & 1 \end{pmatrix}. \tag{2.51}$$

Then, for an expression to be invariant under our quasi-2D symmetry group, it must satisfy

$$M^L_{ab} T_{ai} T_{bj} \mathrm{A}_{\alpha i} \mathrm{A}^*_{\beta j} = M^L_{ij} \mathrm{A}_{\alpha i} \mathrm{A}^*_{\beta j}, \tag{2.52}$$

which implies

$$M^L_{ab} T_{ai} T_{bj} = M^L_{ij} \implies T^T M^L T = M^L. \tag{2.53}$$

Solving this equation, we can see that

$$M^L = \begin{pmatrix} \alpha_1 & \alpha_3 & 0 \\ -\alpha_3 & \alpha_1 & 0 \\ 0 & 0 & \alpha_2 \end{pmatrix}. \tag{2.54}$$

However, this term breaks time-reversal symmetry $\mathcal{T}$ when α_3 is non-zero. So finally, we have

$$M^L = \begin{pmatrix} \alpha_1 & 0 & 0 \\ 0 & \alpha_1 & 0 \\ 0 & 0 & \alpha_2 \end{pmatrix}. \tag{2.55}$$

Now we can see that the quadratic invariants look like

$$\sum_{\mu=1}^{3} \left[\alpha_1 \sum_{i=1,2} \mathrm{A}_{\mu i} \mathrm{A}^*_{\mu i} + \alpha_2 \sum_{i=3} \mathrm{A}_{\mu i} \mathrm{A}^*_{\mu i} \right] \tag{2.56}$$

in the quasi-2d regime. Let us define two new matrices

$$\mathrm{A}_\perp = \begin{pmatrix} \mathrm{A}_{1,1} & \mathrm{A}_{1,2} \\ \mathrm{A}_{2,1} & \mathrm{A}_{2,2} \\ \mathrm{A}_{3,1} & \mathrm{A}_{3,2} \end{pmatrix}, \tag{2.57}$$

and

$$\mathrm{A}_z = \begin{pmatrix} \mathrm{A}_{1,3} \\ \mathrm{A}_{2,3} \\ \mathrm{A}_{3,3} \end{pmatrix}. \tag{2.58}$$

The quasi-2D quadratic invariants can be more easily written down as

$$\alpha_1 \mathrm{tr}(\mathrm{A}_\perp \mathrm{A}_\perp^\dagger) + \alpha_2 \mathrm{tr}(\mathrm{A}_z \mathrm{A}_z^\dagger). \tag{2.59}$$

We can see that there are now two independent mass terms, but only one of these can change signs first. The coupling constant that changes sign first will drive the phase transition, and the other term can be ignored near the superfluid phase transition. Using the microscopic physics of ^{3}He, it can be determined that α_1 drives the phase transition [25]. Finally, our new quadratic invariant is

$$\alpha \mathrm{tr}(\mathrm{A}_\perp \mathrm{A}_\perp^\dagger). \tag{2.60}$$

$\mathrm{A}_\perp$ is our new order parameter.

Now we see if we can introduce new quartic invariants of the form

$$M_{\alpha\beta\gamma\delta abcd} \mathrm{A}_{\alpha a} \mathrm{A}_{\beta b} \mathrm{A}^*_{\gamma c} \mathrm{A}^*_{\delta d}. \tag{2.61}$$

I	$M_{\alpha\beta\gamma\delta abcd}$
$\mathrm{tr}(AA^\dagger)^2$	$\delta_{\alpha\gamma}\delta_{\beta\delta}\delta_{ac}\delta_{bd} + \delta_{\alpha\delta}\delta_{\beta\gamma}\delta_{ad}\delta_{bc}$
$\lvert\mathrm{tr}(AA^T)\rvert^2$	$\delta_{\alpha\beta}\delta_{\gamma\delta}\delta_{ab}\delta_{cd}$
$\mathrm{tr}(AA^TA^*A^\dagger)$	$\delta_{\alpha\gamma}\delta_{\beta\delta}\delta_{ab}\delta_{cd} + \delta_{\alpha\delta}\delta_{\beta\gamma}\delta_{ab}\delta_{cd}$
$\mathrm{tr}(AA^\dagger A^*A^T)$	$\delta_{\alpha\beta}\delta_{\gamma\delta}\delta_{ac}\delta_{bd} + \delta_{\alpha\beta}\delta_{\gamma\delta}\delta_{ad}\delta_{bc}$
$\mathrm{tr}(AA^\dagger AA^\dagger)$	$\delta_{\alpha\gamma}\delta_{\beta\delta}\delta_{ac}\delta_{bd} + \delta_{\alpha\delta}\delta_{\beta\gamma}\delta_{ac}\delta_{bd}$

Table 2.2: Invariants and their M-tensors

Here the $U(1)$ symmetry enforces that we must have equally many A's and A*'s in each term in the invariant. In the 3D free energy, the five quartic invariants can be derived using the same techniques as before. A table of invariants and their corresponding M-tensor is provided in table 2.2.

Intuitively, our results in the quasi-2D case should look similar to table 2.2, but while separating terms involving A_z and $A_\perp$, similarly to eq. (2.59).
Let us now consider our matrix M to act trivially on the spin as we did before, and let us restrict our angular momentum interactions. We get

$$M = \mathbb{I}^{\otimes 2} \otimes M^L = \mathbb{I} \otimes \mathbb{I} \otimes P \otimes Q. \tag{2.62}$$

Here, we assumed our tensor M^L could be decomposed into the tensor product of two matrices P and Q. This assumption is supported by the fact that all the terms above are just the sums of terms that can be decomposed in this way. We can write this tensor equation in component form with

$$\implies M_{\alpha\beta\gamma\delta abcd} = \delta_{\alpha\beta}\delta_{\gamma\delta}P_{ab}Q_{cd}. \tag{2.63}$$

Now we apply a $SO(2)_{L_z}$ rotation T to our order parameter A and impose invariance under quasi-2D symmetry and get

$$P_{ab}Q_{cd}T_{ai}T_{bj}T_{ck}T_{d\ell}\mathrm{A}_{\alpha i}\mathrm{A}_{\alpha j}\mathrm{A}^*_{\gamma k}\mathrm{A}^*_{\gamma \ell} = P_{ij}Q_{k\ell}\mathrm{A}_{\alpha i}\mathrm{A}_{\alpha j}\mathrm{A}^*_{\gamma k}\mathrm{A}^*_{\gamma \ell}. \tag{2.64}$$

This simplifies to

$$\implies [TPT^T] \otimes [TQT^T] = P \otimes Q, \tag{2.65}$$

which gives similar results as eq. (2.55). We can use one of the 3D quartic terms to derive what the quartic term would decompose into in the quasi-2D case as follows:

$$\beta_1 \mathrm{tr}(\mathrm{A}\mathrm{A}^\dagger)^2 = \beta_1 \sum_{\mu\nu}\sum_{ij} \mathrm{A}_{\mu i}\mathrm{A}^*_{\mu i}\mathrm{A}_{\nu j}\mathrm{A}^*_{\nu j} \longrightarrow \tag{2.66}$$

$$\begin{aligned}\sum_{\mu\nu}\Bigg[&\beta_{1,1}\sum_{ij=1,2}\mathrm{A}_{\mu i}\mathrm{A}^*_{\mu i}\mathrm{A}_{\nu j}\mathrm{A}^*_{\nu j} + \beta_{1,2}\sum_{i=1,2/j=3}\mathrm{A}_{\mu i}\mathrm{A}^*_{\mu i}\mathrm{A}_{\nu j}\mathrm{A}^*_{\nu j}\\ &+\beta_{1,3}\sum_{i=3/j=1,2}\mathrm{A}_{\mu i}\mathrm{A}^*_{\mu i}\mathrm{A}_{\nu j}\mathrm{A}^*_{\nu j} + \beta_{1,4}\sum_{ij=3}\mathrm{A}_{\mu i}\mathrm{A}^*_{\mu i}\mathrm{A}_{\nu j}\mathrm{A}^*_{\nu j}\Bigg]\end{aligned} \tag{2.67}$$

We can divide the quasi-2D GL free energy, F_{2D} into three parts based on the appearance of $\mathrm{A}_\perp$ and A_z as

$$F_{2D} = F_{\perp\perp} + F_{\perp z} + F_{zz}, \tag{2.68}$$

where the parts of the free energy can be defined as

$$\begin{aligned}F_{2D} = \alpha\mathrm{tr}(\mathrm{A}_\perp\mathrm{A}^\dagger_\perp) + \beta_1|\mathrm{tr}(\mathrm{A}_\perp\mathrm{A}^T_\perp)|^2 + \beta_2[\mathrm{tr}(A_\perp A^\dagger_\perp)]^2\\ +\beta_3\mathrm{tr}(A_\perp A^T_\perp A^*_\perp A^\dagger_\perp) + \beta_4\mathrm{tr}(A_\perp A^\dagger_\perp A_\perp A^\dagger_\perp) + \beta_5\mathrm{tr}(A_\perp A^\dagger_\perp A^*_\perp A^T_\perp)\end{aligned} \tag{2.69}$$

$$F_{zz} = \sigma_1\mathrm{tr}(A_z A^\dagger_z) + \rho_1|\mathrm{tr}(\mathrm{A}_z\mathrm{A}^T_z)|^2 + \rho_2[\mathrm{tr}(\mathrm{A}_z\mathrm{A}^\dagger_z)]^2. \tag{2.70}$$

$F_{\perp z}$ can be constructed similarly by taking the cross terms between $A_\perp$ and A_z. Since the $A_\perp$ mass term changes sign first, both F_{zz} and $F_{\perp z}$ are not relevant to the phase transition since A_z does not contribute to the long-range order. That implies our quasi-2D free energy is just the 3D one with the order parameter A replaced with $A_\perp$ as shown below:

$$\begin{aligned}F_{\perp\perp} = \alpha\mathrm{tr}(A_\perp A^\dagger_\perp) + \beta_1|\mathrm{tr}(A_\perp A^T_\perp)|^2 + \beta_2[\mathrm{tr}(A_\perp A^\dagger_\perp)]^2\\ +\beta_3\mathrm{tr}(A_\perp A^T_\perp A^*_\perp A^\dagger_\perp) + \beta_4\mathrm{tr}(A_\perp A^\dagger_\perp A_\perp A^\dagger_\perp) + \beta_5\mathrm{tr}(A_\perp A^\dagger_\perp A^*_\perp A^T_\perp)\end{aligned} \tag{2.71}$$

Not only is the 2D free energy similar to the 2D case, the inverse-propagator is also given by eq. (2.39), with the summation angular momentum indices stopping at $i = j = 2$ rather $i = j = 3$.

2.5.1 2D Order Parameter

Now, we will take our 3×2 order parameter and find the mean-field value of its order parameter through minimization. Conveniently, it happens that in quasi-2D, the A phase is still energetically favourable, as well as a truncated version of the B phase known as the planar phase [25]. In quasi-2D, the order parameter of the planar phase, which is the counterpart to the 3D B phase, looks like

$$A_{2b} = \begin{pmatrix} \Delta_{2b} & 0 \\ 0 & \Delta_{2b} \\ 0 & 0 \end{pmatrix}. \tag{2.72}$$

Then, the free energy is given by

$$F_{2D}[A_{2b}] = 2\alpha\Delta_{2b}^2 + 2(2\beta_{12} + \beta_{345})\Delta_{2b}^4 \tag{2.73}$$

The minimum of this is given by

$$\Delta_{2b}^2 = \frac{-\alpha}{2(2\beta_{12} + \beta_{345})}. \tag{2.74}$$

The A phase is given by

$$A_{2a} = \begin{pmatrix} \Delta_{2a} & i\Delta_{2a} \\ 0 & 0 \\ 0 & 0 \end{pmatrix}, \tag{2.75}$$

or equivalently

$$A_{2a} = \begin{pmatrix} 0 & 0 \\ 0 & 0 \\ \Delta_{2a} & i\Delta_{2a} \end{pmatrix}. \tag{2.76}$$

Then, the free energy is given by

$$F[A_{2a}] = 2\alpha\Delta_{2a}^2 + 4\beta_{245}\Delta_{2a}^4 \tag{2.77}$$

The minimum of this is given by

$$\Delta_{2a}^2 = \frac{-\alpha}{4\beta_{245}} \tag{2.78}$$

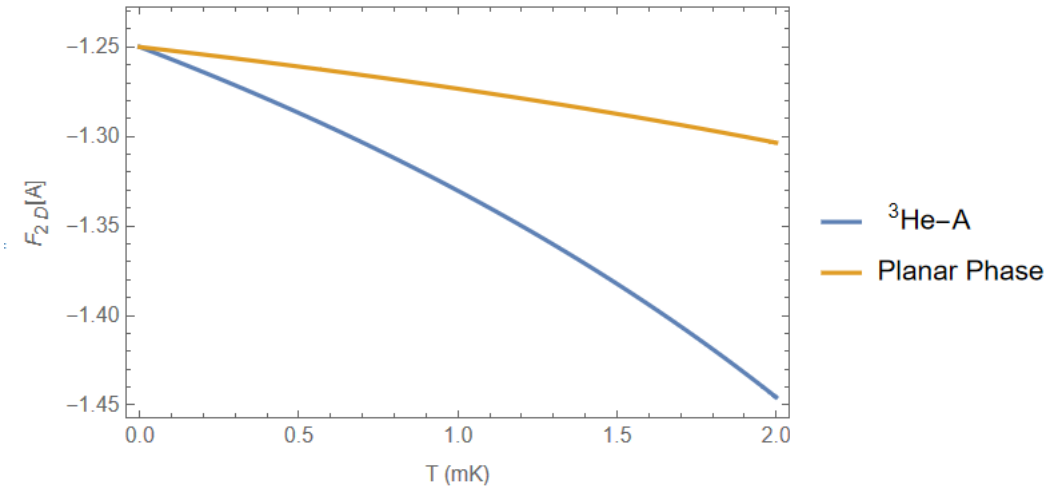

Figure 2.5: **Strong-coupling corrections to 2D free energy.** The free energy of ^{3}He-A and the planar phase under strong-coupling corrections with a pressure of 20 bars. The energy degeneracy between the two phases is broken, and ^{3}He-A is favoured.

For the A phase to dominate over the B phase. We have

$$
\begin{aligned}
& F[A_{2b}] > F[A_{2a}] \\
\implies -\frac{\alpha^2}{2(2\beta_{12}+\beta_{345})} > -\frac{\alpha^2}{4(\beta_{245})} & \implies \frac{\alpha^2}{2(2\beta_{12}+\beta_{345})} < \frac{\alpha^2}{4(\beta_{245})} \\
& \implies \beta_{12} + \frac{1}{2}\beta_{345} > \beta_{245} \\
& \implies C_{AP} = \beta_1 + \frac{1}{2}(\beta_3 - \beta_{45}) > 0. \qquad (2.79)
\end{aligned}
$$

At weak coupling, A phase and B phase have the same free energy

$$F[A_{2a}] = F[A_{2b}] = -\frac{5}{4}, \qquad (2.80)$$

so we have to look beyond the mean-field level and consider fluctuations of the order parameter to decide which of these two phases wins. The degeneracy between the planar and A phase is lifted in the strong-coupling corrections, where the A phase is favoured at all calculated temperatures and pressures, as shown in fig. 2.5 for various temperatures.

Chapter 3

The Renormalization Group

3.1 Introduction

Now that we have analyzed ^{3}He through the lenses of mean-field theory and strong-coupling behaviour, the next step is to observe the effects of fluctuations using RG. In perturbative RG, the contributions of fluctuations to the effective free energy are written in a perturbative series about the weak-coupling free energy. These series are expanded in orders of coupling constants, and each term consists of momentum space integrals, which can be represented as Feynman diagrams. The Trace-Log formula allows us to easily evaluate the sum of all one-loop Feynman diagrams in our Ginzburg-Landau theory. However, the presence of Goldstone modes at all length scales leads to IR divergences of these Feynman diagrams. This leads us to apply a regularization scheme by considering the appropriate length scales of our system and using the Wilsonian RG scheme to identify the effects of fluctuations on the phase transition.

3.1.1 An Overview of the Renormalization Group

RG provides a practical framework for understanding second-order phase transitions. As we approach the critical point, fluctuations in the order parameter become large, and interactions must be considered. The GL free energy describes the effects of these fluctuations and interactions near the phase transition. For a real order parameter

$\phi(x)$, the GL free energy might have the form

$$F[\phi(x)] = \int d^d\mathbf{x} \left[\frac{1}{2}\nabla\left(\phi(\mathbf{x})\right) \cdot \nabla\left(\phi(\mathbf{x})\right) + U(\phi(\mathbf{x}))\right], \tag{3.1}$$

where U is the effective potential, which contains terms constrained by the symmetries of the theory. U generally depends on a number of coupling constants $g = (g_1, g_2 \dots)$. For example, it could take the form

$$U(\phi) = g_1\phi^2 + g_2\phi^4 + \dots \tag{3.2}$$

We fix the gradient term to have a coefficient of $\frac{1}{2}$ for simplicity, but it can be multiplied by a coupling constant called the Wavefunction Renormalization for a more comprehensive analysis. Let us set $\beta = (k_B T)^{-1}$ to unity for simplicity. We are interested in computing the partition function

$$\mathcal{Z} = \int \mathcal{D}\phi e^{-F[\phi]}, \tag{3.3}$$

which is a path integral over the space of order parameters (see appendix B for further discussion). Informally, we can think of the path integral measure as the continuous-infinite product of one-dimensional measures

$$\mathcal{D}\phi = \prod_{\mathbf{k}} d\phi_{\mathbf{k}} \tag{3.4}$$

Our Ginzburg-Landau theory is also no longer valid for momenta higher than our ultraviolet cut-off Λ. Using this cut-off, we can remove UV divergences in our one-loop corrections, but we must use the renormalization group scheme to overcome the IR divergences.

We will use a momentum space renormalization group scheme. We first describe our order parameter in terms of its momentum component rather than its spatial dependence using the Fourier transform

$$\phi_{\mathbf{k}} = \int d^d\mathbf{x}\phi(\mathbf{x})e^{i\mathbf{k}\cdot\mathbf{x}}. \tag{3.5}$$

Let $k = \|\mathbf{k}\|$. We can impose that the Fourier modes $\phi_{\mathbf{k}}$ of the order parameter obey

$$\phi_{\mathbf{k}} = 0 \text{ for } k > \Lambda. \tag{3.6}$$

Now we suppose our system is restricted to a box of finite size, such that the smallest momentum possible in the box is

$$\Lambda' = \frac{\Lambda}{b}, \tag{3.7}$$

for some $b > 1$. This allows us to regularize the IR divergences momentarily. However, we will eventually consider our system at infinite size by taking $b \to \infty$.

Using this regularization scheme, we can break our order parameter into 'short' and 'long' wavelength components.

$$\phi_{\mathbf{k}} = \phi^{<}_{\mathbf{k}} + \phi^{>}_{\mathbf{k}}, \tag{3.8}$$

where $\phi^{<}_{\mathbf{k}}$ are the long wavelength modes given by

$$\phi^{<}_{\mathbf{k}} = \begin{cases} \phi_{\mathbf{k}} & k < \Lambda' \\ 0 & k > \Lambda' \end{cases}, \tag{3.9}$$

and $\phi^{>}_{\mathbf{k}}$ are the short wavelength modes given by

$$\phi^{>}_{\mathbf{k}} = \begin{cases} \phi_{\mathbf{k}} & \Lambda' < k < \Lambda \\ 0 & \text{otherwise} \end{cases} \tag{3.10}$$

We can now decompose our free energy in Fourier space and expand it in terms of these short long wavelength fields as

$$F[\phi_{\mathbf{k}}] = F_0[\phi^{<}_{\mathbf{k}}] + F_0[\phi^{>}_{\mathbf{k}}] + F_I[\phi^{<}_{\mathbf{k}}, \phi^{>}_{\mathbf{k}}], \tag{3.11}$$

where F_0 is the part that only depends on one field, and F_I involves products of the shot and long wavelength fields. Our partition function in terms of these variables is given by

$$\mathcal{Z} = \prod_{k<\Lambda} \int d\phi_{\mathbf{k}} e^{-F} = \prod_{k<\Lambda'} \int d\phi^{<}_{\mathbf{k}} e^{-F_0[\phi^{<}_{\mathbf{k}}]} \left(\prod_{\Lambda'<k<\Lambda} \int d\phi^{>}_{\mathbf{k}} e^{-F_0[\phi^{>}_{\mathbf{k}}] + F_I[\phi^{<}_{\mathbf{k}}, \phi^{>}_{\mathbf{k}}]} \right). \tag{3.12}$$

$$= \int \mathcal{D}\phi^{<} e^{-F_0[\phi^{<}]} \left(\int \mathcal{D}\phi^{>} e^{-F_0[\phi^{>}] + F_I[\phi^{<}, \phi^{>}]} \right) \tag{3.13}$$

$$\equiv \int \mathcal{D}\phi^{<} e^{-F_W[\phi^{<}]} \tag{3.14}$$

We want to evaluate this integral over the short-wavelength modes to obtain the Wilsonian effective free energy, F_W, which is a free energy for the long-wavelength modes. F_W can be written as

$$e^{-F_W[\phi^<]} = e^{-F_0[\phi^<]}\left(\int \mathcal{D}\phi^> e^{-F_0[\phi^>]+F_I[\phi^<,\phi^>]}\right) \tag{3.15}$$

We have not done anything to break the symmetry of the system, so F_W will be of the same form as F with shifted or *renormalized* coupling constants. We write F_W as

$$F_W[\phi^<] = \int d^dx \left[\frac{1}{2}\gamma'(b)\nabla\phi^< \cdot \nabla\phi^< + g_1'(b)\left(\phi^<\right)^2 + g_2'(b)\left(\phi^<\right)^4 + \dots\right]. \tag{3.16}$$

We can see that long wavelength modes 'experience' different coupling constants. The integrals in F_W are bound by $q \leq \Lambda/b$, while the integrals in F are bound by $q \leq \Lambda$. To ensure these two free energies are comparable, we must ensure they have the same limits. We can do this by 'zooming out' by rescaling to momentum and position as follows

$$k \to bk, \quad x \to \frac{x}{b}. \tag{3.17}$$

This ensures the cut-off for F_W, Λ/b, gets rescaled to Λ. However, now the gradient term in F_W is no longer normalized, so we rescale the field $\phi^<$ to get rid of this. We transform the field as

$$\phi'(x') = b^{\frac{2-d}{2}}\sqrt{\gamma'}\phi^<(x). \tag{3.18}$$

This gives us our new free energy in terms of these rescaled fields as

$$F_W[\phi'] = \int d^dx \left[\frac{1}{2}\nabla\phi' \cdot \nabla\phi' + g_1(b)\left(\phi'\right)^2 + g_2(b)\left(\phi'\right)^4 + \dots\right]. \tag{3.19}$$

We can see that we have parameterized a set of theories in terms of b, with our original UV theory being at $b = 1$, and the IR theory at $b = \infty$. Any set of renormalized coupling constants will take the form

$$g_i(b) = b^{\mathcal{O}_i}\Big(g_i(0) + \delta g_i(b)\Big), \tag{3.20}$$

where $\mathcal{O}_i$ is the scaling of the coupling constant g_i, $g_i(0)$ is the initial value of the coupling constant (the mean-field value in our case), and $\delta g_i(b)$ are corrections to

the coupling constants. $\mathcal{O}_i$ plays an important role in determining the importance of coupling constants. When $\mathcal{O}_i < 0$, then g_i is referred to as an *irrelevant* coupling because as b approaches infinity, the renormalized coupling constant will decay to zero, indicating the coupling constant is not relevant for the phase transition of interest. When $\mathcal{O}_i = 0$, g_i is referred to as *marginal* and if $\mathcal{O}_i > 0$, then g_i is a *relevant* coupling constant. We are only interested in considering relevant coupling to the flow, and in $d = 4$, any terms of higher order than quartic terms turn out to be irrelevant. This is why we truncated our free energy to the fourth order.

Because we usually cannot solve for these renormalized coupling constants directly, we can define a set of differential equations, called the flow equations, that have the form

$$\frac{\mathrm{d}g_i(b)}{\mathrm{d}\ln b} = B_{g_i}(g_1, g_2, \dots), \tag{3.21}$$

where $\{g_i\}$ are the set of coupling constants, and B_{g_i} is called the beta functions for the coupling constant g_i. We can view renormalization as a 'flow' in the space of coupling constants. For an infinitely sized system, we aim to solve these equations for the flow of the renormalized coupling constants at $\ln b \to \infty$, while for a finite system, we will see that we must stop at some finite b_f determined by the size of the system. The initial conditions of the coupling constants at $\ln b = 0$ are determined by mean-field theory. The coupling constants will begin with their mean-field values and slowly add longer and longer fluctuations as b increases, eventually including fluctuations of all wavelengths.

As b flows to infinity, the coupling constants may approach a fixed point. A fixed point corresponds to a free energy with special values for its coupling constants such that they remain unchanged under the renormalization group flow defined in eq. (3.21). The correlation length of the system, ξ, can have two possible fixed points under the rescaling $\xi \to \frac{\xi}{b}$: either $\xi = 0$ or $\xi = \infty$. At $\xi = 0$, the system is uncorrelated and uninteresting. At $\xi = \infty$, we have fluctuations at all length scales, and the free energy becomes scale-invariant. Second-order phase transitions correspond

to stable fixed points.

The stability of a fixed point $g_\star = (g_{1\star}, g_{2\star}, \dots)$ is determined by computing its stability matrix

$$M_{ij} = \frac{\partial B_{g_i}}{\partial g_j}\Big|_{g=g_\star}. \tag{3.22}$$

This matrix must have purely negative eigenvalues for an infrared-stable fixed point. When the coupling constants of a free energy are sufficiently close to a stable fixed point, or within its 'basin of attraction', the couplings will flow to that fixed point under RG. Every theory also has a Gaussian fixed point, which corresponds to all coupling constants being zero, and this is a repulsive fixed point with entirely positive eigenvalues.

We can also numerically solve for the running of the coupling constants themselves to understand the phase transition. This can be especially useful when we cannot find a stable fixed point but still have access to theoretical mean-field values. We can substitute the values of the renormalized coupling constants at the end of our flow back into our free energy to obtain our renormalized free energy. The minimum of the free energy will determine the phase that is favoured after considering fluctuations up to a length scale $\lambda_{typ} \sim \frac{b}{\Lambda}$.

3.1.2 Trace-log formula

The trace-log formula provides an easy way to integrate over the slow modes up to one-loop order for constant order parameters $\phi(\mathbf{x}) = \phi$ [20]. We start by writing the trace-log formula

$$\Delta U = \frac{1}{2}\int_{\mathbf{q}} \operatorname{tr}\log \mathcal{G}^{-1}(\phi, \mathbf{q}), \tag{3.23}$$

where $\mathcal{G}(\phi, q)$ is the propagator in momentum space and can be decomposed as

$$\mathcal{G}^{-1}(\phi, \mathbf{q}) = \mathcal{G}_0^{-1}(\mathbf{q}) + \mathcal{V}(\phi), \tag{3.24}$$

where $\mathcal{G}_0(q)$ is independent of the order parameter, and $\mathcal{V}(\phi)$ is independent of momentum $\mathbf{q}$. The trace-log formula is valid only for small quartic couplings; However,

the scaling dimension of quartic couplings is $\mathcal{O} = 4 - d$, and the couplings will grow out of the perturbative regime quickly for $d < 4$. Additionally, the quartic coupling constants must have relevant scaling to consider the effects of interactions, and this only occurs when $d < 4$. The solution is to consider RG 'close' to 4 dimensions. We use a parameter $\epsilon = 4 - d$ to regulate our integrals, where $\epsilon \ll 1$.

These integrals often have infrared and ultraviolet divergences. The UV divergence is taken care of by restricting the integrals to momenta with magnitudes less than Λ. To alleviate the IR divergence around $\mathbf{q} = 0$, we introduce an RG parameter b, and integrate momentum shells with $q \in \left[\frac{\Lambda}{b}, \Lambda\right]$, and take the limit as b approaches ∞ will approach the IR divergence more closely. We use the notation

$$\int_{\mathbf{q}}'(\dots) = \int_{\Lambda/b}^{\Lambda} \mathrm{d}^d\mathbf{q}(\dots) = \int_{\Lambda/b}^{\Lambda} \mathrm{d}q \int_{S^{d-1}} \mathrm{d}\Omega\Big[q^{d-1}(\dots)\Big] \tag{3.25}$$

for momentum shell integration. Here, Ω represents the angular coordinates over the $d-1$ dimensional sphere S^{d-1}. Integration over the momentum shells gives us progressive corrections to the effective potential

$$\delta U(b) = \frac{1}{2}\int_{\mathbf{q}}' \mathrm{tr}\log\mathcal{G}^{-1}(\phi, q). \tag{3.26}$$

However, our goal is to determine the corrections to the individual coupling constants. Luckily, we can take derivatives of our effective potential to extract coupling constants [20]. For example, in ^{3}He

$$\frac{\partial^2}{\partial \mathrm{A}_{1,1}\partial \mathrm{A}^*_{1,1}}\bigg|_{A=0} U(\mathrm{A}) = \alpha \tag{3.27}$$

for both the 3D and 2D effective potentials. We can do this for all the other coupling constants as well and obtain an operator $\hat{P}_i$ for each coupling constant such that

$$\hat{P}_i\Big|_{\mathrm{A}=0} U(\phi) = g_i. \tag{3.28}$$

These operators must be a linear combination of derivatives in the order parameter [20]. We can use these to get fluctuation corrections to the coupling constants

$$\delta g_i(b) = \hat{P}_i \delta U(\phi) = \frac{1}{2}\int_{\mathbf{q}}' \mathrm{tr}\ \hat{P}_i\Big|_{\phi=0} \log\mathcal{G}^{-1}(\phi, q). \tag{3.29}$$

Calculating $\mathcal{G}(\phi, q)$ is very computationally intensive, so alternatively, we use algebra to calculate the derivatives of the matrix-logarithm (see appendix B). If we assume that $\hat{P}_i$ took on the simplest possible form and this ϕ is a complex matrix order parameter, then

$$\hat{P}_i = \frac{\partial^4}{\partial\phi_{\mu,i}\partial\phi_{\nu,j}\partial\bar{\phi}_{\rho,k}\partial\bar{\phi}_{\sigma,l}}, \tag{3.30}$$

then

$$\begin{aligned}\delta g_i = \frac{1}{2}\mathrm{tr}\int_{\mathbf{q}}^{'} \mathcal{G}_0\frac{\partial^2\mathcal{V}}{\partial\phi_{\mu,i}\partial\phi_{\nu,j}}\mathcal{G}_0\frac{\partial^2\mathcal{V}}{\partial\bar{\phi}_{\rho,k}\partial\bar{\phi}_{\sigma,l}} \\ +\mathcal{G}_0\frac{\partial^2\mathcal{V}}{\partial\phi_{\mu,i}\partial\bar{\phi}_{\rho,k}}\mathcal{G}_0\frac{\partial^2\mathcal{V}}{\partial\phi_{\nu,j}\partial\bar{\phi}_{\sigma,l}} + \mathcal{G}_0\frac{\partial^2\mathcal{V}}{\partial\phi_{\mu,i}\partial\bar{\phi}_{\sigma,l}}\mathcal{G}_0\frac{\partial^2\mathcal{V}}{\partial\bar{\phi}_{\rho,k}\partial\phi_{\nu,j}}.\end{aligned} \tag{3.31}$$

We obtain our RG equations as a system of differential equations by taking derivatives with respect to the RG parameter $t = \ln b$.

Once we have our RG equations, we can integrate them numerically using various methods, such as the Runge-Kutta method. Since we are using a system of finite size, we must stop our integration when the RG parameter b is at some final b_f value. The RG parameter allows us to limit fluctuations to a maximum wavelength of $\lambda_{max} \sim b/\Lambda$, whereas a system will only allow fluctuations as large as its length L, assuming our system is a cube with side length L. As $b \to \infty$, we start including fluctuations that cannot fit in our finite system. Instead of stopping our flow at $b = \infty$, which corresponds to an infinite system size, we should rather stop our flow at $b_f \sim L\Lambda$.

3.2 Renormalization Group Example

As an introductory example, we will calculate the RG flow of a complex scalar order parameter $\phi(x)$ with $U(1)$ symmetry and d spatial dimensions. We will approach it without using the trace-log formula to illustrate the intricacies of Wilsonian RG better. The free energy of this theory is given by

$$F_{GL}[\phi] = \int d^d x \left(\frac{1}{2}|\nabla\phi|^2 + U(\phi(x))\right), \tag{3.32}$$

with

$$U(\phi) = \alpha|\phi|^2 + \frac{\lambda}{2}|\phi|^4. \tag{3.33}$$

We take the Fourier transform of the free energy, with

$$\phi(x) = \int \frac{d^d k}{(2\pi)^d} \phi_k e^{-ikx}, \tag{3.34}$$

and this allows us to write the free energy as

$$\begin{aligned} F_{GL}[\phi] = &\int_0^\Lambda d^d q \left(q^2 + \alpha\right) \phi_k \phi_k^* \\ &+ \frac{\lambda}{2} \int_0^\Lambda \frac{d^d k_1 d^d k_2 d^d k_3 d^d k_4}{(2\pi)^{3d}} \delta(k_1 + k_2 - k_3 - k_4) \phi_{k_4}^* \phi_{k_3}^* \phi_{k_2} \phi_{k_1}. \end{aligned} \tag{3.35}$$

We break the field ϕ into long wavelength modes $\phi^<$, and short-wavelength modes $\phi^>$ with

$$\phi_k = \phi_k^< + \phi_k^>. \tag{3.36}$$

We can substitute eq. (3.36) into eq. (3.35), and seperate the free energy as follows

$$F[\phi] = F_0[\phi^<] + F_0[\phi^>] + F_I[\phi^<, \phi^>]. \tag{3.37}$$

Here F_0 is the same as F_{GL}, which describes the energy of the slow and fast modes independently. F_I describes the integration energy between the slow and fast modes, and is described by an expression of 16 terms. Before we write out F_I, we can conveniently throw out some of its terms by taking advantage of some properties of Gaussian Integrals (see appendix A). We can throw away all terms that have an odd power in the fields $\phi^<$ and $\phi^>$, because they will have zero contribution to the path integral. This includes terms like $\phi_{k_1}^{*<} \phi_{k_2}^{*<} \phi_{k_3}^< \phi_{k_4}^>$. Our aim is to solve for the effective action of the long wavelength modes which is given by

$$e^{-F_W[\phi_k^<]} = e^{-F_0[\phi_k^<]} \int \mathcal{D}\phi_k^> e^{-F_0[\phi_k^>]} e^{-F_I[\phi_k^>, \phi_k^<]}, \tag{3.38}$$

which involves integrating out all the short wavelength modes. This can be rewritten in a condensed notation as

$$e^{-F_W[\phi_k^<]} = e^{-F_0[\phi_k^<]} Z_0^> \left\langle e^{-F_I[\phi_k^>, \phi_k^<]} \right\rangle_>, \tag{3.39}$$

where $\langle\cdot\rangle_>$ is a Gaussian integration over the short wavelength modes $\phi_k^>$ (see appendix A). We can pick a normalization of our path integrals such that $\langle 1\rangle_> = Z_0^> = 1$. We can further write the effective free energy as

$$F_W[\phi_k^<] = F_0[\phi^<] - \log\left\langle e^{-F_I[\phi_k^>,\phi_k^<]}\right\rangle_> . \tag{3.40}$$

This can be expanded in powers of F_I

$$\log\left\langle e^{-F_I[\phi_k^>,\phi_k^<]}\right\rangle_> = \log\left\langle 1 - F_I + \frac{1}{2}F_I^2 + \dots \right\rangle_> \tag{3.41}$$

$$= \left\langle 1 - F_I + \frac{1}{2}F_I^2 + \dots \right\rangle_> + \frac{1}{2}\left\langle 1 - F_I\right\rangle_>^2 \tag{3.42}$$

$$= -\left\langle F_I\right\rangle_> + \frac{1}{2}\left[\left\langle F_I^2\right\rangle - \left\langle F_I\right\rangle^2\right] + \dots . \tag{3.43}$$

We can expand our Wilson effective free energy in orders of λ as

$$F_W[\phi_k^<] = F_0[\phi^<] + \left\langle F_I\right\rangle_> - \frac{1}{2}\left[\left\langle F_I^2\right\rangle - \left\langle F_I\right\rangle^2\right] + O(\lambda^3) \tag{3.44}$$

We will compute F_W up to the first order in λ. We must first solve for $\left\langle F_I\right\rangle_>$, where F_I is expanded into 16 terms in terms of $\phi_k^<$ and $\phi_k^>$ and their complex conjugates. We can now apply properties of Gaussian integrals seen in appendix A to get the following identities for our calculations:

$$\langle\phi_{k_1}\phi_{k_2}^*\rangle = G^{-1}(\phi = 0, k_1 - k_2) = \frac{(2\pi)^d}{k_1^2 + \alpha}\delta(k_1 - k_2), \tag{3.45}$$

$$\langle\phi_{k_2}^*\rangle = \langle\phi_{k_2}\rangle = \langle\phi_{k_1}^*\phi_{k_2}\phi_{k_3}\rangle = 0, \tag{3.46}$$

$$\langle\phi_{k_3}^*\phi_{k_4}^*\phi_{k_2}\phi_{k_1}\rangle = \langle\phi_{k_1}\phi_{k_3}^*\rangle\langle\phi_{k_2}\phi_{k_4}^*\rangle + \langle\phi_{k_2}\phi_{k_3}^*\rangle\langle\phi_{k_3}\phi_{k_4}^*\rangle. \tag{3.47}$$

When we expand $\left\langle F_I\right\rangle_>$in terms of the long and short wavelength modes, we will see only certain terms contribute. Firstly, there must be an even number of $\phi^>$ in a term for it to be non-zero. Secondly, terms with four short wavelength modes, such as $\phi_{k_3}^{*>}\phi_{k_4}^{*>}\phi_{k_2}^>\phi_{k_1}^>$ will contribute an overall constant that we can ignore for our purposes. Terms with 4 $\phi_{k_3}^{*<}\phi_{k_4}^{*<}\phi_{k_2}^<\phi_{k_1}^<$, trivially come out of the integral and reproduce the original quartic term. The terms we are interested in, therefore, must have only two

short and two long wavelength fields, with only one of the short wavelength fields complex conjugated. For example, terms like $\phi^{*<}_{k_4}\phi^{*>}_{k_3}\phi^{>}_{k_2}\phi^{<}_{k_1}$. There are 4 such terms, and they contribute equally. Our correction to the effective energy is given by

$$4\frac{\lambda}{2}\int_0^{\Lambda/b}\frac{d^dk_1d^dk_2d^dk_3d^dk_4}{(2\pi)^{3d}}\delta(k_1+k_2-k_3-k_4)\phi^{*<}_{k_4}\langle\phi^{*>}_{k_3}\phi^{>}_{k_2}\rangle_>\phi^{<}_{k_1} \tag{3.48}$$

$$=4\frac{\lambda}{2}\int_0^{\Lambda/b}\frac{d^dk_1d^dk_2d^dk_3d^dk_4}{(2\pi)^{2d}}\frac{\delta(k_1+k_2-k_3-k_4)\delta(k_3-k_2)\phi^{*<}_{k_4}\phi^{<}_{k_1}}{k_2^2+\alpha} \tag{3.49}$$

$$=4\frac{\lambda}{2}\int_0^{\Lambda/b}\frac{d^dk_1d^dk_2d^dk_3}{(2\pi)^{2d}}\frac{\delta(k_3-k_2)\phi^{*<}_{k_1+k_2-k_3}\phi^{<}_{k_1}}{k_2^2+\alpha} \tag{3.50}$$

$$=4\frac{\lambda}{2}\int_0^{\Lambda/b}\frac{d^dk_1d^dk_2}{(2\pi)^{2d}}\frac{\phi^{*<}_{k_1}\phi^{<}_{k_1}}{k_2^2+\alpha}, \tag{3.51}$$

which can be written as

$$=4\frac{\lambda}{2(2\pi)^{3d}}\int_0^{\Lambda/b}d^dk\phi^{*<}_k\phi^{<}_k\int_{\Lambda/b}^{\Lambda}d^dq\frac{1}{q^2+\alpha}, \tag{3.52}$$

which only corrects the second-order term (mass term, appendix on path integrals). We can write F_W as

$$F_W[\phi^<_k]=\int_0^{\Lambda/b}\frac{d^dk}{(2\pi)^d}\left(k^2+\alpha+4\frac{\lambda}{2(2\pi)^d}\int_{\Lambda/b}^{\Lambda}d^dq\frac{1}{q^2+\alpha}\right)\phi^<_k\phi^{*<}_k \tag{3.53}$$

$$+\frac{\lambda}{2}\int_0^{\Lambda/b}\frac{d^dk_1d^dk_2d^dk_3d^dk_4}{(2\pi)^{3d}}\delta(k_1+k_2-k_3-k_4)\phi^{*<}_{k_4}\phi^{*<}_{k_3}\phi^{<}_{k_2}\phi^{<}_{k_1}. \tag{3.54}$$

We can rescale the momenta with $k\to bk$ and the field with $\phi^<\to k^{\frac{4-d}{2}}\phi^<$, which makes

$$F_W[\phi^<_k]=\int_0^{\Lambda}b^d\frac{d^dk}{(2\pi)^d}\left(b^2k^2+\alpha+4\frac{\lambda}{2(2\pi)^d}k^{d-2}\int_{\Lambda/b}^{\Lambda}d^dq\frac{1}{q^2+\alpha}\right)b^{4-d}\phi^<_k\phi^{*<}_k \tag{3.55}$$

$$+\frac{\lambda}{2}b^{4-d}\int_0^{\Lambda}\frac{d^dk_1d^dk_2d^dk_3d^dk_4}{(2\pi)^{3d}}\delta(k_1+k_2-k_3-k_4)\phi^{*<}_{k_4}\phi^{*<}_{k_3}\phi^{<}_{k_2}\phi^{<}_{k_1}. \tag{3.56}$$

We can write the renormalized coupling constants

$$\alpha(b)=b^2\left(\alpha+4\frac{\lambda}{2(2\pi)^d}\int_{\Lambda/b}^{\Lambda}d^dq\frac{1}{q^2+\alpha}\right)=b^2\left(\alpha+4\alpha\lambda\ln b\right) \tag{3.57}$$

$$\lambda(b)=b^{4-d}\lambda. \tag{3.58}$$

To get corrections to λ, we must calculate F_W up to order λ^2. We must calculate $\langle F_I^2 \rangle$ which can be expressed as

$$\langle F_I^2 \rangle = \frac{\lambda^2}{2} \int_0^\Lambda \frac{\prod_i dp_i dq_i}{(2\pi)^{6d}} \delta(q_1+q_2-q_3-q_4)\delta(k_1+k_2-k_3-k_4)\langle \phi^*_{q_4}\phi^*_{q_3}\phi_{q_2}\phi_{q_1}\phi^*_{k_4}\phi^*_{k_3}\phi_{k_2}\phi_{k_1}\rangle_> \tag{3.59}$$

We can calculate the expectation value using Wick's theorem. Corrections to $\lambda(b)$ will be of the form

$$\frac{\lambda^2}{2} \int_0^\Lambda \frac{\prod_i dp_i dq_i}{(2\pi)^{6d}} \delta(q_1+q_2-q_3-q_4)\delta(k_1+k_2-k_3-k_4)\phi^{*<}_{q_4}\phi^{*<}_{q_3}\phi^{<}_{q_2}\phi^{<}_{q_1}\langle \phi^{*>}_{k_4}\phi^{*>}_{k_3}\phi^{>}_{k_2}\phi^{>}_{k_1}\rangle_> \tag{3.60}$$

Wick's theorem allows us to decompose our expectation values as

$$\langle \phi^{*>}_{k_4}\phi^{*>}_{k_3}\phi^{>}_{k_2}\phi^{>}_{k_1}\rangle_> = \langle \phi^{*>}_{k_4}\phi^{>}_{k_1}\rangle_>\langle \phi^{*>}_{k_3}\phi^{>}_{k_2}\rangle_> + \langle \phi^{*>}_{k_4}\phi^{>}_{k_2}\rangle_>\langle \phi^{*>}_{k_3}\phi^{>}_{k_1}\rangle_> + \langle \phi^{>}_{k_4}\phi^{>}_{k_2}\rangle_>\langle \phi^{*>}_{k_3}\phi^{*>}_{k_1}\rangle_>. \tag{3.61}$$

$$= \langle \phi^{*>}_{k_4}\phi^{>}_{k_1}\rangle_>\langle \phi^{*>}_{k_3}\phi^{>}_{k_2}\rangle_> + \langle \phi^{*>}_{k_4}\phi^{>}_{k_2}\rangle_>\langle \phi^{*>}_{k_3}\phi^{>}_{k_1}\rangle_> \tag{3.62}$$

which gives us

$$-\frac{\lambda^2}{2} \int_0^{\Lambda/b} \frac{\prod_i dp_i dq_i}{(2\pi)^{6d}} \delta(q_1+q_2-q_3-q_4)\delta(k_1+k_2-k_3-k_4)\phi^{*<}_{q_4}\phi^{*<}_{q_3}\phi^{<}_{q_2}\phi^{<}_{q_1}\times$$
$$\left[16\int_{\Lambda/b}^\Lambda \frac{d\vec{q}}{(2\pi)^d}\frac{1}{(q^2+\alpha)}\frac{1}{((q+k_2-k_4)^2+\alpha)} + 4\int_{\Lambda/b}^\Lambda \frac{d\vec{q}}{(2\pi)^d}\frac{1}{(q^2+\alpha)}\frac{1}{((q-k_1-k_2)^2+\alpha)}\right].$$

The two integrals have the same value, which simplifies our equation to

$$-10\lambda^2 \int_0^{\Lambda/b} \frac{\prod_i dp_i dq_i}{(2\pi)^{6d}} \phi^{*<}_{q_4}\phi^{*<}_{q_3}\phi^{<}_{q_2}\phi^{<}_{q_1}\delta(q_1+q_2-q_3-q_4)\times \tag{3.63}$$

$$\delta(k_1+k_2-k_3-k_4)\left[\int_{\Lambda/b}^\Lambda \frac{d\vec{q}}{(2\pi)^d}\frac{1}{(q^2+\alpha)^2}\right]. \tag{3.64}$$

$$\tag{3.65}$$

Then, we have

$$\tilde{\lambda}(b) = b^{4-d}\left(\tilde{\lambda} - 10\tilde{\lambda}^2 \ln b\right). \tag{3.66}$$

Let $t = \ln b$, where $t = 0$ corresponds to the UV regime while $t = \infty$ is identified with the IR. Our flow becomes

$$\frac{d}{dt}\tilde{\alpha} = 2\tilde{\alpha} - 4\tilde{\alpha}\tilde{\lambda} \tag{3.67}$$

$$\frac{d}{dt}\tilde{\lambda} = \epsilon\tilde{\lambda} - 10\tilde{\lambda}^2 \tag{3.68}$$

when $\ln b \to \infty$, the Wilson-Fisher fixed-point is $\tilde{\alpha}_\star = 0$ and $\tilde{\lambda}_\star = \frac{\epsilon}{10}$. The 2×2 stability matrix at the fixed point

$$M_{ij} = \left.\frac{\partial B_{g_i}}{\partial g_j}\right|_{g=g_\star}, \tag{3.69}$$

with $g = (\tilde{\alpha}, \tilde{\lambda})$ reads

$$M = \begin{pmatrix} 2 - \frac{2\epsilon}{5} & 0 \\ 0 & -\epsilon \end{pmatrix}. \tag{3.70}$$

The eigenvalues of the stability matrix inform us about the stability of a fixed point. Negative eigenvalues correspond to stable directions that result in RG flow heading towards the fixed point, whereas positive eigenvalues correspond to unstable directions, which will result in the flow moving away from the fixed point. M has a positive eigenvalue in the direction of α and a negative eigenvalue associated with λ. This fixed point is stable in the quartic couplings, therefore it corresponds to a second-order phase transition.

3.3 Renormalization Group of ^{3}He

3.3.1 3D System

Understanding the RG analysis in a 3D system is crucial because ^{3}He is experimentally well-understood in that context, allowing us to determine the effectiveness and limitations of RG. We are interested in predicting what phase is favoured during the phase transition and perhaps what kind of phase transition it is. In 3D, we let our

order parameter be the full 3×3 matrix. We use the invariants

$$I_1 = \left|\mathrm{tr}\left(\mathrm{AA^T}\right)\right|^2 \tag{3.71}$$

$$I_2 = \left|\mathrm{tr}\left(\mathrm{AA^\dagger}\right)\right|^2 \tag{3.72}$$

$$I_3 = \mathrm{tr}\left(\mathrm{AA^T A^* A^\dagger}\right) \tag{3.73}$$

$$I_4 = \mathrm{tr}\left(\mathrm{AA^\dagger AA^\dagger}\right) \tag{3.74}$$

$$I_5 = \mathrm{tr}\left(\mathrm{AA^\dagger A^* A^T}\right). \tag{3.75}$$

We assume the Einstein summation convention, so repeated indices are summed over. We define our free energy as

$$F[\mathrm{A}] = \int^{\Lambda} d^3\mathbf{q}\left\{U(\mathrm{A}) + (\gamma - 1) q_i \mathrm{A}^*_{\mu i} q_j \mathrm{A}_{\mu j} + q_i \mathrm{A}^*_{\mu j} q_i \mathrm{A}_{\mu j}\right\}, \tag{3.76}$$

where $\Lambda \sim \sqrt{T}$ is our UV cutoff since it is the smallest fluctuation scale of the Goldstone modes. The effective potential is defined as

$$U(\mathrm{A}) = \alpha \mathrm{tr} \mathrm{AA^\dagger} + \sum_n \beta_n I_n(\mathrm{A}). \tag{3.77}$$

each component of A is complex, so we define it in terms of two real parameters

$$\mathrm{A}_{\mu i} = \frac{1}{\sqrt{2}}\left(\psi_{\mu i} + \bar{\psi}_{\mu i}\right) + \frac{i}{\sqrt{2}}\left(\psi_{\mu i} - \bar{\psi}_{\mu i}\right). \tag{3.78}$$

Using ψ and $\bar{\psi}$ simplifies our analysis by making the propagator a diagonal matrix when $\gamma = 1$. We are interested in calculating the renormalized coupling constants, which will have the form

$$\bar{\beta}_a(b) = b^\epsilon\Big(\bar{\beta}_a(0) + \delta\bar{\beta}_a(b)\Big), \tag{3.79}$$

$\bar{\beta}_a(0)$ is the mean-field value of $\bar{\beta}_a$ and $\delta\bar{\beta}_a(b)$ is the one-loop correction. The scaling dimension of $\bar{\beta}_a$ is $\epsilon = 4 - d = 1$. The mean-field values of the coupling constants are

$$\bar{\boldsymbol{\beta}}_{\mathrm{MF}} = -\beta_{1,MF}\Big(-1, 2, 2, 2, -2\Big) \tag{3.80}$$

$$\gamma_{\mathrm{MF}} = 3. \tag{3.81}$$

We begin by relating our coupling constants to derivatives of the free energy following eq. (3.28)

$$\begin{pmatrix} \bar{\beta}_1 \\ \bar{\beta}_2 \\ \bar{\beta}_3 \\ \bar{\beta}_4 \\ \bar{\beta}_5 \end{pmatrix} = \frac{1}{16} \begin{pmatrix} 0 & 2 & 0 & 0 & 0 \\ 0 & 2 & 0 & 2 & 0 \\ 1 & -2 & -1 & 0 & 0 \\ 0 & 0 & 1 & -2 & 1 \\ 1 & -2 & 0 & 0 & -1 \end{pmatrix} \begin{pmatrix} \frac{\partial^4}{\partial\psi_{1,1}^2\partial\bar{\psi}_{1,1}^2} \\ \frac{\partial^4}{\partial\psi_{1,1}\partial\psi_{2,2}\partial\bar{\psi}_{1,1}\partial\bar{\psi}_{2,2}} \\ \frac{\partial^4}{\partial\psi_{1,3}^2\partial\bar{\psi}_{1,1}^2} \\ \frac{\partial^4}{\partial\psi_{2,3}^2\partial\bar{\psi}_{1,1}^2} \\ \frac{\partial^4}{\partial\psi_{1,1}^2\partial\bar{\psi}_{2,1}^2} \end{pmatrix} \Bigg|_{\mathrm{A}=0} U(\mathrm{A}), \quad (3.82)$$

where A depends implicitly on ψ and $\bar{\psi}$. We can write eq. (3.82) in a more compact form

$$\bar{\boldsymbol{\beta}} = \mathbf{T}\hat{P}\Big|_{\mathrm{A}=0} U(\mathrm{A}). \quad (3.83)$$

Then

$$\delta\bar{\boldsymbol{\beta}}(b) = \mathbf{T}\hat{P}\Big|_{A=0} \delta U(b). \quad (3.84)$$

We are interested in the phase transition from the Fermi liquid state to any superfluid phase, so we can set $\alpha = 0$, which corresponds to $T = T_c$. After substituting in the trace-log formula, we get

$$\delta\bar{\boldsymbol{\beta}}(b) = \frac{1}{2}\mathbf{T}\hat{P}\Big|_{A=0} \int_{\mathbf{q}}^{'} \mathrm{tr}\ln\mathcal{G}^{-1}(\mathrm{A}, q). \quad (3.85)$$

Using eq. (3.31), we can evaluate the corrections analytically. The corrections take the form

$$\delta\bar{\beta}_a(b) = \frac{\mathcal{C}_a(\gamma, \bar{\boldsymbol{\beta}})}{\gamma^2} \int_{\mathbf{q}}^{'} \frac{1}{q^4}, \quad (3.86)$$

where each $\mathcal{C}_a(\gamma, \bar{\boldsymbol{\beta}})$ is a quadratic form in our quartic coupling constants $\bar{\boldsymbol{\beta}}$. The renormalized coupling constants become

$$\bar{\beta}_a(b) = b^\epsilon\Big(\bar{\beta}_a(0) + \frac{\mathcal{C}_a(\gamma, \bar{\boldsymbol{\beta}})}{\gamma^2} \int_{\mathbf{q}}^{'} \frac{1}{q^4}\Big). \quad (3.87)$$

The flow equation becomes

$$\frac{\mathrm{d}\bar{\beta}_a(b)}{\mathrm{d}\ln b} = \epsilon b^\epsilon\left(\beta_a(0) + \frac{\mathcal{C}_a(\gamma, \bar{\boldsymbol{\beta}})}{\gamma^2} \int_{\mathbf{q}}^{'} \frac{1}{q^4}\right) + b^\epsilon \frac{\mathcal{C}_a(\gamma, \bar{\boldsymbol{\beta}})}{\gamma^2} \frac{\mathrm{d}}{\mathrm{d}\ln b} \int_{\mathbf{q}}^{'} \frac{1}{q^4} \quad (3.88)$$

$$= \epsilon\bar{\beta}_a(b) + b^\epsilon \frac{\mathcal{C}_a(\gamma, \bar{\boldsymbol{\beta}})}{\gamma^2}\Big(\frac{b^\epsilon}{\Lambda^\epsilon}\Big). \quad (3.89)$$

The evaluation of $\int_{\mathbf{q}}' \frac{1}{q^4}$ is shown in appendix C.1. We impose self-consistency on our coupling constants such that $b^\epsilon \beta_a \to \beta_a(b)$, which leads to

$$\frac{\mathrm{d}\bar{\beta}_a(b)}{\mathrm{d}\ln b} = \epsilon\bar{\beta}_a(b) + \frac{\mathcal{C}_a\Big(\gamma, \bar{\boldsymbol{\beta}}(b)\Big)}{\gamma^2}\frac{1}{\Lambda^\epsilon} \tag{3.90}$$

We can also absorb Λ by rescaling

$$\beta_a(b) = \frac{\bar{\beta}_a(b)}{\Lambda^\epsilon}. \tag{3.91}$$

The quadratic nature of $\mathcal{C}_a$ causes Λ to be cancelled from both sides of the flow equation. Now that we have renormalized everything, we can drop the b-dependence in $\beta_a(b)$ and call it β_a, and refer to $C_a(\gamma, \boldsymbol{\beta}(b))$ as $C_a(\gamma)$ for simplicity. Let $t = \ln b$, and our flow equations take the form

$$\frac{\mathrm{d}\beta_a}{\mathrm{d}t} = \epsilon\beta_a + \frac{1}{\gamma^2}\mathcal{C}_a(\gamma). \tag{3.92}$$

The flow will start at $t = 0$ and end at $t_f = \ln b_f$, where

$$t_f = \ln(b_f) \sim \ln(\Lambda L)_{\exp} = \ln\frac{1\text{ mm}}{30\text{ nm}} \approx 10. \tag{3.93}$$

The length scale of the system in ref. [6] is $L_x \sim L_y$, which is 1 mm. The UV cut-off is given by $\Lambda \sim \lambda_T^{-1}$, where λ_T thermal fluctuation wavelength $\sqrt{\frac{2\pi\hbar^2}{mk_{\mathrm{B}}T_c}}$, and m is the mass of a ^{3}He atom. For the 3D case, when $\epsilon = 1$, we compute the values of $\mathcal{C}_a(\gamma)$ using eq. (3.31), and get

$$\begin{aligned}\mathcal{C}_1(\gamma) =& -6\beta_1^2\left(2\gamma^2+1\right) - \frac{1}{15}\beta_1\left(10\left(\beta_4+3\beta_5\right)\left(5\gamma^2+1\right) + \beta_2(\gamma(133\gamma+34)+13)\right.\\ &+3\beta_3(\gamma(41\gamma-2)+21)) - \frac{1}{60}\beta_5\left(\beta_3\left(366\gamma^2+68\gamma+46\right)\right.\\ &\left.\left.+\ 12\beta_2(\gamma-1)^2 + 3\left(2\beta_4+3\beta_5\right)(\gamma-1)^2\right)\right),\end{aligned} \tag{3.94}$$

$$\begin{aligned}\mathcal{C}_2(\gamma) =& \frac{1}{60}\Big[-4\beta_3^2\left(17\gamma^2+\gamma+12\right) - 2\beta_5\left(20\beta_2\left(15\gamma^2+\gamma+8\right) + \beta_3(\gamma(163\gamma-66)+23)\right.\\ &+\beta_4(\gamma(73\gamma-6)+53)) - 16\beta_1^2(7\gamma(\gamma+3)+2) - 4\beta_1\left(10\beta_2(\gamma(14\gamma-5)+3)\right.\\ &\left.+(\gamma-1)\left(3\beta_3(\gamma-1)+\beta_4(23\gamma+7)+\beta_5(53\gamma+37)\right)\right) - 4\beta_2^2(\gamma(229\gamma+42)+119)\\ &-12\beta_4^2(\gamma(16\gamma+3)+11) + \beta_5^2(7-\gamma(13\gamma+114)) - 16\beta_2\beta_3(\gamma(37\gamma-4)+27)\\ &\left.-\ 4\beta_4\left(\beta_2(\gamma(233\gamma-16)+143) + \beta_3(\gamma(51\gamma-32)+41)\right)\right],\end{aligned} \tag{3.95}$$

$$\begin{aligned}\mathcal{C}_3(\gamma) =&\frac{1}{60}\Big[-423\beta_3^2\gamma^2 - 152\beta_4^2\gamma^2 - 634\beta_3\beta_4\gamma^2 + 186\beta_3^2\gamma + 124\beta_4^2\gamma - 552\beta_3\beta_4\gamma.\\ &-2\beta_1^2(\gamma-1)(61\gamma-1) - \beta_2^2(\gamma-1)(91\gamma+29) - \beta_5^2(\gamma-1)(143\gamma+37)\\ &+2\beta_5\left(\beta_3(17-\gamma(33\gamma+104)) - 8\beta_4(\gamma-1)(11\gamma+4)\right) - 123\beta_3^2 + 28\beta_4^2\\ &-4\beta_1\left(5\beta_2(\gamma-1)(5\gamma-2) - 2\beta_3(\gamma-1)(29\gamma+1) + \beta_4(7-\gamma(58\gamma+69))\right)\\ &-\beta_5(\gamma(43\gamma+69)+8) + 2\beta_2\left(-6\beta_3(\gamma(41\gamma+23)-4) - 14\beta_3\beta_4\right.\\ &\left.-(\gamma-1)\left(\beta_4(121\gamma+59) + 5\beta_5(17\gamma+7)\right)\right)\Big],\end{aligned} \tag{3.96}$$

$$\begin{aligned}\mathcal{C}_4(\gamma) =&\frac{1}{60}\Big[-283\beta_3^2\gamma^2 - 452\beta_4^2\gamma^2 - 474\beta_3\beta_4\gamma^2 - 314\beta_3^2\gamma - 176\beta_4^2\gamma + 248\beta_3\beta_4\gamma\\ &-2\beta_1^2(\gamma-1)(61\gamma-1) - \beta_2^2(\gamma-1)(91\gamma+29) - \beta_5^2(\gamma(373\gamma+14)+213)\\ &+2\beta_5\left(\beta_3(\gamma-1)(7\gamma+23) - 4\beta_4(7\gamma(\gamma+3)+2)\right) + 2\beta_2\left(-2\beta_3(\gamma-1)(68\gamma+37)\right.\\ &\left.-3\beta_4(\gamma(77\gamma+46)-3) + 15\beta_5(\gamma-1)(3\gamma+1)\right) + 4\beta_1\left(15\beta_2(\gamma-1)\gamma - 4\beta_3(7\gamma(\gamma+3)+2)\right.\\ &\left.-\beta_4(\gamma-1)(8\gamma-23) + \beta_5(31(1-3\gamma)\gamma - 58)\right) - 3\beta_3^2 - 92\beta_4^2 - 14\beta_3\beta_4\Big],\end{aligned} \tag{3.97}$$

$$\begin{aligned}\mathcal{C}_5(\gamma) =&\frac{1}{30}\Big[-4\beta_1\left(10\beta_4\left(5\gamma^2+1\right) + 3\beta_2(\gamma-1)^2 + \beta_3(\gamma(43\gamma+14)+3)\right)\\ &-3\beta_5^2(\gamma(43\gamma+14)+3) - 2\beta_5\left(4\beta_2(\gamma(34\gamma+7)+4) + \beta_3(\gamma(53\gamma-6)+13)\right.\\ &\left.+\beta_4(\gamma(213\gamma+14)+73)\right)\Big].\end{aligned} \tag{3.98}$$

Computing these corrections while leaving γ fully general is a major result. The flow of γ can be found by calculating the second loop order corrections. The following results are taken from [26]. We have

$$\frac{\mathrm{d}\gamma}{\mathrm{d}t} = \frac{1}{3}(1-\gamma)\Big(\frac{1}{\gamma^2}+3\Big)f_\gamma, \tag{3.99}$$

where $f_\gamma > 0$ is a positive definite function given by

$$\begin{aligned}f_\gamma =& \,12\beta_1^2 + 2\beta_1\beta_2 + 8\beta_1\beta_3 + 2\beta_1\beta_4 + 6\beta_1\beta_5 + \frac{13}{2}\beta_2^2 + 4\beta_2\beta_3\\ &+ 7\beta_2\beta_4 + 5\beta_2\beta_5 + 8\beta_3^2 + 4\beta_3\beta_4 + \frac{13}{2}\beta_4^2 + 5\beta_4\beta_5 + \frac{15}{2}\beta_5^2.\end{aligned} \tag{3.100}$$

Because f_γ is positive definite, the flow of γ has an infrared-stable fixed point at $\gamma_\star = 1$ independently of the rest of the couplings. Near the beginning of the flow, when $b \sim 1$, the value of $\gamma \neq 1$, and this plays an important role in destroying the fixed ratios in the couplings given in eq. (3.80). At $\gamma = 1$, the equations simplify greatly to the well-known equations by Jones, Love and Moore in ref. [26]. At $\gamma = 1$, our corrections $C_a(1)$ are given by

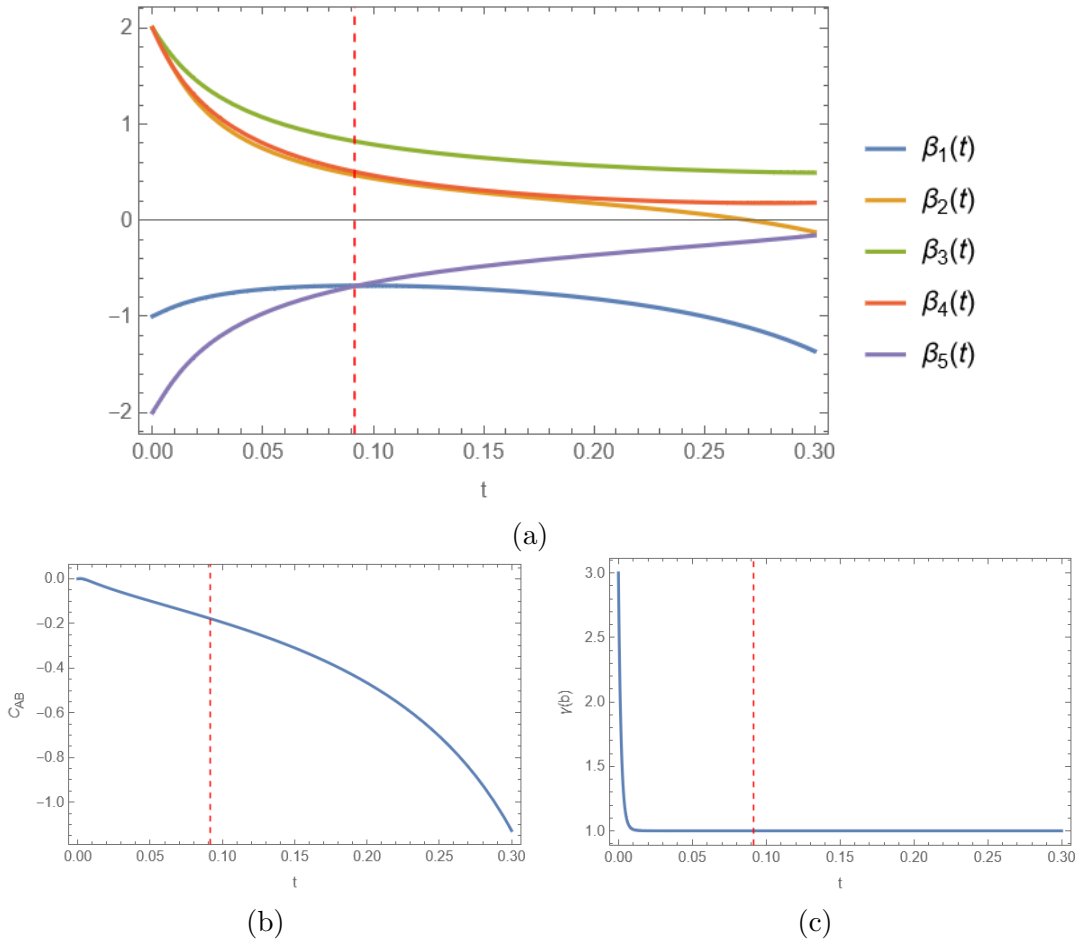

Figure 3.1: **RG flow in 3D.** *a)* RG flow of the five quartic couplings $\beta_a(b)$, where b represents the typical wavelength of fluctuations according to $\lambda \sim b\lambda_T$, the thermal wavelength. The flow is numerically determined and plotted against $t = \ln b$. The fixed ratios of the quartic couplings change significantly. The flow becomes unphysical at the red dotted line where the free energy of the B phase diverges. *b)* The flow of C_{AB}, which is positive when the A phase is favoured and negative when the B-phase is favoured, is plotted against t. The B phase is shown to be favoured in the valid region of our RG. *c)* The RG flow of γ with respect to t. γ decays rapidly to its fixed point at $\gamma = 1$.

$$\mathcal{C}_1(1) = -2\Big[9\beta_1^2 + 6\beta_1\beta_2 + 6\beta_1\beta_3 + 2\beta_1\beta_4 + 6\beta_1\beta_5 + 4\beta_3\beta_5\Big], \tag{3.101}$$

$$\mathcal{C}_2(1) = -2\Big[4\beta_1^2 + 13\beta_2^2 + \beta_3^2 + 3\beta_4^2 + \beta_5^2 + 4\beta_1\beta_2 + 8\beta_2\beta_3 + 2\beta_3\beta_4 + 2\beta_4\beta_5 + 2\beta_3\beta_5 + 12\beta_2\beta_4 + 8\beta_2\beta_5\Big], \tag{3.102}$$

$$\mathcal{C}_3(1) = -2\Big[3\beta_3^2 + 4\beta_1\beta_4 + 4\beta_1\beta_5 + 6\beta_2\beta_3 + 10\beta_3\beta_4 + 2\beta_3\beta_5\Big], \tag{3.103}$$

$$\mathcal{C}_4(1) = -2\Big[5\beta_3^2 + 6\beta_4^2 + 5\beta_5^2 + 4\beta_1\beta_3 + 4\beta_1\beta_5 + 6\beta_2\beta_4 + 2\beta_4\beta_3 + 2\beta_4\beta_5\Big], \tag{3.104}$$

$$\mathcal{C}_5(1) = -2\Big[3\beta_5^2 + 4\beta_1\beta_3 + 4\beta_1\beta_4 + 6\beta_2\beta_5 + 2\beta_3\beta_5 + 10\beta_4\beta_5\Big], \tag{3.105}$$

where γ has been set to 1 [26], and $\epsilon = 4 - d$. The fixed point occurs when

$$(\beta_{1\star}, \beta_{2\star}, \beta_{3\star}, \beta_{4\star}, \beta_{5\star}, \gamma_\star) = \Big(0, \frac{\epsilon}{26}, 0, 0, 0, 1\Big). \tag{3.106}$$

We can substitute the values of the coupling constants at the Wilson-Fisher fixed point into the free energy and see that the A phase and B phase are energetically degenerate at this fixed point. The stability matrix at the Wilson-Fisher fixed point is

$$M_{3D} = \begin{pmatrix} \frac{7}{13}\epsilon & 0 & 0 & 0 & 0 \\ -\frac{4}{13}\epsilon & -\epsilon & -\frac{8}{13}\epsilon & -\frac{12}{13}\epsilon & -\frac{8}{13}\epsilon \\ 0 & 0 & \frac{7}{13}\epsilon & 0 & 0 \\ 0 & 0 & 0 & \frac{7}{13}\epsilon & 0 \\ 0 & 0 & 0 & 0 & \frac{7}{13}\epsilon \end{pmatrix}, \tag{3.107}$$

and its eigenvalues are $\Big(-\epsilon, \frac{7}{13}\epsilon, \frac{7}{13}\epsilon, \frac{7}{13}\epsilon, \frac{7}{13}\epsilon\Big)$. The fixed point is attractive in the β_2 direction, and repulsive otherwise. At face value, our result suggests that the superfluid transition in ^{3}He is not second-order. Additionally, it was determined that the Wilson–Fischer fixed point is unstable for the 3×2 matrix order parameter as well [26]. This is in stark contrast to the clear second-order phase transition in experiment [6, 27]. There are several potential explanations for this. Fluctuation-induced first-order transitions often correspond to an unstable RG fixed point, and such transitions at low enough resolution can appear to be second-order. However, the resolution of the experiments excludes such a possibility.

A more favourable explanation is that this is a shortcoming of perturbative RG at the one-loop level. The Wilson–Fisher fixed point is computed as a correction to the Gaussian fixed point through expansion in the small parameter $\epsilon \ll 1$. Though this fixed point is unstable for $\epsilon = 1$, it is still 'less unstable' than the Gaussian fixed point with eigenvalues $(\epsilon, \epsilon, \epsilon, \epsilon, \epsilon)$. Even the positive eigenvalues are reduced from ϵ to $\frac{7}{13}\epsilon$, so it is plausible that the second or third order corrections could give us a fully stable fixed point. However, computing these higher-order corrections for 5 coupling constants and 18 real fields would be very challenging. Even computing these first-order corrections without the techniques outlined in ref. [20] would be extremely cumbersome. Additionally, stable fixed points are usually found for simpler theories with only one coupling constant, such as the Wilson–Fisher fixed point of classical O(N)-models. In contrast, many tensor field theories with multiple coupling constants do not have stable fixed points in the perturbative RG, see Refs.[19, 26, 28–34]. Our free energy, has *five* quartic couplings, so it is unreasonable to expect a single one-loop calculation to change the sign of five eigenvalues to yield an infrared-stable fixed point.

We conclude that we can not extract useful information from the fixed points because of the limitations of one-loop RG. We can, on the other hand, numerically solve the RG flow and determine what phase is favoured in the phase transition.

We solved the RG flow equations in the 3D-limit, and the results are plotted in fig. 3.1. The five quartic coupling constants $\beta_a(t)$ deviate significantly from the fixed ratios of the mean-field initial conditions in eq. (3.80). This lifts the accidental energetic degeneracy of the A-phase and B-phase. The coefficients $\beta_a(t)$ in the early stages $t \sim 0$ indicate that C_{AB} becomes increasingly negative, so the B-phase continues to be favoured over the A-phase.

The coupling constants β_a quickly take on unphysical values that cause the free energy to become unbounded from below. We detect this when the A-phase or B-phase free energies become singular. Because of the complex nature of the free energy,

numerous conditions in the form of a system of inequalities must be upheld for the free energy to be bounded below. For example

$$\beta_{12345} > 0. \tag{3.108}$$

Finding a complete list of these inequalities is challenging and beyond the scope of this thesis. The inequality that appears to be violated is

$$\beta_5 > \beta_1. \tag{3.109}$$

These divergences could result from cutting off our free energy at the fourth degree. Our perturbative RG equations can no longer be applied in this unphysical regime. For all physical values of the RG, the B-phase is energetically favoured over the A-phase.

3.3.2 2D System

We can extend our analysis of RG in 3D systems to 2D systems and gain an understanding of ^{3}He under complete confinement when the order parameter's last column vanishes completely. The order parameter is given by

$$\mathrm{A}_\perp = \begin{pmatrix} \mathrm{A}_{1,1} & \mathrm{A}_{1,2} \\ \mathrm{A}_{2,1} & \mathrm{A}_{2,2} \\ \mathrm{A}_{3,1} & \mathrm{A}_{3,2} \end{pmatrix}. \tag{3.110}$$

The free energy is

$$F_\perp[\mathrm{A}_\perp] = \int d^2\mathbf{q}_\perp \left\{ U(\mathrm{A}_\perp) + (\gamma - 1) q_i \mathrm{A}^*_{\perp\mu i} q_j \mathrm{A}_{\perp\mu j} + q_i \mathrm{A}^*_{\perp\mu j} q_i \mathrm{A}_{\perp\mu j} \right\}, \tag{3.111}$$

where $\mathbf{q}_\perp = (q_x, q_y)$. The effective potential is defined as

$$U(\mathrm{A}_\perp) = \alpha \mathrm{tr} \mathrm{A}_\perp \mathrm{A}^\dagger_\perp + \sum_n \beta_n I_n(\mathrm{A}_\perp). \tag{3.112}$$

Each component of $\mathrm{A}_\perp$ is complex, so we define it in terms of two real parameters

$$\mathrm{A}_{\perp\mu i} = \frac{1}{\sqrt{2}} \left(\psi_{\mu i} + \bar{\psi}_{\mu i} \right) + \frac{i}{\sqrt{2}} \left(\psi_{\mu i} - \bar{\psi}_{\mu i} \right). \tag{3.113}$$

Now we will calculate the RG flow in 2D, setting $\epsilon = 2$. We are interested in calculating the renormalized coupling constants, which will have the form

$$\beta_a(b) = b^{\epsilon}\Big(\beta_a(0) + \delta\beta_a(b)\Big), \tag{3.114}$$

$\beta_a(0)$ are the mean-field values in the 2D case, which have the same ratios as the 3D case [25]. $\delta\beta_a(b)$ is the one-loop correction. The mean-field values are

$$\boldsymbol{\beta}_{\mathrm{MF}} = \beta_{2,MF}\Big(-1, 2, 2, 2, -2\Big), \tag{3.115}$$

$$\gamma_{\mathrm{MF}} = 3 \tag{3.116}$$

We begin by relating our coupling constants to derivatives of the free energy following eq. (3.28)

$$\begin{pmatrix} \beta_1 \\ \beta_2 \\ \beta_3 \\ \beta_4 \\ \beta_5 \end{pmatrix} = \frac{1}{12}\begin{pmatrix} 0 & 3 & -3 & 0 & 0 \\ 0 & 3 & 3 & 0 & 0 \\ 1 & -3 & 3 & -3 & 0 \\ 0 & 0 & -6 & 3 & 3 \\ 1 & -3 & 3 & 0 & -3 \end{pmatrix}\begin{pmatrix} \frac{\partial^4}{\partial\psi_{1,1}^4} \\ \frac{\partial^4}{\partial^2\psi_{1,2}\partial^2\psi_{2,1}} \\ \frac{\partial^4}{\partial\psi_{3,1}^2\partial\bar{\psi}_{2,2}^2} \\ \frac{\partial^4}{\partial\psi_{1,2}^2\partial\bar{\psi}_{1,1}^2} \\ \frac{\partial^4}{\partial\psi_{1,1}^2\partial\bar{\psi}_{3,1}^2} \end{pmatrix}\Bigg|_{\mathrm{A}_\perp=0} U(\mathrm{A}_\perp), \tag{3.117}$$

The derivation of the flow equations is identical to the 3D case. Our flow equations are of the form

$$\frac{\mathrm{d}\beta_i}{\mathrm{d}t} = \epsilon\beta_i - \frac{1}{\gamma^2}\tilde{\mathcal{C}}_i(\gamma), \tag{3.118}$$

where $\epsilon = 2$ in the 2D case. We compute the values of $\tilde{\mathcal{C}}_i$ using eq. (3.31), and get

$$\begin{aligned}\tilde{\mathcal{C}}_1(\gamma) =& \frac{1}{4}\Big[24\beta_1^2\left(\gamma^2+1\right) + 4\beta_1\left(2\left(\beta_4+3\beta_5\right)\left(\gamma^2+1\right) + 3\beta_2(\gamma+1)^2 + \beta_3(\gamma(5\gamma-2)+5)\right) \\ &+ \beta_5\left(4\beta_2(\gamma-1)^2 + \left(2\beta_4+3\beta_5\right)(\gamma-1)^2 + 2\beta_3(\gamma(5\gamma+6)+5)\right)\Big],\end{aligned} \tag{3.119}$$

$$\begin{aligned}\tilde{\mathcal{C}}_2(\gamma) =& \frac{1}{4}\Big[4\beta_1\left(4\beta_2\left(\gamma^2+1\right) + \left(\beta_3+\beta_4+\beta_5\right)(\gamma-1)^2\right) + 2\left(6\beta_4^2\left(\gamma^2+1\right)\right. \\ &+\beta_2^2(\gamma(17\gamma+6)+17) + 2\beta_2\left(\beta_3(\gamma(9\gamma-2)+9) + \beta_4(\gamma(11\gamma-2)+11)\right) \\ &+\beta_3^2(\gamma(3\gamma-2)+3) + 8\beta_3\beta_4((\gamma-1)\gamma+1)\Big) + 2\beta_5\left(12\beta_2\left(\gamma^2+1\right)\right. \\ &+\left(\beta_3+\beta_4\right)(\gamma(5\gamma-2)+5)) + 4\beta_1^2(\gamma(\gamma+6)+1) + \beta_5^2(\gamma(\gamma+6)+1)\Big],\end{aligned} \tag{3.120}$$

$$\tilde{\mathcal{C}}_3(\gamma) = \frac{1}{4}\Big[\beta_4^2(\gamma-1)^2 + \beta_5^2(\gamma-1)^2 + 2\left(2\beta_1^2+\beta_2^2\right)(\gamma-1)^2 + 2\beta_3^2(\gamma(7\gamma-6)+7)$$
$$+4\beta_3\left(\beta_1(\gamma-1)^2 + 3\beta_2(\gamma+1)^2\right) + 4\beta_4\left(\beta_2(\gamma-1)^2 + \beta_1(\gamma(\gamma+6)+1)\right.$$
$$\left.+4\beta_3(\gamma(\gamma+3)+1)\right) + 2\beta_5\left(\beta_4(\gamma-1)^2 + (2\beta_1+\beta_3)(\gamma(\gamma+6)+1)\right)\Big], \tag{3.121}$$

$$\tilde{\mathcal{C}}_4(\gamma) = \frac{1}{4}\Big[\left(2\beta_1^2+\beta_2^2\right)(\gamma-1)^2 + 2\beta_3^2(\gamma(3\gamma+14)+3) + 4\beta_4^2(\gamma(3\gamma+4)+3)$$
$$+\beta_5^2(\gamma(17\gamma-2)+17) + 4\beta_3\left(\beta_2(\gamma-1)^2 + \beta_1(\gamma(\gamma+6)+1)\right) + 4\beta_4\left(\beta_1(\gamma-1)^2\right.$$
$$\left.+3\beta_2(\gamma+1)^2 + 4\beta_3((\gamma-1)\gamma+1)\right) + 2\beta_5\left(\beta_3(\gamma-1)^2 + 2\beta_1(\gamma(5\gamma-2)+5)\right.$$
$$\left.+\beta_4(\gamma(\gamma+6)+1)\right)\Big], \tag{3.122}$$

$$\tilde{\mathcal{C}}_5(\gamma) = \frac{1}{2}\Big[4\beta_1\left(2\beta_4\left(\gamma^2+1\right) + \beta_2(\gamma-1)^2 + \beta_3(\gamma+1)^2\right) + \beta_5\left(8\beta_2\left(\gamma^2+\gamma+1\right)\right.$$
$$\left.+3\beta_5(\gamma+1)^2 + 2\beta_3(\gamma(3\gamma-2)+3) + 2\beta_4(\gamma(7\gamma+2)+7)\right)\Big]. \tag{3.123}$$

The flow of γ is identical to the 3D case given in eq. (3.99) and (3.102).

We solved the RG flow equations in the 2D-limit, and the results are plotted in fig. 3.2. The five quartic coupling constants $\beta_a(t)$ deviate significantly from the fixed ratios of the mean-field initial conditions in eq. (3.80). This lifts the accidental energetic degeneracy of the A-phase and planar phase. The coefficients $\beta_a(t)$ in the early stages $t \sim 0$ indicate the C_{AP} becomes increasingly negative, so the planar phase is favoured over the A-phase.

We notice that the decay of $\gamma(t)$ to $\gamma_\star = 1$ is much slower than the 3D case. This allows for a greater effect on the ratios of the coupling constants, and this implies a larger physical effect. Fluctuations often are much more pronounced in lower dimensional systems.

The coupling constants β_a quickly take on unphysical values that cause the free energy to become unbounded below. We detect this when the A-phase's or the planar phase's free energies become singular. Similarly to the 3D case, the inequality that appears to be violated is

$$\beta_5 > \beta_1. \tag{3.124}$$

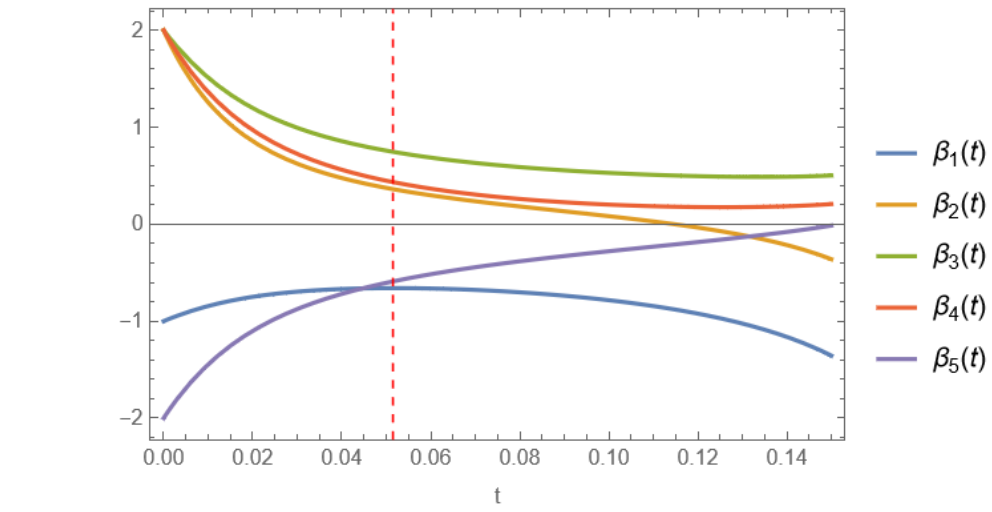

(a)

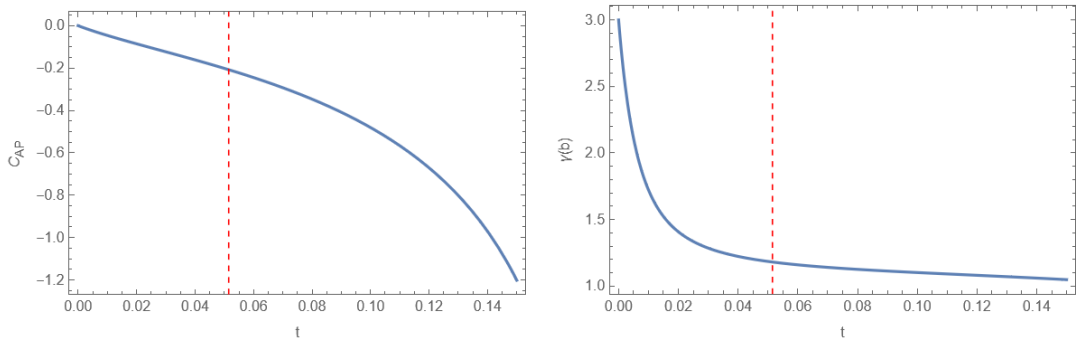

(b) (c)

Figure 3.2: **RG flow in 2D.** *a)* RG flow of the five quartic couplings $\beta_a(b)$, where the flow is numerically determined and plotted against $t = \ln b$. The fixed ratios of the quartic couplings change significantly but only differ from the 3D flow quantitatively. The flow becomes unphysical at the red dotted line where the free energy of the planar phase diverges. *b)* The flow of C_{AP}, which is positive when the A phase is favoured and negative when the planar phase is favoured, is plotted against t. The planar phase is shown to be favoured in the valid region of our RG. *c)* The RG flow of γ with respect to t. γ decays slowly to its fixed point at $\gamma = 1$, inc comparison to 3D.

Our perturbative RG equations can no longer be applied in this unphysical regime. For all physical values of the RG, the planar phase is energetically favoured over the A-phase.

3.3.3 Quasi-2D System

When ^{3}He uniaxial nanoscale confinement to confinement length L_z, which is much smaller than the length scale of the system, the 3D rotational symmetry of the system

reduces to only a 2D symmetry, and the symmetry of the system reduces to

$$\mathrm{SO(3)_S} \times \mathrm{SO(2)_L} \times \mathrm{U(1)}. \tag{3.125}$$

This implies that the order parameter in this case will be the 3×2 order parameter. We are effectively considering the 2D case while allowing fluctuations of the order parameter in the z-direction. This is nontrivial because there is a mismatch between the number of spatial dimensions, which is three, and the number of angular momentum indices, which is two. The confinement also leads to the quantization of the confined momentum q_z with

$$q_z = \frac{\pi}{L_z} n, \tag{3.126}$$

We assume $\mathrm{A}(x_\perp, z)$ is periodic in z, which signifies specular reflection at the boundary walls. q_x and q_y also take on discrete values proportional $\frac{\pi}{L_x}$ and $\frac{\pi}{L_y}$, but the spectrum is sufficiently tightly spaced to be approximated as a continuum. We replace the integral over q_z with a sum

$$\sum_{q_z} = \frac{1}{L_z} \sum_{n=1}^{\infty}. \tag{3.127}$$

The quasi-2D free energy is

$$F[\mathrm{A}_\perp] = \frac{1}{L_z} \sum_{n=1}^{\infty} \int d^2\mathbf{q}_\perp \left\{ \sum_a \beta_a I_a(\mathrm{A}_\perp) + (\gamma - 1) q_i \mathrm{A}^*_{\perp \mu i} q_j \mathrm{A}_{\perp \mu j} + \left(\alpha + q^2\right) \mathrm{tr} \mathrm{A}_\perp \mathrm{A}^\dagger_\perp \right\}, \tag{3.128}$$

where $\boldsymbol{q} = (q_x, q_y, q_z) = (q_\perp \cos\theta, q_\perp \sin\theta, \frac{n\pi}{L})$, and $\boldsymbol{q}_\perp = (q_x, q_y)$. The q_z-dependence is entirely held within $q^2 = q_\perp^2 + q_z^2$.

The quasi-2D free energy interpolates between the 2D and 3D free energies. When $L_z = 0$ we will recover the 2D free energy, and when $L_z \to \infty$, this will recover the 3D free energy with the last column of the order parameter set to zero. The value of L_z is on the order of 1000 nm in Ref. [6], so

$$(L_z \Lambda)_{exp} \sim 30. \tag{3.129}$$

We will investigate $L_z\Lambda \in [10, 50]$ to cover all confinement ranges of the experiment. In the quasi-2D case, the value of α during the phase transition should offset the non-zero kinetic energy and make the denominator of the propagator singular to incorporate Goldstone modes. We have

$$\alpha = -\frac{\pi^2}{L_z^2} \tag{3.130}$$

during the phase transition, and so $q_z^2 + \alpha = \Delta q_z^2$ with

$$\Delta q_z^2 = \frac{\pi^2}{L_z^2}(n^2 - 1). \tag{3.131}$$

The modes with $n > 1$ are massive, but they still can lead to a quantitative effect in the RG equations. The momentum shell integral in this case will be

$$\int_{\mathbf{q}}'(\dots) := \frac{1}{L_z}\sum_{n=1}^{\infty}\int_{\Lambda/b}^{\Lambda} \mathrm{d}^2\mathbf{q}_\perp(\dots) = \frac{1}{L_z}\sum_{n=1}^{\infty}\int_{\Lambda/b}^{\Lambda}\mathrm{d}q_\perp \int_0^{2\pi}\mathrm{d}\theta\Big[q_\perp(\dots)\Big]. \tag{3.132}$$

Using the same derivatives as the 2D case in eq. (3.117), we can apply eq. (3.31) and get the corrections to be of the form

$$\delta\bar{\beta}_a = -\int_{\mathbf{q}_\perp}' \frac{\tilde{\mathcal{C}}_a(\gamma)q_\perp^4 + \tilde{\mathcal{C}}_a(1)[(\gamma+1)q_\perp^2\Delta q_z^2 + \Delta q_z^4]}{(q_\perp^2 + \Delta q_z^2)^2(\gamma q_\perp^2 + \Delta q_z^2)^2}. \tag{3.133}$$

During the RG procedure, we rescale the length scale which results in the rescaling of L_z so we define a new reduced confinement length

$$\tilde{L}_z = \frac{\Lambda L_z}{b}. \tag{3.134}$$

Applying eq. (C.2) this simplifies to

$$\delta\bar{\beta}_a = -\frac{1}{L_z}\Big(\frac{\Lambda}{b}\Big)^2\sum_{n=1}^{\infty}\frac{\tilde{\mathcal{C}}_a(\gamma)\Big(\frac{\Lambda}{b}\Big)^4 + \tilde{\mathcal{C}}_a(1)\Big[(\gamma+1)\Big(\frac{\Lambda}{b}\Big)^2\Delta q_z^2 + \Delta q_z^4\Big]}{\Big(\Big(\frac{\Lambda}{b}\Big)^2 + \Delta q_z^2\Big)^2\Big(\gamma\Big(\frac{\Lambda}{b}\Big)^2 + \Delta q_z^2\Big)^2}. \tag{3.135}$$

We can substitute eq. (3.134) into this equation and simplify it to

$$-\frac{\Lambda}{\Lambda L_z}\Big(\frac{\Lambda}{b}\Big)^2\sum_{n=1}^{\infty}\frac{\tilde{\mathcal{C}}_a(\gamma)\Big(\frac{\Lambda}{b}\Big)^4 + \tilde{\mathcal{C}}_a(1)\Big[(\gamma+1)\Big(\frac{\Lambda}{b}\Big)^2\frac{\pi^2\Lambda^2}{b^2\tilde{L}_z^2}(n^2-1) + \Big(\frac{\pi^2\Lambda^2}{b^2\tilde{L}_z^2}(n^2-1)\Big)^2\Big]}{\Big(\Big(\frac{\Lambda}{b}\Big)^2 + \frac{\pi^2\Lambda^2}{b^2\tilde{L}_z^2}(n^2-1)\Big)^2\Big(\gamma\Big(\frac{\Lambda}{b}\Big)^2 + \frac{\pi^2\Lambda^2}{b^2\tilde{L}_z^2}(n^2-1)\Big)^2}. \tag{3.136}$$

$$= -\frac{1}{\Lambda L_z}\Big(\frac{b^2}{\Lambda}\Big)\sum_{n=1}^{\infty}\frac{\tilde{\mathcal{C}}_a(\gamma) + \tilde{\mathcal{C}}_a(1)\Big[(\gamma+1)\frac{\pi^2}{\tilde{L}_z^2}(n^2-1) + \frac{\pi^4}{\tilde{L}_z^4}(n^2-1)^2\Big]}{\Big(1 + \frac{\pi^2}{\tilde{L}_z^2}(n^2-1)\Big)^2\Big(\gamma + \frac{\pi^2}{\tilde{L}_z^2}(n^2-1)\Big)^2}. \tag{3.137}$$

Now, we can apply similar steps as eq. (3.90) and (3.92), and obtain that the renormalized couplings obey the following flow equation

$$\frac{\mathrm{d}\beta_a}{\mathrm{d}\ln b} = \epsilon\beta_a - H_a(\gamma, \tilde{L}_z), \tag{3.138}$$

where

$$H_a(\gamma, \tilde{L}_z) = \frac{1}{\Lambda L_z}\sum_{n=1}^{\infty} \frac{\tilde{\mathcal{C}}_a(\gamma) + \tilde{\mathcal{C}}_a(1)\Big[(\gamma+1)\frac{\pi^2}{\tilde{L}_z^2}(n^2-1) + \frac{\pi^4}{\tilde{L}_z^4}(n^2-1)^2\Big]}{\Big(1+\frac{\pi^2}{\tilde{L}_z^2}(n^2-1)\Big)^2\Big(\gamma+\frac{\pi^2}{\tilde{L}_z^2}(n^2-1)\Big)^2} \tag{3.139}$$

The summand expression decays as $\frac{1}{n^4}$, so summing this to some large N will get us a sufficiently accurate answer. The expressions for $\tilde{\mathcal{C}}_a(1)$ are given by

$$\tilde{\mathcal{C}}_1(1) = 4(3\beta_1^2 + 3\beta_1\beta_2 + 2\beta_1\beta_3 + \beta_1\beta_4 + 3\beta_1\beta_5 + 2\beta_3\beta_5) \tag{3.140}$$

$$\begin{aligned}\tilde{\mathcal{C}}_2(1) = 2(&4\beta_1^2 + 4\beta_1\beta_2 + 10\beta_2^2 + 8\beta_2\beta_3 + 10\beta_2\beta_4 + \beta_5^2 \\ &+ 6\beta_2\beta_5 + \beta_3^2 + 2\beta_3\beta_4 + 2\beta_3\beta_5 + 3\beta_4^2 + 2\beta_4\beta_5)\end{aligned} \tag{3.141}$$

$$\tilde{\mathcal{C}}_3(1) = 4(2\beta_1\beta_4 + 2\beta_1\beta_5 + 3\beta_2\beta_3 + \beta_3^2 + 5\beta_3\beta_4 + \beta_3\beta_5) \tag{3.142}$$

$$\tilde{\mathcal{C}}_4(1) = 2(4\beta_1\beta_3 + 4\beta_1\beta_5 + 6\beta_2\beta_4 + 5\beta_3^2 + 2\beta_3\beta_4 + 5\beta_4^2 + 2\beta_4\beta_5 + 4\beta_5^2) \tag{3.143}$$

$$\tilde{\mathcal{C}}_5(1) = 2(4\beta_1\beta_3 + 4\beta_1\beta_4 + 6\beta_2\beta_5 + 2\beta_3\beta_5 + 8\beta_4\beta_5 + 3\beta_5^2). \tag{3.144}$$

We can analytically perform the summation over n when $\gamma = 1$. We have

$$H_a(1, \tilde{L}_z) = \frac{\mathcal{C}_a(1)}{\tilde{L}_z}\sum_{n=1}^{\infty}\frac{1}{\Big(1+\frac{\pi}{\tilde{L}_z}(n^2-1)\Big)} \tag{3.145}$$

$$= \mathcal{C}_a(1)\frac{\tilde{L}_z^3}{4}\frac{-2+\eta\ \coth(\eta)+\eta^2/\sinh^2(\eta)}{\eta^4} > 0, \tag{3.146}$$

with $\eta = \sqrt{\tilde{L}_z^2 - \pi^2}$. Here we assumed $\eta > 0$ as applies to the physical system.

We solved the RG flow equations in the quasi-2D limit, and the results are plotted in fig. 3.3. The five quartic coupling constants $\beta_a(t)$ deviate significantly from the fixed ratios of the mean-field initial conditions in eq. (3.80). This lifts the accidental energetic degeneracy of the A-phase and planar phase just as it did in the 2D limit. The coefficients $\beta_a(t)$ in the early stages $t \sim 0$ indicate the C_{AP} becomes increasingly

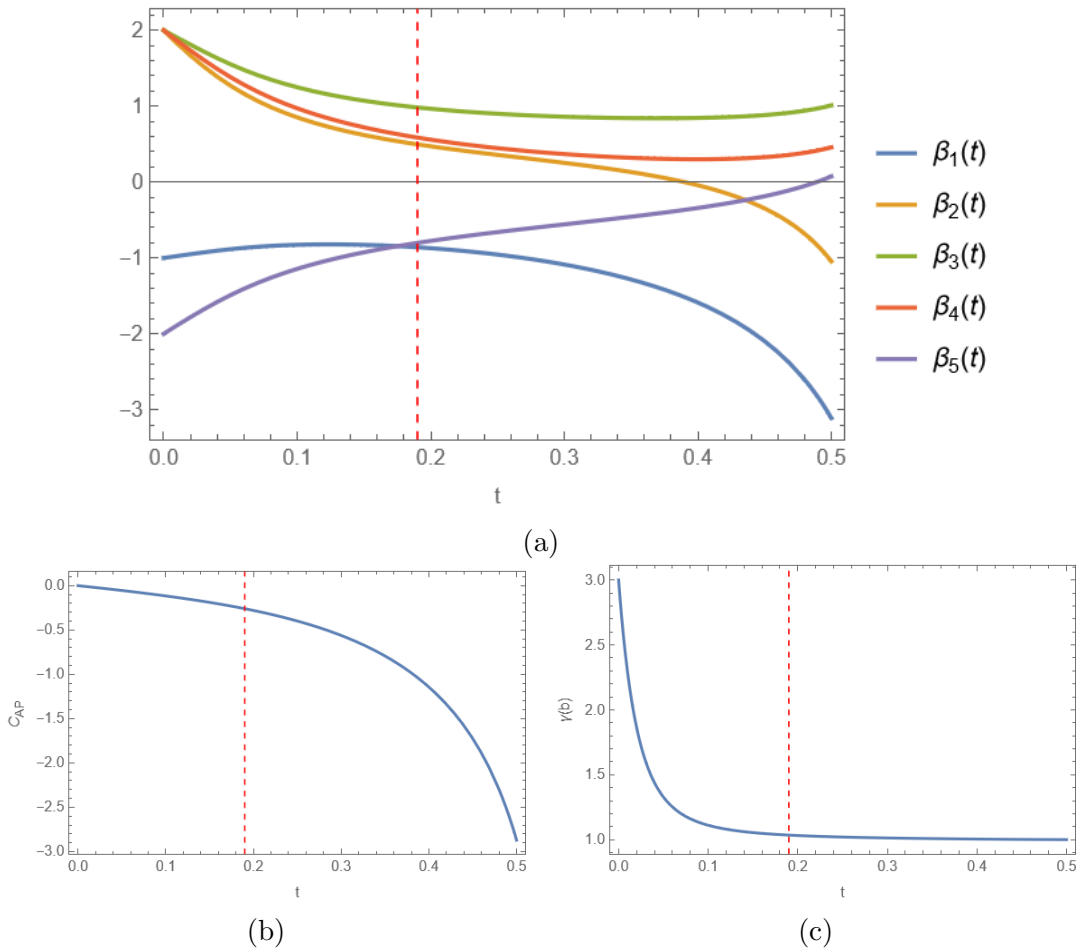

Figure 3.3: **RG flow in the quasi-2D limit.** *a)* RG flow of the five quartic couplings $\beta_a(b)$, where the flow is numerically determined and plotted against $t = \ln b$ for $L_z\Lambda = 30$. The summation limit N was increased until 10, after which the flow did not have observable changes from increasing N. The fixed ratios of the quartic couplings change significantly but only differ from the 2D and 3D flow quantitatively. The flow becomes unphysical at the red dotted line where the free energy of the planar phase diverges. *b)* The flow of C_{AP}, which is positive when the A phase is favoured and negative when the planar phase is favoured, is plotted against t. The planar phase is shown to be favoured in the valid region of our RG, similar to the 2D case. *c)* The RG flow of γ with respect to t. γ decays slower than the 3D case but faster than the 2D case.

negative, so the planar phase is favoured over the A-phase. We find that the planar phase is favoured in all confinement scales within the context of the experiment.

We notice that the decay of $\gamma(t)$ to $\gamma_\star = 1$ is much slower than the 3D case, but faster than the 2D case. This allows for a greater effect on the ratios of the coupling

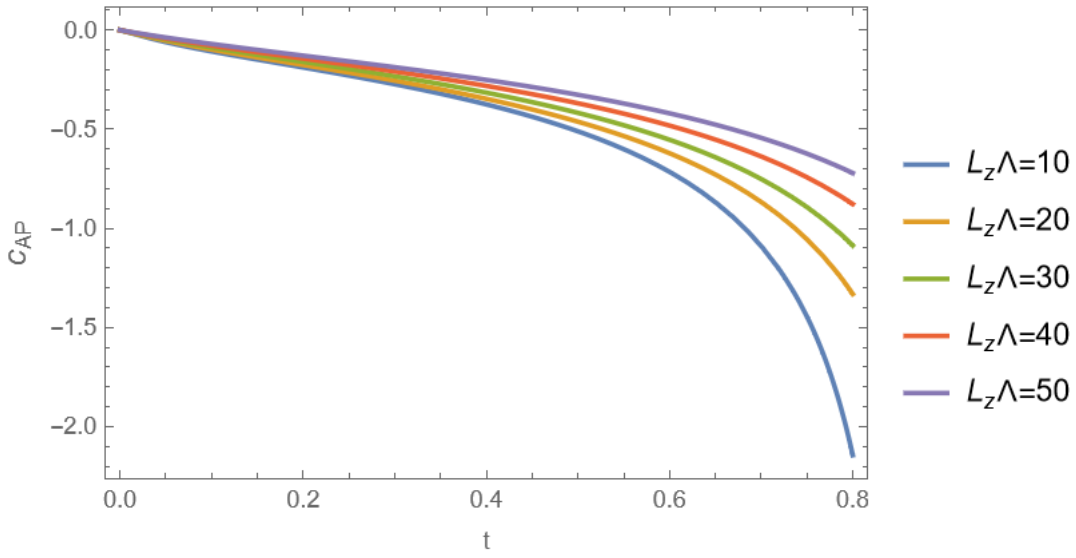

Figure 3.4: **Quasi-2D RG flow for various levels of confinement.** We plotted the RG flow of $C_{AP}(t)$ for various levels of confinement against $t = \ln b$. The summation limit N was increased until 10, after which the flow did not have observable changes from increasing N. The degeneracy between the planar phase and A-phase is broken for all confinement lengths. The planar phase is favoured for all levels of confinement considered.

constants, and this implies a larger physical effect. However, this is not enough to cause the A-phase to be favoured.

The coupling constants β_a quickly take on unphysical values that cause the free energy to become unbounded below. We detect this when the A-phase or planar phase free energies become singular. Similarly to the 3D case, the inequality that appears to be violated is

$$\beta_5 > \beta_1. \tag{3.147}$$

Our perturbative RG equations can no longer be applied in this unphysical regime. For all physical values of the RG, the planar phase is energetically favoured over the A-phase, in contradiction with the experiment. Perturbative RG at the one-loop level is insufficient to explain the emergence of A-phase at low pressures under confinement. The next step is to move on from perturbative RG to more powerful methods.

Chapter 4

Functional Renormalization Group

4.1 Introduction

Perturbative RG only allowed us to compute corrections up to the first order in the quartic couplings, and it did not reveal the A-phase. The Functional Renormalization Group (FRG) allows us to compute our partition function exactly using the Wetterich equation [35]. Although solving the Wetterich equation exactly is very difficult, with the appropriate approximations, FRG allows us to include corrections far beyond first-order, including non-perturbative corrections. However, FRG's promise is countered by the fact that we cannot control or predict which corrections will be included in our FRG equations. FRG has successfully accurately modelled numerous phase transitions [36–38].

The ideas used in FRG are very similar to the ones in perturbative RG despite their very different use of notation. We have listed some relationships between FRG and perturbative RG in table 4.1. The central goal of FRG is to solve for the effective action $\Gamma[\phi]$, which encodes all the physics relevant to the system. Just like in perturbative RG, we cannot solve for Γ directly, so we derive a system of differential equations that depend on an IR momentum cutoff parameter k. The parameter k has a very similar function to b in perturbative RG, but the momentum shell integration is replaced by the use of a regulator $R_k(q)$. Rather than using the trace-log formula, we use the far superior Wetterich equation to solve for Γ_k. Our ansatz gives the initial

Perturbative RG	FRG
$F_{eff}[\phi]$	$\Gamma[\phi]$
$t = \ln b$	$t = \ln \frac{\Lambda}{k}$
$g(b)$	g_k
$\int_q'$	$R_k(q)$
$G(\phi, q)$	$G_k(\phi, q)$
trace-log formula	Wetterich equation

Table 4.1: Relation between concepts and notation from perturbative RG and FRG.

value for Γ_k at $k = \Lambda$, which in our case will be the GL free energy $F[\phi]$. The final value of the flow is given by $\Gamma_{k=0} = \Gamma$, which contains our corrections.

We want to mathematically define the notation we have introduced in FRG using powerful mathematical machinery borrowed from quantum field theory. We start by defining our partition function over a real scalar field ϕ, for simplicity, with a source J

$$Z[J] = \int \mathcal{D}\phi \exp\Big(-F[\phi] + \int_{\mathbf{r}} J\phi\Big) \tag{4.1}$$

$$= \int \mathcal{D}\phi \exp\Big(-\int_{\mathbf{r}} \frac{1}{2} q^2 \phi\phi + \int_{\mathbf{r}} U(\phi) + \int_{\mathbf{r}} J\phi\Big). \tag{4.2}$$

Let $W[J] = \log Z[J]$, then we can find correlation functions as follows (see appendix A)

$$G^{(n)}_{\{i_j\}}[\{r_j\}; J] = \left.\frac{\delta^n W[J]}{\delta J_{i_1}(r_1) \dots \delta J_{i_n}(r_n)}\right|_{J=0} = \langle T\phi_{i_1}(r_1) \dots \phi_{i_1}(r_n)\rangle, \tag{4.3}$$

where T is time ordering. Then we have

$$\left.\frac{\delta W[J]}{\delta \phi_i(r)}\right|_{J=0} = \langle T\phi_i(r)\rangle = \int D\phi e^{-F[\phi]}\phi_i(r) = \varphi_i(r). \tag{4.4}$$

To get the effective action from this, we use a Legendre transformation, where W and Γ are conjugate

$$\Gamma[\varphi] = -W[J] + \int_{\mathbf{r}} J\phi. \tag{4.5}$$

Now we add a correction to our free energy that includes our regulator

$$\Delta F_k = \int \frac{d^d\mathbf{q}}{(2\pi)^d}\phi(\mathbf{q})R_k(\mathbf{q})\phi(\mathbf{q}). \tag{4.6}$$

Here, $R_k(\mathbf{q})$ acts as a smooth UV and IR cutoff. Some common examples of regulators include $\frac{q^2}{\exp(q^2/k^2)-1}$ and $(k^2-q^2)\theta(k^2-q^2)$. Then, we define our regularized partition function as

$$Z_k(J) = \int \mathcal{D}\phi \exp\Big(-F[\phi] - \Delta F_k + \int_{\mathbf{r}} J\phi\Big). \tag{4.7}$$

A regulator must satisfy

$$R_{k=\Lambda}(\mathbf{q}) \sim \Lambda^2 \tag{4.8}$$

$$R_{k=0}(\mathbf{q}) = 0. \tag{4.9}$$

The initial value of the regulator should be very large and have little contribution of order e^{-k^2}. When $k \to 0$, then our regulator should vanish and leave the original partition function. R_k grows like k^2 for low momentum and decays exponentially for high momenta with characteristic width k. The regulator can be reduced to the form

$$R_k(\mathbf{q}) = q^2 r\Big(\frac{q^2}{k^2}\Big). \tag{4.10}$$

For the regulator to properly regularize UV and IR divergences, it must satisfy two conditions. For the IR regularization at

$$r(y) \sim \frac{1}{y} \text{ as } y \to 0, \tag{4.11}$$

and for the UV regularization

$$r(y) \sim \frac{1}{y^{d/2}} \text{ as } y \to \infty. \tag{4.12}$$

This gives ultraviolet and infrared conditions. The first limit is to suppress low momentum modes, such as Goldstone modes, as the propagator acquires additional mass at low momentum below k. However, renormalization is required to deal with

the cut-off. The second limit guarantees it decays exponentially fast to avoid UV divergences. Now, using our regulator, we will define a regularized effective action.

Let $W_k = \log Z_k$, we can now write our k-dependent effective action as

$$\Gamma_k[\varphi] = -W_k[J] + \int_r J \cdot \phi - \Delta F_k. \tag{4.13}$$

Our goal is to solve Γ_k, with initial conditions at $k = \Lambda$ and ending at $k = 0$. The Wetterich equation is the exact flow equation for Γ_k and is given by

$$\partial_t \Gamma_k = \frac{1}{2} \mathrm{Tr} \left[\left(\Gamma_k^{(2)} + R_k \right)^{-1} \partial_t R_k \right] \tag{4.14}$$

$$= \frac{1}{2} \int \frac{\mathrm{d}^d \mathbf{q}}{(2\pi)^d} \mathrm{tr} \Big[\mathcal{G}_k(\phi, \mathbf{q}) \partial_t R_k(\mathbf{q}) \Big]. \tag{4.15}$$

Here, $\Gamma_k^{(2)}$ is the second functional derivative, or Hessian, of Γ_k. Tr is a trace over matrix indices and spatial degrees of freedom via integration. t is the RG time and is given by $\log \frac{\Lambda}{k}$, and it runs from $t = 0$ to $t = \infty$. The regularized propagator $\mathcal{G}_k(\phi, \mathbf{q})$ is given by

$$\mathcal{G}_k(\phi, \mathbf{q}) = \Big(\Gamma^{(2)}[\phi] + R_k(\mathbf{q}) \Big)^{-1}. \tag{4.16}$$

The flow of Γ_k does depends on our choice of regulator, but all regulator-dependent flows converge to the same quantum effective action when $k \to 0$. Solving the full Wetterich equation is intractable for any system, so we must truncate the effective action at a finite number of terms. However, this destroys the regulator-independence of our effective action. Despite this, choosing tried and tested regulators will generally provide accurate results.

4.2 U(1) theory

We now do a simple calculation using FRG, similar to what we did for the Wilsonian Renormalization Group. We first make an ansatz for the effective free energy being

the same as our GL free energy

$$\Gamma_k[\phi] = \int d^d x \left(|\nabla\phi(\boldsymbol{x})|^2 + \alpha_k |\phi(\boldsymbol{x})|^2 + \frac{\lambda_k}{2} |\phi(\boldsymbol{x})|^4 \right) \tag{4.17}$$

$$\doteq \int d^d x \left(|\nabla\phi(\boldsymbol{x})|^2 + U_k(\phi(\boldsymbol{x})) \right), \tag{4.18}$$

where U_k is the effective potential. The Hessian of Γ_k is given by its second functional derivatives which is given by

$$\Gamma_k^{(2)}[\phi](\boldsymbol{x},\boldsymbol{y}) = \frac{\delta^2 \Gamma_k[\phi]}{\delta\Phi(\boldsymbol{x})\delta\Phi(\boldsymbol{y})} = \begin{pmatrix} \Gamma^{(2)}_{\phi\phi} & \Gamma^{(2)}_{\phi\phi^*} \\ \Gamma^{(2)}_{\phi^*\phi} & \Gamma^{(2)}_{\phi^*\phi^*} \end{pmatrix}_{(\boldsymbol{x},\boldsymbol{y})} \tag{4.19}$$

$$= \begin{pmatrix} \lambda_k \phi^{*2} & -\nabla^2_{\boldsymbol{x}} + \alpha_k + 2\lambda_k |\phi|^2 \\ -\nabla^2_{\boldsymbol{x}} + \alpha_k + 2\lambda_k |\phi|^2 & \lambda_k \phi^2 \end{pmatrix} \delta^{(d)}(\boldsymbol{x}-\boldsymbol{y}), \tag{4.20}$$

where $\Phi = (\phi, \phi^*)$. Our regulator will have the form

$$\mathcal{R}_k(\boldsymbol{x},\boldsymbol{y}) = \begin{pmatrix} 0 & R_k(-\nabla^2_{\boldsymbol{x}}) \\ R_k(-\nabla^2_{\boldsymbol{x}}) & 0 \end{pmatrix} \delta^{(d)}(\boldsymbol{x}-\boldsymbol{y}). \tag{4.21}$$

The infrared limit corresponds to $k \to 0$. The flow of Γ_k in the infrared limit is defined by the Wetteretich equation

$$\partial_t \Gamma_k[\phi] = -k\frac{d}{dk}\Gamma_k[\phi] = \frac{1}{2}\mathrm{Tr}\left[\dot{\mathcal{R}}_k \left(\Gamma_k^{(2)}[\phi] + \mathcal{R}_k \right)^{-1} \right], \tag{4.22}$$

where $t = \ln\left(\frac{\Lambda}{k}\right)$, which flows to $t = \infty$ in the infrared limit. Λ is the UV cut-off. We assume our field is constant with $\phi(\boldsymbol{x}) = \phi \in \mathbb{R}$. The flow equation for our effective potential becomes

$$\partial_t U_k(\phi) = \frac{1}{2}\mathrm{tr}\int \frac{d^d\mathbf{q}}{(2\pi)^d} \dot{\mathcal{R}}_k(\mathbf{q}) G_k(\mathbf{q},\phi), \tag{4.23}$$

with

$$\mathcal{R}_k(\mathbf{q}) = \begin{pmatrix} 0 & R_k(q) \\ R_k(q) & 0 \end{pmatrix}, \tag{4.24}$$

and the inverse propagator is defined as

$$G_k(\mathbf{q},\phi)^{-1} = \Gamma_k^{(2)}[\phi] + \mathcal{R}_k(\mathbf{q}) \tag{4.25}$$

$$= \begin{pmatrix} \lambda_k\phi^2 & q^2 + R_k(q) + \alpha_k + 2\lambda_k\phi^2 \\ q^2 + R_k(q) + \alpha_k + 2\lambda_k\phi^2 & \lambda_k\phi^2 \end{pmatrix}, \tag{4.26}$$

which lets us determine the propagator as

$$G_k(\mathbf{q},\phi) = \begin{pmatrix} \frac{\lambda_k\phi^2}{\lambda_k^2\phi^4-[q^2+R_k(q)+\alpha_k+2\lambda_k\phi^2]^2} & \frac{-\left[q^2+R_k(q)+\alpha_k+2\lambda_k\phi^2\right]}{\lambda_k^2\phi^4-[q^2+R_k(q)+\alpha_k+2\lambda_k\phi^2]^2} \\ \frac{-\left[q^2+R_k(q)+\alpha_k+2\lambda_k\phi^2\right]}{\lambda_k^2\phi^4-[q^2+R_k(q)+\alpha_k+2\lambda_k\phi^2]^2} & \frac{\lambda_k\phi^2}{\lambda_k^2\phi^4-[q^2+R_k(q)+\alpha_k+2\lambda_k\phi^2]^2} \end{pmatrix}. \tag{4.27}$$

We can now choose a regulator

$$R_k(q) = (k^2-q^2)\theta(k^2-q^2), \tag{4.28}$$

$$\dot{R}_k(q) = -2k^2\theta(k^2-q^2). \tag{4.29}$$

This is the simplest regulator and often simplifies to the trace-log formula corrections. We can now start calculating the flow in the effective potential as

$$\partial_t U_k(\phi) = \frac{1}{2}\int \frac{d^d\mathbf{q}}{(2\pi)^d}\dot{\mathrm{R}}_\mathrm{k}\frac{-2\left[\mathrm{q}^2+\mathrm{R}_\mathrm{k}(\mathrm{q})+\alpha_\mathrm{k}+2\lambda_\mathrm{k}\phi^2\right]}{\lambda_\mathrm{k}^2\phi^4-\left[\mathrm{q}^2+\mathrm{R}_\mathrm{k}(\mathrm{q})+\alpha_\mathrm{k}+2\lambda_\mathrm{k}\phi^2\right]^2} \tag{4.30}$$

$$= -2k^2\int \frac{d^d\mathbf{q}}{(2\pi)^d}\theta(\mathrm{k}^2-\mathrm{q}^2)\frac{\mathrm{k}^2+\alpha_\mathrm{k}+2\lambda_\mathrm{k}\phi^2}{\left[\mathrm{k}^2+\alpha_\mathrm{k}+2\lambda_\mathrm{k}\phi^2\right]^2-\lambda_\mathrm{k}^2\phi^4} \tag{4.31}$$

$$= -2\frac{\Omega_d}{d(2\pi)^d}k^{d+2}\frac{k^2+\alpha_k+2\lambda_k\phi^2}{\left[k^2+\alpha_k+2\lambda_k\phi^2\right]^2-\lambda_k^2\phi^4}. \tag{4.32}$$

From the flow equation of the effective potential we can determine the flow equations of the coupling constants.

$$\alpha_k = U_k''(0), \tag{4.33}$$

$$\lambda_k = \frac{1}{6}U_k^{(4)}(0). \tag{4.34}$$

The flow equations for the coupling constants are given by

$$\partial_t\alpha_k = \dot{U}_k''(0) \tag{4.35}$$

$$\partial_t\lambda_k = \frac{1}{6}\dot{U}_k^{(4)}(0). \tag{4.36}$$

We evaluate these

$$\partial_t\alpha_k = -2\frac{\Omega_d}{d(2\pi)^d}k^{d+2}\,\partial_\phi^2\big|_{\phi=0}\,\frac{k^2+\alpha_k+2\lambda_k\phi^2}{\left[k^2+\alpha_k+2\lambda_k\phi^2\right]^2-\lambda_k^2\phi^4} \tag{4.37}$$

$$= 4\frac{\Omega_d}{d(2\pi)^d}k^{d+2}\frac{\lambda_k}{\left(k^2+\alpha_k\right)^2}, \tag{4.38}$$

$$\partial_t \lambda_k = -\frac{1}{3}\frac{\Omega_d}{d(2\pi)^d} k^{d+2}\, \partial_\phi^4\big|_{\phi=0} \frac{k^2+\alpha_k+2\lambda_k\phi^2}{\left[k^2+\alpha_k+2\lambda_k\phi^2\right]^2-\lambda_k^2\phi^4} \tag{4.39}$$

$$= -\frac{10}{3}\frac{\Omega_d}{d(2\pi)^d} k^{d+2} \frac{\lambda_k^2}{\left(k^2+\alpha_k\right)^3}. \tag{4.40}$$

We can define new dimensionless coupling constants as

$$\tilde{\alpha}_k = \frac{\alpha_k}{k^2}, \tag{4.41}$$

$$\tilde{\lambda}_k = \frac{\lambda_k}{k^{4-d}} \tag{4.42}$$

This transforms as

$$\partial_t \tilde{\alpha}_k = -k\partial_k \frac{\alpha_k}{k^2} = 2\tilde{\alpha}_k + \frac{1}{k^2}\dot{\alpha_k} \tag{4.43}$$

$$\partial_t \tilde{\lambda}_k = -k\partial_k \frac{\lambda_k}{k^{4-d}} = (4-d)\tilde{\lambda}_k + \frac{1}{k^{4-d}}\dot{\lambda_k}. \tag{4.44}$$

Let us define $\epsilon = 4-d$. Our dimensionless flow equations are

$$\partial_t \tilde{\alpha}_k = 2\tilde{\alpha}_k + 4\frac{\Omega_d}{d(2\pi)^d}\frac{\tilde{\lambda}_k}{\left(1+\tilde{\alpha}_k\right)^2} \tag{4.45}$$

$$\partial_t \tilde{\lambda}_k = \epsilon\tilde{\lambda}_k - \frac{10}{3}\frac{\Omega_d}{d(2\pi)^d}\frac{\tilde{\lambda}_k^2}{\left(1+\tilde{\alpha}_k\right)^3}. \tag{4.46}$$

The Wilson Fisher fixed point is given by

$$\tilde{\alpha}_\star = -\frac{1}{11} \tag{4.47}$$

$$\tilde{\lambda}_\star = 2.225 \tag{4.48}$$

4.3 Functional Renormalization of ^{3}He

4.3.1 3D System

We calculate the FRG flow equations in the 3D case using an ansatz that is our free energy

$$\Gamma_\Lambda[A] = F[\mathrm{A}] = \int d^3\mathbf{q}\left\{U(\mathrm{A}) + (\gamma-1)q_i \mathrm{A}^*_{\mu i} q_j \mathrm{A}_{\mu j} + q_i \mathrm{A}^*_{\mu j} q_i \mathrm{A}_{\mu j}\right\}, \tag{4.49}$$

and the effective potential is defined as

$$U(\mathrm{A}) = \alpha \mathrm{tr} \mathrm{A}\mathrm{A}^\dagger + \sum_n \beta_n I_n(\mathrm{A}). \tag{4.50}$$

A has 9 complex components, which can be written in terms of two real components. We will consider the free energy the same as our effective action at the UV scale Γ_Λ. To diagonalize the propagator, we choose the following basis

$$A_{\mu i} = \frac{1}{\sqrt{2}} \left(\psi_{\mu i} + \bar{\psi}_{\mu i} \right) + \frac{i}{\sqrt{2}} \left(\psi_{\mu i} - \bar{\psi}_{\mu i} \right). \tag{4.51}$$

Let $\Psi = (\psi_{1,1}, \psi_{1,2}, \psi_{1,3}, \psi_{2,1} \dots \psi_{3,3})$ and $\bar{\Psi} = (\bar{\psi}_{1,1}, \bar{\psi}_{1,2}, \bar{\psi}_{1,3}, \bar{\psi}_{2,1} \dots \bar{\psi}_{3,3})$. Now we calculate the hessian of $\Gamma[\Psi, \bar{\Psi}]$

$$\Gamma^{(2)}[\Psi, \bar{\Psi}] = \frac{\delta^2 \Gamma[\Psi, \bar{\Psi}]}{\delta \Psi(q) \delta \Psi(q')} = \delta(q - q') \begin{pmatrix} \frac{\delta^2 \Gamma}{\delta \psi^2} & \frac{\delta^2 \Gamma}{\delta \bar{\psi} \delta \psi} \\ \frac{\delta^2 \Gamma}{\delta \psi \delta \bar{\psi}} & \frac{\delta^2 \Gamma}{\delta \bar{\psi}^2} \end{pmatrix}. \tag{4.52}$$

This will be a rank 4 tensor since the order parameter is rank 2. As we calculated in Sec. 2.3

$$\Gamma^{(2)}_{\mu i, \nu j}[\Psi, \bar{\Psi}] = \delta_{\mu\nu} \Big((q^2 + \alpha) \delta_{ij} + (\gamma - 1) q_i q_j \Big) \begin{pmatrix} 1 & 0 \\ 0 & 1 \end{pmatrix} + \mathcal{V}_{\mu i, \nu j}(\Psi, \bar{\Psi}). \tag{4.53}$$

We can easily calculate the inverse of this to get the propagator. Let $q^2 = q_x^2 + q_y^2 + q_z^2$. Let $\hat{q}_i = \frac{q_i}{q}$, with $\sum_i {\hat{q}_i}^2 = 1$. In spherical coordinates this is $\hat{\mathbf{q}}_i = \Big(\cos\theta \sin\phi, \sin\theta \sin\phi, \cos\phi \Big)$. We can now choose the following regulator

$$\mathcal{R}_k(q) = \delta_{\mu\nu} (k^2 - q^2) \theta(k^2 - q^2) \Big(\delta_{ij} + (\gamma - 1) \hat{q}_i \hat{q}_j \Big) \begin{pmatrix} 1 & 0 \\ 0 & 1 \end{pmatrix}, \tag{4.54}$$

where $\theta(x)$ is the Heaviside step function given by

$$\theta(x) = \begin{cases} 1 & x \geq 0 \\ 0 & x < 0 \end{cases}. \tag{4.55}$$

We proceed by deriving the regulator and getting

$$\dot{\mathcal{R}}_k(q) = k \frac{d}{dk} \mathcal{R}_k = \delta_{\mu\nu} \Big(2k^2 \delta_{ij} + 2(\gamma - 1) k^2 \hat{q}_i \hat{q}_j \Big) \begin{pmatrix} 1 & 0 \\ 0 & 1 \end{pmatrix}. \tag{4.56}$$

We can write the inverse propagator when the order parameter is zero as

$$\mathcal{G}_k^{-1}(0,q) = \Gamma^{(2)}[0] + \mathcal{R}_k = \delta_{\mu\nu}\Big((k^2+\alpha)\delta_{ij} + (\gamma-1)[k^2\hat{q}_i\hat{q}_j]\Big)\begin{pmatrix} 1 & 0 \\ 0 & 1 \end{pmatrix} \tag{4.57}$$

The zero field propagator is given by

$$\mathcal{G}_k(0,q) = \mathcal{G}_0 = \delta_{\mu\nu}\left(\frac{\delta_{ij}}{(k^2+\alpha)} - \frac{(\gamma-1)k^2\hat{q}_i\hat{q}_j}{(k^2+\alpha)(\gamma k^2+\alpha)}\right)\begin{pmatrix} 1 & 0 \\ 0 & 1 \end{pmatrix} \tag{4.58}$$

Since Γ_k only has k-dependence in its effective potential, we will calculate the flow of U_k.

$$\partial_t U_k = \frac{1}{2}\int d^d\mathbf{q}\ \mathrm{tr}\left[\left(\Gamma^{(2)}[\Psi,\bar{\Psi}] + \mathcal{R}_k(q)\right)^{-1}\dot{\mathcal{R}}_k(q)\right], \tag{4.59}$$

where $t = \ln\left(\frac{\Lambda}{k}\right)$, where Λ and k are the ultraviolet and infrared cutoffs, respectively.

Similarly to Chapter 3, we can relate the coupling constants to the effective potential by taking a linear combination of derivatives as follows

$$\begin{pmatrix} \beta_1 \\ \beta_2 \\ \beta_3 \\ \beta_4 \\ \beta_5 \end{pmatrix} = \frac{1}{16}\begin{pmatrix} 0 & 2 & 0 & 0 & 0 \\ 0 & 2 & 0 & 2 & 0 \\ 1 & -2 & -1 & 0 & 0 \\ 0 & 0 & 1 & -2 & 1 \\ 1 & -2 & 0 & 0 & -1 \end{pmatrix}\begin{pmatrix} \frac{\partial^4}{\partial\psi_{1,1}^2\partial\bar{\psi}_{1,1}^2} \\ \frac{\partial^4}{\partial\psi_{1,1}\partial\psi_{2,2}\partial\bar{\psi}_{1,1}\partial\bar{\psi}_{2,2}} \\ \frac{\partial^4}{\partial\psi_{1,3}^2\partial\bar{\psi}_{1,1}^2} \\ \frac{\partial^4}{\partial\psi_{2,3}^2\partial\bar{\psi}_{1,1}^2} \\ \frac{\partial^4}{\partial\psi_{1,1}^2\partial\bar{\psi}_{2,1}^2} \end{pmatrix}\Bigg|_{\mathrm{A}=0} U(\mathrm{A}), \tag{4.60}$$

Additionally, we have the following relation for α

$$\frac{\partial^2}{\partial\psi_{1,1}^2}\Big|_{\mathrm{A}=0} U(\mathrm{A}) = \alpha. \tag{4.61}$$

Unlike with RG, we will calculate the flow equations for α as well for greater accuracy in our result. We can summarize the relationship between U and the coupling constants with the relation

$$\hat{P}_g U(A) = g. \tag{4.62}$$

From eq. (4.59), we can derive the flow equation for our coupling constants

$$\partial_t g_k = \partial_t\Big(\hat{P}_g U_k\Big) = \frac{1}{2}\int \frac{d^d\mathbf{q}}{(2\pi)^d}\mathrm{tr}\dot{R}_k\hat{P}_g\mathcal{G}_k(\Psi,\bar{\Psi},q). \tag{4.63}$$

From appendix B we can analytically find derivatives of the propagator. For a second derivative, the formula is given by

$$\frac{\partial^2}{\partial\psi_{\mu,i}\partial\psi_{\nu,j}}\Big|_{A=0}\mathcal{G}_k(\Psi,\bar{\Psi},\boldsymbol{q}) = -\mathcal{G}_0\frac{\partial^2\mathcal{V}}{\partial\psi_{\mu,i}\partial\psi_{\nu,j}}\mathcal{G}_0 \tag{4.64}$$

The fourth-derivative case is given by

$$\begin{aligned}\frac{\partial^4}{\partial\psi_{\mu,i}\partial\psi_{\nu,j}\partial\bar{\psi}_{\rho,k}\partial\bar{\psi}_{\sigma,l}}\Big|_{A=0}\mathcal{G}_k(\Psi,\bar{\Psi},\boldsymbol{q}) &= \mathcal{G}_0\frac{\partial^2\mathcal{V}}{\partial\psi_{\mu,i}\partial\psi_{\nu,j}}\mathcal{G}_0\frac{\partial^2\mathcal{V}}{\partial\bar{\psi}_{\rho,k}\partial\bar{\psi}_{\sigma,l}}\mathcal{G}_0\\ +\mathcal{G}_0\frac{\partial^2\mathcal{V}}{\partial\psi_{\mu,i}\partial\bar{\psi}_{\rho,k}}\mathcal{G}_0\frac{\partial^2\mathcal{V}}{\partial\psi_{\nu,j}\partial\bar{\psi}_{\sigma,l}}\mathcal{G}_0 &+ \mathcal{G}_0\frac{\partial^2\mathcal{V}}{\partial\psi_{\mu,i}\partial\bar{\psi}_{\sigma,l}}\mathcal{G}_0\frac{\partial^2\mathcal{V}}{\partial\bar{\psi}_{\rho,k}\partial\psi_{\nu,j}}\mathcal{G}_0.\end{aligned} \tag{4.65}$$

We have selected $\mathcal{R}_k$ such that all instances of q cancel out from $\mathcal{G}_\prime$ and only angular dependence is left. Our flow equation simplifies to a radial integral over the solid angle Ω below

$$\partial_t g_k = \frac{k^d}{2d(2\pi)^d}\int d\Omega\ \ \mathrm{tr}\Big[\dot{R}_k\hat{P}_i\mathcal{G}_k(\Psi,\bar{\Psi},q)\Big]. \tag{4.66}$$

We perform the substitution $\alpha_k \to k^2\tilde{\alpha}_k$ and $\beta_{ik} \to k^2\tilde{\beta}_{ik}$ to arrive at our renormalized flow equation. From simple dimensional analysis, we can see that the dimensionless equations will have a prefactor k^{4-d} for the quartic couplings and k^2 for α. We now solve for the flow equations in the dimensionless coupling constants

$$\partial_t\beta_{ik} = \partial_t\Big(k^{4-d}\tilde{\beta}_{ik}\Big) = k^{4-d}\tilde{B}_{\beta_i} \tag{4.67}$$

$$\implies k^{4-d}\partial_t\tilde{\beta}_{ik} - (4-d)k^{4-d}\tilde{\beta}_{ik} = k^{4-d}\tilde{B}_{\beta_i} \tag{4.68}$$

$$\implies \partial_t\tilde{\beta}_{ik} = (4-d)\tilde{\beta}_{ik} + \tilde{B}_{\beta_i}, \tag{4.69}$$

where $\tilde{B}_{\beta_i}$ depends only on the renormalized couplings. For a coupling constant g, we define the functions $\tilde{B}_g$ as the dimensionless version of B_g. We determine B_{β_i} have the form

$$B_{\beta_i} = \frac{-2\mathcal{C}_i(1)\Big[3(\alpha-1)^2 + (\gamma-1)(\alpha-1)(\alpha-5) + 2(\gamma-1)^2\Big] + \alpha(\gamma-1)^2\mathcal{D}_i}{3\pi^2(\alpha-1)^2(\alpha-\gamma)^2}, \tag{4.70}$$

where $\mathcal{C}_i(1)$ are defined in eqs. (3.101) to (3.105).

The values of $\mathcal{D}_i$ are given by

$$\mathcal{D}_1 = 8\beta_1\left(\beta_3 - 4\beta_2\right) + 2\beta_5\left(4\beta_2 - 8\beta_3 + 2\beta_4 + 3\beta_5\right) \tag{4.71}$$

$$\begin{aligned}\mathcal{D}_2 = 2\Big[&-16\beta_1^2 + 4\left(\beta_3 + \beta_4 + \beta_5\right)\beta_1 - 8\beta_2^2 + \beta_3^2 - \beta_4^2 \\ &- 4\beta_5^2 + 8\beta_3\beta_4 + 4\beta_2\left(\beta_3 + \beta_4\right) + 2\beta_3\beta_5 + 2\beta_4\beta_5\Big]\end{aligned} \tag{4.72}$$

$$\begin{aligned}\mathcal{D}_3 = 2\Big[&4\beta_1^2 + 4\left(\beta_3 - 4\left(\beta_4 + \beta_5\right)\right)\beta_1 + 2\beta_2^2 + 6\beta_3^2 + 4\beta_4^2 \\ &+ \beta_5^2 - 32\beta_3\beta_4 + 4\beta_2\left(\beta_4 - 4\beta_3\right) - 8\beta_3\beta_5 + 2\beta_4\beta_5\Big]\end{aligned} \tag{4.73}$$

$$\begin{aligned}\mathcal{D}_4 = 2\Big[&4\beta_1^2 + 4\left(-4\beta_3 + \beta_4 + \beta_5\right)\beta_1 + 2\beta_2^2 - 19\beta_3^2 - 11\beta_4^2 \\ &+ \beta_5^2 + 8\beta_3\beta_4 + 4\beta_2\left(\beta_3 - 4\beta_4\right) + 2\beta_3\beta_5 - 8\beta_4\beta_5\Big]\end{aligned} \tag{4.74}$$

$$\mathcal{D}_5 = -2\Big[\beta_1\left(12\beta_3 - 8\beta_2\right) + \beta_5\left(12\beta_2 - 4\beta_3 + 6\beta_4 + 9\beta_5\right)\Big] \tag{4.75}$$

The flow equation for the dimensionless α is given by

$$\partial_t\tilde{\alpha}_k = 2\tilde{\alpha}_k + \tilde{B}_\alpha, \tag{4.76}$$

We computed B_α to be

$$B_\alpha = \frac{2\left(\alpha^2(\gamma+2) - 6\alpha\gamma + 2\gamma^2 + \gamma\right)\left(\beta_1 + 5\beta_2 + 2\beta_3 + 3\beta_4 + 2\beta_5\right)}{3\pi^2(\alpha-1)^2(\alpha-\gamma)^2}. \tag{4.77}$$

We also apply the flow equations of γ from [26], and we have listed the equations in Appendix C. The initial conditions for our coupling constants are

$$\beta_i(0) = -\beta_{1,MF}\Big(-1, 2, 2, 2, -2\Big) \tag{4.78}$$

$$\alpha(0) = 0 \tag{4.79}$$

$$\gamma(0) = 3; \tag{4.80}$$

We numerically integrated the FRG flow equations in the 3D limit, and the results are plotted in fig. 4.1. The five quartic coupling constants $\beta_a(t)$ deviate significantly from the fixed ratios of the mean-field initial conditions in eq. (4.103). The coefficients $\beta_a(t)$ in the early stages $t \sim 0$ indicate the C_{AB} remains negative, despite briefly flowing towards positive C_{AB}, so the B-phase is favoured over the A-phase. However,

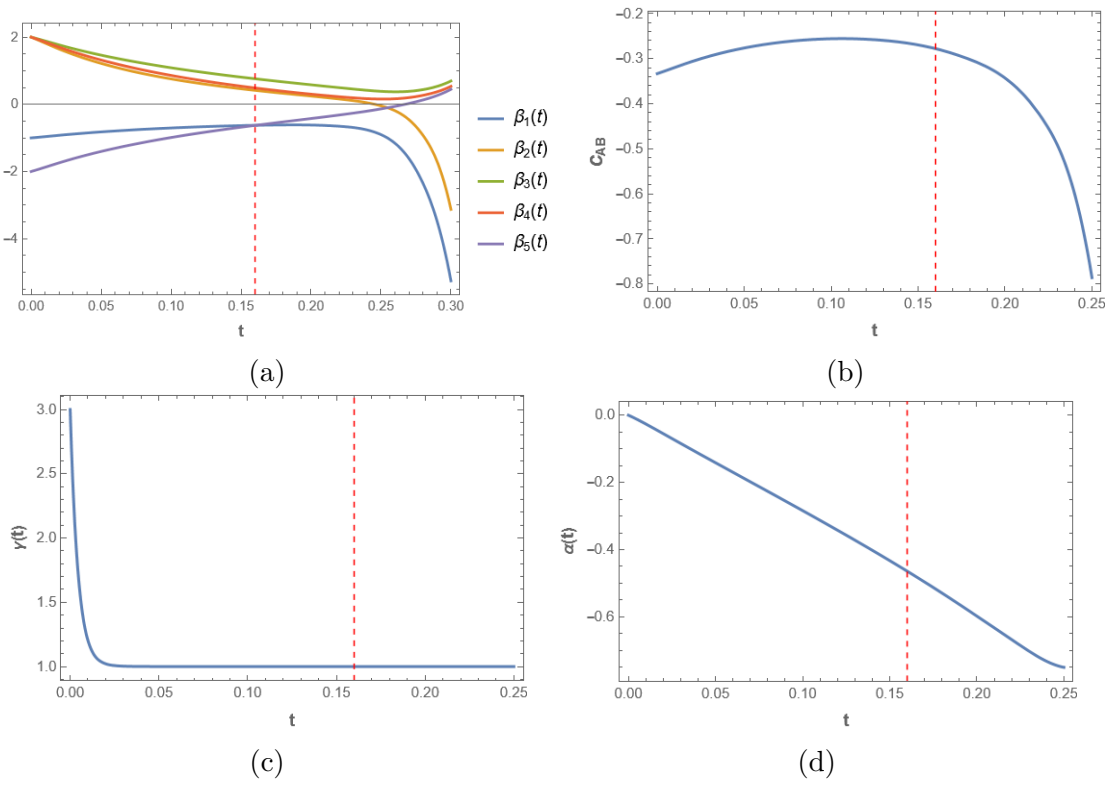

Figure 4.1: **FRG flow in the 3D limit.** *a)* FRG flow of the five quartic couplings $\beta_a(t)$, where the flow is numerically determined and plotted against $t = \ln \frac{\Lambda}{k}$. The fixed ratios of the quartic couplings change significantly, and the flow is qualitatively similar to the 3D RG flow. The flow becomes unphysical at the red dotted line because the free energy of the planar phase diverges. *b)* The flow of C_{AB}, which is positive when the A phase is favoured and negative when the B phase is favoured, is plotted against t. The B-phase is shown to be favoured in the valid region of our FRG, but in comparison to the 3D RG flow of C_{AB}, we find that the FRG reveals that there is an initial tendency towards the A-phase. *c)* The RG flow of γ with respect to t. γ decays quickly to $\gamma = 1$.*d)* The flow of α. α starts at the phase transition and flows to the negative, indicating that the system transitioned into a symmetry-broken state.

this indicates that the higher-order corrections included are pushing the flow towards the A-phase.

We notice that the decay of $\gamma(t)$ to $\gamma_\star = 1$ is quite rapid, but it is similar to the 3D RG case. When $\gamma = 1$, the flow equations for the quartic couplings become identical. Because γ is the primary driver for changing the fixed ratios between the quartic couplings, its rapid decay leads to a smaller effect on the quartic couplings. α starts at the phase transition with $\alpha = 0$ and flows to the negative, indicating that the

system transitioned into a symmetry-broken state. This indicates that the superfluid phase transition occurs.

The coupling constants β_a quickly take on unphysical values that cause the free energy to become unbounded below. We detect this when the A-phase or B-phase free energies become singular. The inequality that appears to be violated is

$$3\beta_{12} + \beta_{345} > 0, \tag{4.81}$$

which leads to our effective potential becoming unbounded below. Our FRG flow equations can no longer be applied in this unphysical regime. For all physical values of the FRG, the B-phase is energetically favoured over the A-phase. This is consistent with experiment [6].

4.3.2 2D System

We can extend our analysis of FRG to the 2D limit and gain an understanding of ^{3}He under complete confinement when the order parameter's last column vanishes completely. The order parameter is given by

$$\mathrm{A}_\perp = \begin{pmatrix} \mathrm{A}_{1,1} & \mathrm{A}_{1,2} \\ \mathrm{A}_{2,1} & \mathrm{A}_{2,2} \\ \mathrm{A}_{3,1} & \mathrm{A}_{3,2} \end{pmatrix}. \tag{4.82}$$

The free energy is

$$\Gamma_\Lambda = F[\mathrm{A}_\perp] = \int d^2\mathbf{q}_\perp \left\{ U(\mathrm{A}_\perp) + (\gamma - 1) q_i \mathrm{A}^*_{\perp\mu i} q_j \mathrm{A}_{\perp\mu j} + q_i \mathrm{A}^*_{\perp\mu j} q_i \mathrm{A}_{\perp\mu j} \right\}, \tag{4.83}$$

where $\mathbf{q}_\perp = (q_x, q_y)$. The effective potential is defined as

$$U(\mathrm{A}_\perp) = \alpha \mathrm{tr} \mathrm{A}_\perp \mathrm{A}^\dagger_\perp + \sum_n \beta_n I_n(\mathrm{A}_\perp). \tag{4.84}$$

The propagator is defined similarly to the 3D case

$$\Gamma^{(2)}_{\mu i,\nu j}[\Psi, \bar{\Psi}] = \delta_{\mu\nu} \Big((q_\perp^2 + \alpha)\delta_{ij} + (\gamma - 1) q_{\perp i} q_{\perp j} \Big) \begin{pmatrix} 1 & 0 \\ 0 & 1 \end{pmatrix} + \mathcal{V}_{\mu i,\nu j}(\Psi, \bar{\Psi}). \tag{4.85}$$

Here we define $q_\perp^2 = q_x^2 + q_y^2$. The other main difference between the 3D and 2D propagators is that i and j run over two spatial coordinates rather than three. Our regulator is defined as

$$\mathcal{R}_k(q_\perp) = \delta_{\mu\nu}(k^2 - q_\perp^2)\theta(k^2 - q_\perp^2)\Big(\delta_{ij} + (\gamma - 1)\hat{q}_{\perp i}\hat{q}_{\perp j}\Big)\begin{pmatrix} 1 & 0 \\ 0 & 1 \end{pmatrix}. \tag{4.86}$$

In polar coordinates, we have $\hat{\mathbf{q}}_{\perp i} = \Big(\cos\theta, \sin\theta\Big)$. We proceed by deriving the regulator and getting

$$\dot{\mathcal{R}}_k(q) = k\frac{d}{dk}R_k(q) = R_k(q) = \delta_{\mu\nu}\Big(2k^2\delta_{ij} + 2(\gamma - 1)k^2\hat{q}_i\hat{q}_j\Big)\begin{pmatrix} 1 & 0 \\ 0 & 1 \end{pmatrix}. \tag{4.87}$$

Now, we can write the inverse propagator when the order parameter is zero as

$$\mathcal{G}_k^{-1}(0,q) = \Gamma^{(2)}[0] + \mathcal{R}_k = \delta_{\mu\nu}\Big((k^2 + \alpha)\delta_{ij} + (\gamma - 1)[k^2\hat{q}_{\perp i}\hat{q}_{\perp j}]\Big)\begin{pmatrix} 1 & 0 \\ 0 & 1 \end{pmatrix}. \tag{4.88}$$

The propagator at zero order parameter is given by

$$\mathcal{G}_k(0,q) = \mathcal{G}_0 = \delta_{\mu\nu}\left(\frac{\delta_{ij}}{(k^2 + \alpha)} - \frac{(\gamma - 1)k^2\hat{q}_{\perp i}\hat{q}_{\perp j}}{(k^2 + \alpha)(\gamma k^2 + \alpha)}\right)\begin{pmatrix} 1 & 0 \\ 0 & 1 \end{pmatrix}. \tag{4.89}$$

Now, we will solve the Wetterich Equation using our ansatz. is given by

$$\partial_t U_k = \frac{1}{2}\int d^d\mathbf{q}_\perp \mathrm{tr}\left[\Big(\Gamma^{(2)}[\Psi, \bar{\Psi}] + \mathcal{R}_k(q)\Big)^{-1}\dot{\mathcal{R}}_k(q)\right] \tag{4.90}$$

In 2D, we can relate the coupling constant to the effective potential with the following linear combinations of derivatives

$$\begin{pmatrix} \beta_1 \\ \beta_2 \\ \beta_3 \\ \beta_4 \\ \beta_5 \end{pmatrix} = \frac{1}{12}\begin{pmatrix} 0 & 3 & -3 & 0 & 0 \\ 0 & 3 & 3 & 0 & 0 \\ 1 & -3 & 3 & -3 & 0 \\ 0 & 0 & -6 & 3 & 3 \\ 1 & -3 & 3 & 0 & -3 \end{pmatrix}\begin{pmatrix} \frac{\partial^4}{\partial\psi_{1,1}^4} \\ \frac{\partial^4}{\partial^2\psi_{1,2}\partial^2\psi_{2,1}} \\ \frac{\partial^4}{\partial\psi_{3,1}^2\partial\bar{\psi}_{2,2}^2} \\ \frac{\partial^4}{\partial\psi_{1,2}^2\partial\bar{\psi}_{1,1}^2} \\ \frac{\partial^4}{\partial\psi_{1,1}^2\partial\bar{\psi}_{3,1}^2} \end{pmatrix}\Bigg|_{\mathrm{A}_\perp=0} U(\mathrm{A}_\perp), \tag{4.91}$$

and

$$\frac{1}{2}\frac{\partial^2 U(A_\perp)}{\partial\psi_{1,1}^2}\Big|_{A_\perp=0} = 0. \tag{4.92}$$

The rest of the derivation is identical to the 3D case. The flow of our dimensionless quartic couplings are given by

$$\partial_t \beta_{ik} = \partial_t \Big(\hat{P}_i U_k \Big) = \frac{1}{2} \int \frac{d^d \mathbf{q}}{(2\pi)^d} \mathrm{tr} \dot{R}_k \hat{P}_i \mathcal{G}_k(\Psi, \bar{\Psi}, q). \tag{4.93}$$

We find the flow equations take the form

$$\partial_t \tilde{\beta}_{ik} = (4-d)\tilde{\beta}_{ik} - \tilde{C}_{\beta_i} \tag{4.94}$$

$$\partial_t \tilde{\alpha}_k = 2\tilde{\alpha}_k - \tilde{C}_\alpha. \tag{4.95}$$

For a coupling constant g, we define the functions $\tilde{C}_g$ as the dimensionless version of C_g.

$$C_{\beta_i} = \frac{\tilde{\mathcal{C}}_i(1)\Big[(\alpha-1)^2 + \frac{1}{2}(\alpha-3)(\alpha-1)(\gamma-1) + \frac{1}{2}(\gamma-1)^2\Big] + \alpha(\gamma-1)^2 \tilde{\mathcal{D}}_i}{(\alpha-1)^2(\alpha-\gamma)^2}, \tag{4.96}$$

where $\tilde{\mathcal{C}}_i(1)$ are defined in eqs. (3.140) to (3.144). The flow equation for α can be determined using eq. (4.64), and the beta function is given by

$$C_\alpha = \frac{(2\beta_1 + 7\beta_2 + 4\beta_3 + 5\beta_4 + 3\beta_5)\left(\alpha^2(\gamma+1) - 4\alpha\gamma + \gamma(\gamma+1)\right)}{\pi(1-\alpha)^2(\gamma-\alpha)^2} \tag{4.97}$$

The values of $\tilde{\mathcal{D}}_i$ are listed below

$$\tilde{\mathcal{D}}_1 = 3\beta_5^2 + 4\beta_2\beta_5 - 6\beta_3\beta_5 + 2\beta_4\beta_5 - 12\beta_1\beta_2 + 4\beta_1\beta_3 \tag{4.98}$$

$$\begin{aligned}\tilde{\mathcal{D}}_2 = \Big[&-12\beta_1^2 + 4\beta_3\beta_1 + 4\beta_4\beta_1 + 4\beta_5\beta_1 - 6\beta_2^2 + 2\beta_3^2 - 3\beta_5^2 \\ &+ 4\beta_2\beta_3 + 4\beta_2\beta_4 + 8\beta_3\beta_4 + 2\beta_3\beta_5 + 2\beta_4\beta_5\Big]\end{aligned} \tag{4.99}$$

$$\begin{aligned}\tilde{\mathcal{D}}_3 = \Big[&4\beta_1^2 + 4\beta_3\beta_1 - 12\beta_4\beta_1 - 12\beta_5\beta_1 + 2\beta_2^2 + 6\beta_3^2 + 4\beta_4^2 \\ &+ \beta_5^2 - 12\beta_2\beta_3 + 4\beta_2\beta_4 - 24\beta_3\beta_4 - 6\beta_3\beta_5 + 2\beta_4\beta_5\Big]\end{aligned} \tag{4.100}$$

$$\begin{aligned}\tilde{\mathcal{D}}_4 = \Big[&4\beta_1^2 - 12\beta_3\beta_1 + 4\beta_4\beta_1 + 4\beta_5\beta_1 + 2\beta_2^2 - 14\beta_3^2 - 8\beta_4^2 \\ &+ \beta_5^2 + 4\beta_2\beta_3 - 12\beta_2\beta_4 + 8\beta_3\beta_4 + 2\beta_3\beta_5 - 6\beta_4\beta_5\Big]\end{aligned} \tag{4.101}$$

$$\tilde{\mathcal{D}}_5 = -6\beta_5^2 - 8\beta_2\beta_5 + 4\beta_3\beta_5 - 4\beta_4\beta_5 + 8\beta_1\beta_2 - 8\beta_1\beta_3. \tag{4.102}$$

We also apply the flow equations of γ from [26], and we have listed the equations in Appendix C. The initial conditions for our coupling constants are

$$\beta_i(0) = -\beta_{1,MF}\Big(-1, 2, 2, 2, -2\Big) \tag{4.103}$$

$$\alpha(0) = 0 \tag{4.104}$$

$$\gamma(0) = 3; \tag{4.105}$$

We numerically integrated the FRG flow equations in the 2D-limit, and the results are plotted in fig. 4.2. The five quartic coupling constants $\beta_a(t)$ deviate significantly from the fixed ratios of the mean-field initial conditions in eq. (4.103). The coefficients $\beta_a(t)$ in the early stages $t \sim 0$ indicate the C_{AP} becomes negative, breaking the degeneracy between the planar phase and A-phase, and favouring the planar phase. We expected to see the A-phase dominate as theoretically shown in Ref. [25]. The flow diverges quickly at $t \sim 0.05$ compared to the RG flows in Chapter 3, and the 3D FRG flows. This means we have taken into account fewer fluctuations, and we do not capture the effects of the Goldstone modes to the same extent. This may be why we fail to see the A-phase emerge in our flow.

We notice that the decay of $\gamma(t)$ to $\gamma_\star = 1$ is quite rapid, and it is similar to the 3D FRG case. α starts at the phase transition with $\alpha = 0$ and flows to the negative, indicating that the system transitioned into a symmetry-broken state. We expect to see this since we want to see what phase is favoured after the transition.

The coupling constants β_a quickly take on unphysical values that cause the free energy to become unbounded below. We detect this when the A-phase or planar phase free energies become singular. The inequality that appears to be violated is

$$2\beta_{12} + \beta_{345} > 0, \tag{4.106}$$

which leads to our effective potential becoming unbounded below. Our FRG flow equations can no longer be applied in this unphysical regime. For all physical values of the FRG, the planar phase is energetically favoured over the A-phase.

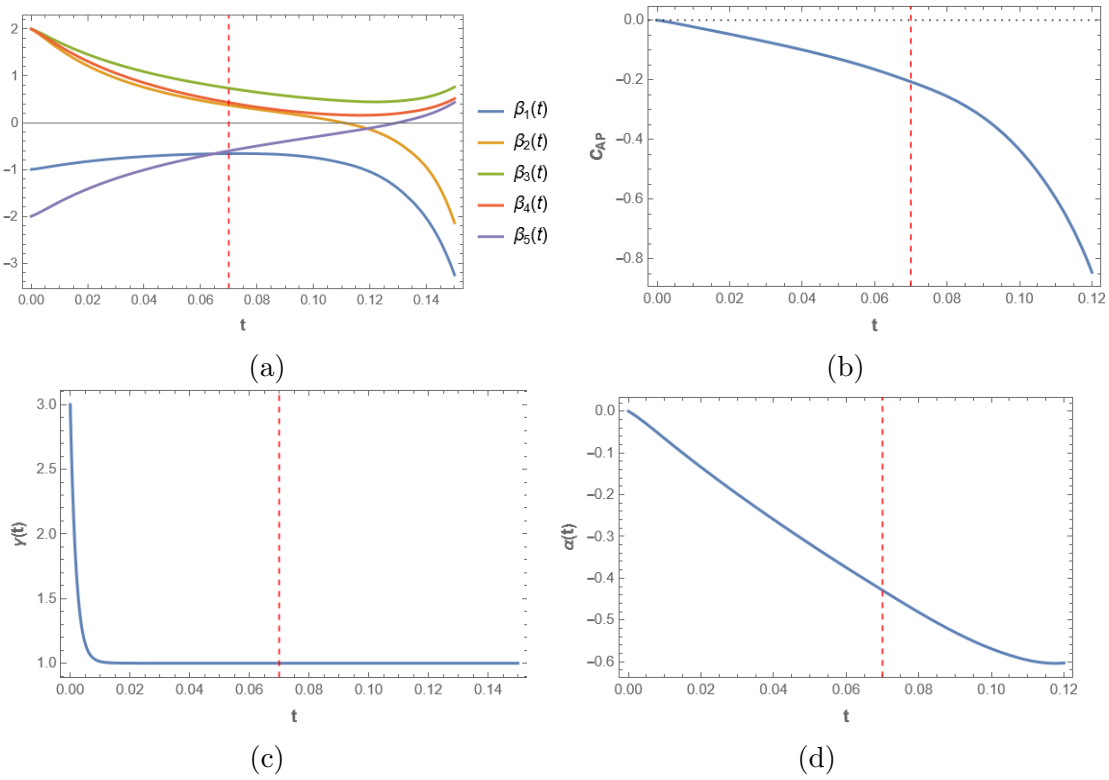

Figure 4.2: **FRG flow in the 2D limit.** *a)* FRG flow of the five quartic couplings $\beta_a(t)$, where the flow is numerically determined and plotted against $t = \ln \frac{\Lambda}{k}$. The fixed ratios of the quartic couplings change significantly, and the flow is qualitatively similar to the 3D FRG flow. The flow becomes unphysical at the red dotted line because the free energy of the planar phase diverges. The flow stops at t$\tilde{0}$.05, which is much earlier than the 3D case. *b)* The flow of C_{AP}, which is positive when the A phase is favoured and negative when the planar phase is favoured, is plotted against t. The degeneracy between the A-phase and the planar phase is broken, and the planar phase is shown to be favoured in the valid region of our FRG. *c)* The RG flow of γ with respect to t. γ decays quickly to $\gamma = 1$. *d)* The flow of α with respect to t. α starts at the phase transition, with $\alpha = 0$, and flows to the negative, indicating that the system transitioned into a symmetry-broken state.

4.3.3 Quasi-2D System

We can extend our analysis of FRG to the quasi-2D limit. We quantize our confined momentum

$$q_z \to k_n = \frac{n\pi}{L_z}, \tag{4.107}$$

where L_z is the nanoscale confinement length. q_x and q_y also take on discrete values proportional $\frac{\pi}{L_x}$ and $\frac{\pi}{L_y}$, but the spectrum is sufficiently tightly spaced to be

approximated as a continuum. Unlike in the RG case, which used momentum shell integration for all cases, our method for regulating our integrals will change in quasi-2D. The order parameter $A_\perp$ is the same as the 2D case, and our anstaz for the free energy is given by the quasi-2D free energy

$$\Gamma[\mathrm{A}_\perp] = F[\mathrm{A}_\perp] = \frac{1}{L_z}\sum_{n=1}^{\infty}\int d^2\mathbf{q}_\perp \left\{ \sum_a \beta_a I_a(\mathrm{A}_\perp) + (\gamma-1) q_i \mathrm{A}^*_{\perp\mu i} q_j \mathrm{A}_{\perp\mu j} + \Big(\alpha + q^2\Big)\mathrm{tr}\mathrm{A}_\perp \mathrm{A}^\dagger_\perp \right\}, \tag{4.108}$$

where $q^2 = q_\perp^2 + k_n^2$. The propagator is defined similarly to the 2D case

$$\Gamma^{(2)}_{\mu i,\nu j}[\Psi,\bar{\Psi}] = \delta_{\mu\nu}\Big((q_\perp^2 + k_n^2 + \alpha)\delta_{ij} + (\gamma-1) q_{\perp i} q_{\perp j}\Big) \begin{pmatrix} 1 & 0 \\ 0 & 1 \end{pmatrix} + \mathcal{V}_{\mu i,\nu j}(\Psi,\bar{\Psi}). \tag{4.109}$$

Let us define our regulator as

$$\mathcal{R}_k(q_\perp) = \delta_{\mu\nu}(k^2 - q_\perp^2 - k_n^2)\theta(k^2 - q_\perp^2 - k_n^2)\Big(\delta_{ij} + (\gamma-1)\hat{q}_{\perp i}\hat{q}_{\perp j}\Big) \begin{pmatrix} 1 & 0 \\ 0 & 1 \end{pmatrix}. \tag{4.110}$$

In polar coordinates we have $\hat{\mathbf{q}}_{\perp i} = \Big(\cos\theta, \sin\theta\Big)$. We proceed by deriving the regulator and getting

$$\dot{\mathcal{R}}_k(q) = k\frac{d}{dk}R_k(q) = R_k(q) = 2k^2\delta_{\mu\nu}\Big(\delta_{ij} + (\gamma-1)\hat{q}_i\hat{q}_j\Big) \begin{pmatrix} 1 & 0 \\ 0 & 1 \end{pmatrix}. \tag{4.111}$$

Now, we can write the inverse propagator when the order parameter is zero as

$$\mathcal{G}_k^{-1}(0,q) = \Gamma^{(2)}[0] + \mathcal{R}_k = \delta_{\mu\nu}\Big((k^2+\alpha)\delta_{ij} + (\gamma-1)[(k^2-k_n^2)\hat{q}_{\perp i}\hat{q}_{\perp j}]\Big) \begin{pmatrix} 1 & 0 \\ 0 & 1 \end{pmatrix}. \tag{4.112}$$

The propagator at zero order parameter is given by

$$\mathcal{G}_k(0,q) = \mathcal{G}_0 = \delta_{\mu\nu}\left(\frac{\delta_{ij}}{(k^2+\alpha)} - \frac{(\gamma-1)(k^2-k_n^2)\hat{q}_{\perp i}\hat{q}_{\perp j}}{(k^2+\alpha)(\gamma(k^2-k_n^2)+k_n^2+\alpha)}\right) \begin{pmatrix} 1 & 0 \\ 0 & 1 \end{pmatrix}. \tag{4.113}$$

Now, we will solve the Wetterich Equation using our ansatz. This is given by

$$\partial_t U_k = \frac{1}{2L_z}\sum_{k_n}\int d^2\mathbf{q}_\perp \mathrm{tr}\left[\Big(\Gamma^{(2)}[\Psi,\bar{\Psi}] + \mathcal{R}_k(\mathbf{q})\Big)^{-1}\dot{\mathcal{R}}_k(\mathbf{q})\right]. \tag{4.114}$$

Our flow equations become

$$\partial_t \beta_{ik} = \frac{1}{2L_z} \sum_{k_n=0}^{k} \int_0^{\sqrt{k^2-k_n^2}} q dq \int_0^{2\pi} d\theta \ \mathrm{tr}\left[\hat{P}_i \mathcal{G}_k \dot{\mathcal{R}}_k(\mathbf{q})\right]. \tag{4.115}$$

Since the regulator and the propagator don't depend on the magnitude q, we can write the sum as

$$\partial_t \beta_{ik} = \frac{1}{4L_z} \sum_{n=0}^{\lfloor \frac{L_z k}{\pi} \rfloor} (k^2 - k_n^2) \int_0^{2\pi} d\theta \ \mathrm{tr}\left[\hat{P}_i \mathcal{G}_k \dot{\mathcal{R}}_k(\mathbf{q})\right]. \tag{4.116}$$

Here, $\lfloor \cdot \rfloor$ is the floor function, which comes from the requirement that $k_n < k$. We have seen in fig. 4.2 that our flows survive for very small $t \sim 0.1$. For small t we have

$$\left\lfloor \frac{L_z k}{\pi} \right\rfloor = \left\lfloor \frac{L_z \Lambda e^{-t}}{\pi} \right\rfloor \approx \left\lfloor \frac{L_z \Lambda}{\pi} \right\rfloor. \tag{4.117}$$

We repeat the procedure from the previous section and derive the FRG flow equations for our dimensionless coupling constants. We calculated in section 3.3.3 that the value of $L_z\Lambda$ is roughly around 30 for 1000 nm confinement in ref. [6].

The flow of our dimensionless couplings is given by

$$\partial_t \tilde{\beta}_{ik} = (4-d)\tilde{\beta}_{ik} + \sum_{n=0}^{\lfloor \frac{L_z \Lambda}{\pi} \rfloor} \frac{(1-\tilde{k}_n^2)\tilde{H}_{\beta_i}}{16\pi(1-\tilde{\alpha}_k)^3 \left(\tilde{\alpha}_k - \gamma + (\gamma-1)\tilde{k}_n^2\right)^3} \tag{4.118}$$

$$\partial_t \tilde{\alpha}_k = 2\tilde{\alpha}_k + \sum_{n=0}^{\lfloor \frac{L_z \Lambda}{\pi} \rfloor} \frac{(1-\tilde{k}_n^2)\tilde{H}_{\alpha}}{4\pi(1-\tilde{\alpha}_k)^2 \left(\tilde{\alpha}_k - \gamma + (\gamma-1)\tilde{k}_n^2\right)^2}, \tag{4.119}$$

where $\tilde{k}_n = \frac{k_n}{k}$. We use the same flow equation for γ as in perturbative RG flow. For a coupling constant g, we define the functions $\tilde{H}_g$ as the dimensionless version of H_g. These are given by

$$\begin{aligned} H_\alpha = &\Big(2\beta_1 + 7\beta_2 + 4\beta_3 + 5\beta_4 + 3\beta_5\Big)\Big(\alpha^2(\gamma+1) - 4\alpha\gamma + (\gamma+1)\gamma \\ &+ 2(\gamma-1)(\alpha-\gamma)\tilde{k}_n^2 + (\gamma-1)^2\tilde{k}_n^4\Big) \end{aligned} \tag{4.120}$$

$$\begin{aligned} H_{\beta_i} = \tilde{\mathcal{C}}_i(1)\Big[&2(\alpha-1)^3 + (\gamma-\alpha)^2(\alpha + 3\tilde{k}_n^2 - 4)(\gamma-1) + (\gamma-1)^2(\alpha-1)(2\alpha-\gamma-1) \\ &- 3(\gamma-1)^3(\tilde{k}_n^2 - 1)\Big] + (\alpha-1)(\tilde{k}_n^2-1)(\gamma-1)^2\tilde{\mathcal{E}}_i, \end{aligned} \tag{4.121}$$

where $\tilde{\mathcal{C}}_i(1)$ is defined in eqs. (3.140) to (3.144). We define $\mathcal{E}_i$ in the appendix, in eqs. (C.14) to (C.17) and (C.19). Our flow will have the same initial conditions as the 2D and 3D limits, given by eq. (4.103).

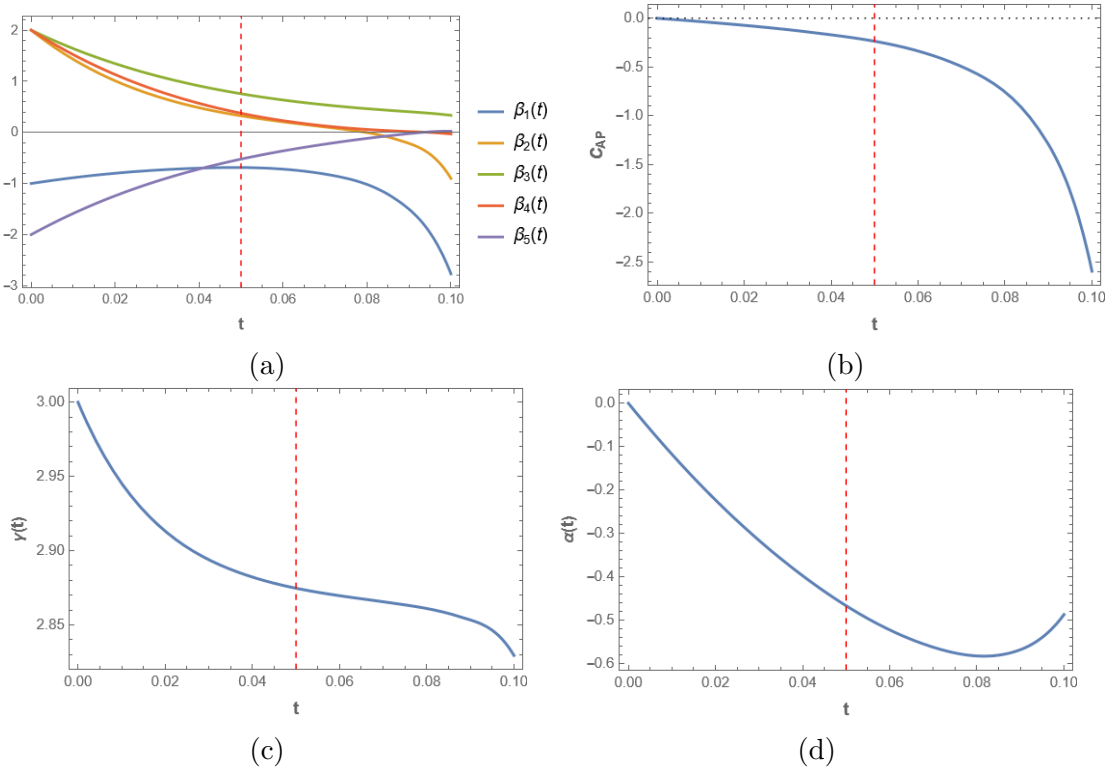

Figure 4.3: **FRG flow in the Quasi-2D limit with 1000 nm confinement.** *a)* RG flow of the five quartic couplings $\beta_a(t)$, where the flow is integrated numerically and plotted against $t = \ln \frac{\Lambda}{k}$ for $L_z\Lambda = 30$ with corresponds to roughly 1000 nm of confinement. The fixed ratios of the quartic couplings change significantly but do not differ qualitatively from the quasi-2D Rg flow and the 2D FRG flow. The flow becomes unphysical at the red dotted line where the free energy of the planar phase diverges. *b)* The flow of C_{AP}, which is positive when the A phase is favoured and negative when the planar phase is favoured, is plotted against t. The planar phase is shown to be favoured in the valid region of our RG, similar to the 2D case. *c)* The RG flow of γ with respect to t. γ decays slower than the 3D case but faster than the 2D case. *d)* The RG flow of $\alpha(t)$. α flows to increasingly negative values in the valid regime of the RG flow.

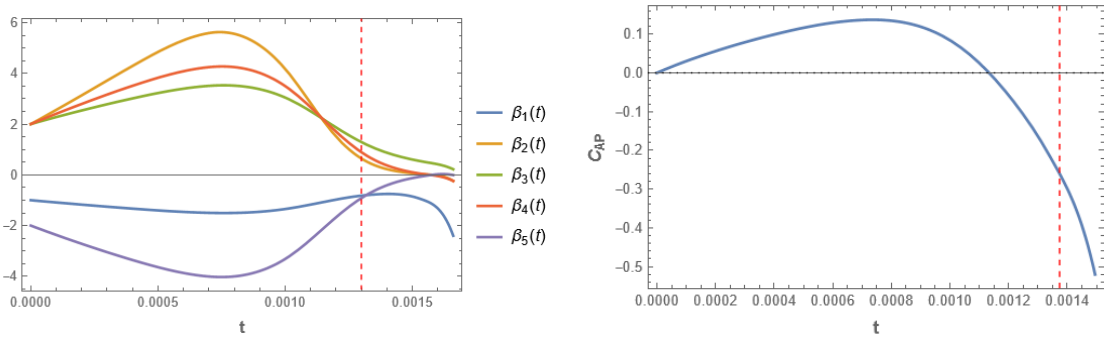

(a) (b)

Figure 4.4: **FRG flow in the Quasi-2D limit with 500 nm confinement.** *a)* RG flow of the five quartic couplings $\beta_a(t)$, where the flow is determined numerically and plotted against $t = \ln \frac{\Lambda}{k}$ for $L_z\Lambda = 18.5$, which corresponds to a confinement of roughly 500 nm. The fixed ratios of the quartic couplings change significantly and differ from the 2D and 3D FRG flow both quantitatively and qualitatively. The flow becomes unphysical at the red dotted line where the free energy of the planar phase diverges. *b)* The flow of C_{AP}, which is positive when the A phase is favoured and negative when the planar phase is favoured, is plotted against t. The A-phase is shown to be favoured in the beginning of our RG flow, bu then the planar phase becomes favoured towards the end of the valid region of our RG.

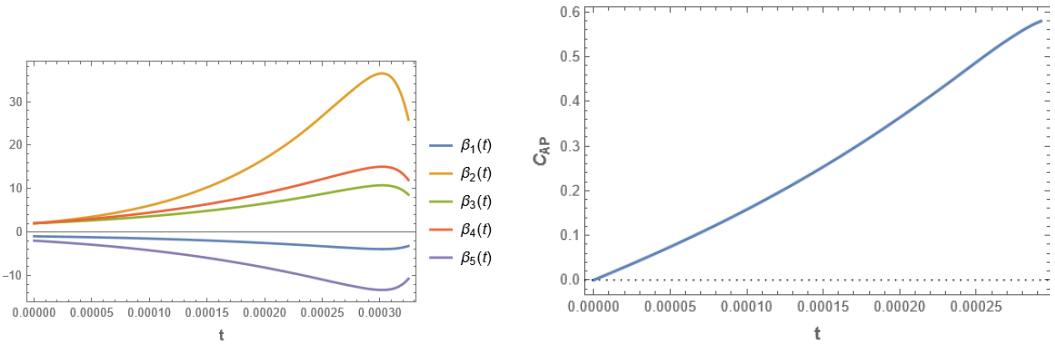

(a) (b)

Figure 4.5: **FRG flow in the Quasi-2D limit with 200 nm confinement.** *a) a)* RG flow of the five quartic couplings $\beta_a(t)$, where the flow is determined numerically and plotted against $t = \ln \frac{\Lambda}{k}$ for $L_z\Lambda = 6$, which corresponds to a confinement of roughly 200 nm. The fixed ratios of the quartic couplings change significantly and differ from the 2D and 3D FRG flow both quantitatively and qualitatively. The flow becomes unphysical at the red dotted line where the free energy of the planar phase diverges. *b)* The flow of C_{AP}, which is positive when the A phase is favoured and negative when the planar phase is favoured, is plotted against t. The A-phase is shown to be favoured throughout the valid region of our RG.

We integrated our FRG flow equations and plotted them at various levels of confinement in Figures 4.3 to 4.5. In all the cases, the flow of γ is qualitatively similar to fig. 4.3c as they flow to $\gamma_\star = 1$. γ decays quite slowly compared to the 3D and 2D limits, leading to a more pronounced deviation of the coupling constants. We note that the quasi-2D FRG does not interpolate between 2D and 3D, because it has a different regulator than them, leading to the quasi-2D FRG flow incorporating different higher order corrections that may not be considered by both the 2D and the 3D case. The flow of α is similar in all three levels of confinement, as it becomes negative, indicating a phase transition. All the flows break down when the effective potential becomes unbounded below when the following inequality is violated

$$2\beta_{12} + \beta_{345} > 0, \tag{4.122}$$

In Figure 4.3, we chose $\Lambda L_z = 30$, which we approximated to correspond to 1000 nm of confinement. Here, Λ is the inverse thermal wavelength. The five quartic coupling constants $\beta_a(t)$ deviate significantly from the fixed ratios of the mean-field initial conditions in eq. (4.103). The coefficients $\beta_a(t)$ in the early stages $t \sim 0$ indicate the C_{AP} becomes negative, breaking the degeneracy between the planar phase and A-phase, and favouring the planar phase. We expected to see the A-phase dominate as theoretically shown in Ref. [25]. In Ref. [6], we see the A-phase at low pressure. We observed a similar flow of C_{AP} for all of the confinement lengths we tested above $\Lambda L_z = 30$, indicating that the planar phase is favoured for confinement lengths greater $L_z\Lambda = 30$.

In Figure 4.4, we chose $\Lambda L_z = 18.5$, which we approximated to be roughly 500 nm of confinement. The five quartic coupling constants $\beta_a(t)$ deviate significantly from the fixed ratios of the mean-field initial conditions in eq. (4.103) as well. The coefficients $\beta_a(t)$ in the early stages $t \sim 0$ indicate the C_{AP} becomes positive, breaking the degeneracy between the planar phase and A-phase, and favouring the A-phase initially and then ultimately favouring the planar phase. We expected to see the

A-phase dominate as theoretically shown in Ref. [25]. We observed a similar flow of C_{AP}, where the A-phase was initially favoured in the RG flow, for confinement lengths within $15 \lesssim \Lambda L_z \lesssim 25$. This indicates that the planar phase is still favoured for confinement lengths greater $L_z\Lambda > 15$, but there is some evidence that the A-phase may appear. Further incorporation of corrections is required to confirm this result.

In Figure 4.4, we chose $\Lambda L_z = 6$, approximating roughly 200 nm of confinement. The five quartic coupling constants $\beta_a(t)$ deviate significantly from the fixed ratios of the mean-field initial conditions in eq. (4.103) as well. The coefficients $\beta_a(t)$ in the early stages $t \sim 0$ indicate the C_{AP} becomes positive, breaking the degeneracy between the planar phase and A-phase, and the A-phase is favoured for the whole flow. We observed a similar flow of C_{AP}, where the A-phase was favoured in the FRG flow, for confinement lengths within $L_z\Lambda \lesssim 10$. This indicates that for sufficient confinement ($L_z\Lambda \lesssim 10$), there is a phase transition from the Fermi liquid phase to the A-phase.

The corrections from FRG still give up the same unstable Wilson Fisher fixed point as perturbative RG, indicating that our phase transition is a fluctuation-induced first-order transition. This may have to do with our choice of a non-smooth regulator $\mathcal{R}_k \sim \theta(k^2 - q^2)$, which provided an easier analysis, but a smooth regulator would provide a more accurate RG flow [35]. Our results indicate that there is a fluctuation-induced first-order phase transition to the planar phase for $\Lambda L_z > 30$ and to the A-phase for $L_z\Lambda \lesssim 10$, and the results are ambiguous in the intermediate confinement scales.

Chapter 5

Summary & Conclusion

In conclusion, we have theoretically investigated the effects of fluctuations in the order parameter on the phase transition of ^{3}He under uniaxial nanoscale confinement. We introduced a reduced symmetry group for our confined system and used it to derive a new quasi-two-dimensional free energy that relies on a 3×2 matrix order parameter instead of the 3×3 matrix order parameter found in the three-dimensional system. We explored candidate phases of the quasi-two-dimensional system by exploring possible subgroups of our reduced symmetry and searching for the phase with the lowest weak-coupling and strong-coupling free energy. We found that the best candidates are two energetically degenerate phases: the A-phase and the planar phase.

Beyond the mean-field approximation, we calculate the perturbative RG flow in the 3D, 2D, and quasi 2D limits. We derive the perturbative flow equations for all quartic coupling constants with non-trivial kinetic factor (for $\gamma \neq 1$) and arbitrary confinement (for $0 \leq L_z < \infty$). In the quasi 2D limit, weak-coupling perturbative renormalization group predicts the planar phase to be energetically favoured, whereas the strong-coupling corrections favour the A-phase observed in experiment. Because of the lack of a stable fixed point, our results indicate that there is a fluctuation-induced first-order transition to the planar phase. However, these results are questionable since perturbative RG could not accurately predict the second-order phase

transition in the 3D system either.

There was a need to consider higher-order corrections, which led us to use the Functional Renormalization Group. We derived FRG flow equations for the 3D, 2D and quasi-2D cases. In the quasi-2D limit, we found that the A-phase was favoured over the planar phase for certain levels of confinement. These confinement scales were also confirmed to have a prominent Fermi liquid to A-phase transition in experiment. Due to the unstable fixed point, we find that under confinement with $L_z\Lambda \lesssim 10$, there is a fluctuation-induced first-order transition to the A-phase. More extensive study needs to be done into the FRG to explore the stability of the fixed point under higher-order corrections.

Bibliography

[1] G.Volovik, *The Universe in a Helium Droplet.* Oxford: Oxford University Press, 2009.

[2] V. Mineev, K. Samokhin, L. Landau, and L. Landau, *Introduction to Unconventional Superconductivity.* Taylor & Francis, 1999, ISBN: 9789056992095. [Online]. Available: https://books.google.ca/books?id=2BXYWT8m068C.

[3] D. Lotnyk *et al.*, "Path-dependent supercooling of the ^{3}He superfluid $A - B$ transition," *Phys. Rev. Lett.*, vol. 126, p. 215 301, 21 2021. DOI: 10.1103/PhysRevLett.126.215301. [Online]. Available: https://link.aps.org/doi/10.1103/PhysRevLett.126.215301.

[4] T. Gentile *et al.*, "SANS polarization analysis with nuclear spin-polarized ^{3}He," *Journal of Applied Crystallography*, vol. 33, no. 3 Part 1, pp. 771–774, 2000. DOI: 10.1107/S0021889800099817. [Online]. Available: https://doi.org/10.1107/S0021889800099817.

[5] M. J. Rudd, P. S. Yapa, A. J. Shook, J. Maciejko, and J. P. Davis, "Strong-coupling corrections to hard domain walls in superfluid ^{3}He$-B$," *Phys. Rev. B*, vol. 104, p. 094 520, 9 2021. DOI: 10.1103/PhysRevB.104.094520. [Online]. Available: https://link.aps.org/doi/10.1103/PhysRevB.104.094520.

[6] A. J. Shook *et al.*, "Stabilized Pair Density Wave via Nanoscale Confinement of Superfluid ^{3}He," *Phys. Rev. Lett.*, vol. 124, p. 015 301, 1 2020. DOI: 10.1103/PhysRevLett.124.015301. [Online]. Available: https://link.aps.org/doi/10.1103/PhysRevLett.124.015301.

[7] B. Bagchi, *Statistical Mechanics for Chemistry and Material Science.* World Scientific, 2018.

[8] H. Choi, J. P. Davis, J. Pollanen, T. M. Haard, and W. P. Halperin, "Strong coupling corrections to the ginzburg-landau theory of superfluid ^{3}He," *Phys. Rev. B*, vol. 75, p. 174 503, 17 2007. DOI: 10.1103/PhysRevB.75.174503. [Online]. Available: https://link.aps.org/doi/10.1103/PhysRevB.75.174503.

[9] H. Choi, J. P. Davis, J. Pollanen, T. M. Haard, and W. P. Halperin, "Erratum: Strong coupling corrections to the ginzburg-landau theory of superfluid ^{3}he [phys. rev. b 75, 174503 (2007)]," *Phys. Rev. B*, vol. 87, p. 019 904, 1 2013. DOI: 10.1103/PhysRevB.87.019904. [Online]. Available: https://link.aps.org/doi/10.1103/PhysRevB.87.019904.

[10] L Levitin *et al.*, "Phase diagram of the topological superfluid 3he confined in a nanoscale slab geometry," *Science (New York, N.Y.)*, vol. 340, pp. 841–844, May 2013. DOI: 10.1126/science.1233621.

[11] Y.-H. Li and T.-L. Ho, "Superfluid ^{3}He in very confined regular geometries," *Phys. Rev. B*, vol. 38, pp. 2362–2370, 4 1988. DOI: 10.1103/PhysRevB.38.2362. [Online]. Available: https://link.aps.org/doi/10.1103/PhysRevB.38.2362.

[12] P. S. Yapa, R. Boyack, and J. Maciejko, "Triangular pair density wave in confined superfluid he3," *Physical Review Letters*, vol. 128, no. 1, Jan. 2022, ISSN: 1079-7114. DOI: 10.1103/physrevlett.128.015301. [Online]. Available: http://dx.doi.org/10.1103/PhysRevLett.128.015301.

[13] L. V. Levitin *et al.*, "Evidence for a spatially modulated superfluid phase of ^{3}He under confinement," *Phys. Rev. Lett.*, vol. 122, p. 085 301, 8 2019. DOI: 10.1103/PhysRevLett.122.085301. [Online]. Available: https://link.aps.org/doi/10.1103/PhysRevLett.122.085301.

[14] A. B. Vorontsov and J. A. Sauls, "Crystalline order in superfluid ^{3}He films," *Phys. Rev. Lett.*, vol. 98, p. 045 301, 4 2007. DOI: 10.1103/PhysRevLett.98.045301. [Online]. Available: https://link.aps.org/doi/10.1103/PhysRevLett.98.045301.

[15] S. Tung, G. Lamporesi, D. Lobser, L. Xia, and E. A. Cornell, "Observation of the presuperfluid regime in a two-dimensional bose gas," *Phys. Rev. Lett.*, vol. 105, p. 230 408, 23 2010. DOI: 10.1103/PhysRevLett.105.230408. [Online]. Available: https://link.aps.org/doi/10.1103/PhysRevLett.105.230408.

[16] R. J. Fletcher *et al.*, "Connecting berezinskii-kosterlitz-thouless and bec phase transitions by tuning interactions in a trapped gas," *Phys. Rev. Lett.*, vol. 114, p. 255 302, 25 2015. DOI: 10.1103/PhysRevLett.114.255302. [Online]. Available: https://link.aps.org/doi/10.1103/PhysRevLett.114.255302.

[17] S. Mandal and I. F. Herbut, "P-wave superconductivity and the axiplanar phase of triple-point fermions," *Physical Review B*, vol. 104, no. 18, 2021. DOI: 10.1103/physrevb.104.l180507. [Online]. Available: https://doi.org/10.1103\%2Fphysrevb.104.l180507.

[18] S. Lammers, I. Boettcher, and C. Wetterich, "Dimensional crossover of nonrelativistic bosons," *Physical Review A*, vol. 93, no. 6, 2016. DOI: 10.1103/physreva.93.063631. [Online]. Available: https://doi.org/10.1103\%2Fphysreva.93.063631.

[19] I. Boettcher and I. F. Herbut, "Critical phenomena at the complex tensor ordering phase transition," *Physical Review B*, vol. 97, no. 6, 2018. DOI: 10.1103/physrevb.97.064504. [Online]. Available: https://doi.org/10.1103%2Fphysrevb.97.064504.

[20] I. Boettcher, J. M. Pawlowski, and S. Diehl, "Ultracold atoms and the functional renormalization group," *Nuclear Physics B - Proceedings Supplements*, vol. 228, pp. 63–135, 2012. DOI: 10.1016/j.nuclphysbps.2012.06.004. [Online]. Available: https://doi.org/10.1016\%2Fj.nuclphysbps.2012.06.004.

[21] M. Kindermann and C. Wetterich, "Phase transitions in liquid ^{3}he," *Phys. Rev. Lett.*, vol. 86, pp. 1034–1037, 6 2001. DOI: 10.1103/PhysRevLett.86.1034. [Online]. Available: https://link.aps.org/doi/10.1103/PhysRevLett.86.1034.

[22] C. Bruder and D. Vollhardt, "Symmetry and stationary points of a free energy: The case of superfluid ^{3}He," *Phys. Rev. B*, vol. 34, pp. 131–146, 1 1986. DOI: 10.1103/PhysRevB.34.131. [Online]. Available: https://link.aps.org/doi/10.1103/PhysRevB.34.131.

[23] D Vollhardt and P Wolfle, "The superfluid phases of helium 3," Jan. 1990. [Online]. Available: https://www.osti.gov/biblio/6233899.

[24] T. Lancaster and S. J. Blundell, *Quantum Field Theory for the Gifted Amateur*. Oxford University Press, Apr. 2014, ISBN: 9780199699322. DOI: 10.1093/acprof:oso/9780199699322.001.0001. [Online]. Available: https://doi.org/10.1093/acprof:oso/9780199699322.001.0001.

[25] C. Sun, A. Attar, and I. Boettcher, "Superfluid phase transition of nanoscale-confined helium-3," *Phys. Rev. B*, vol. 108, p. 144 503, 14 2023. DOI: 10.1103/PhysRevB.108.144503. [Online]. Available: https://link.aps.org/doi/10.1103/PhysRevB.108.144503.

[26] D. R. T. Jones, A. Love, and M. A. Moore, "Phase transitions in superfluid helium 3," *J. Phys. C*, vol. 9, pp. 743–759, 1976. DOI: 10.1088/0022-3719/9/5/015.

[27] J. V. Porto and J. M. Parpia, "Superfluid ^{3}he in aerogel," *Phys. Rev. Lett.*, vol. 74, pp. 4667–4670, 23 1995. DOI: 10.1103/PhysRevLett.74.4667. [Online]. Available: https://link.aps.org/doi/10.1103/PhysRevLett.74.4667.

[28] R. D. Pisarski and D. L. Stein, "Critical behavior of linear Φ^4 models with $G\times G'$ symmetry," *Phys. Rev. B*, vol. 23, p. 3549, 7 1981. DOI: 10.1103/PhysRevB.23.3549. [Online]. Available: https://link.aps.org/doi/10.1103/PhysRevB.23.3549.

[29] R. D. Pisarski and F. Wilczek, "Remarks on the chiral phase transition in chromodynamics," *Phys. Rev. D*, vol. 29, p. 338, 2 1984. DOI: 10.1103/PhysRevD.29.338. [Online]. Available: https://link.aps.org/doi/10.1103/PhysRevD.29.338.

[30] H. Kawamura, "Renormalization-group analysis of chiral transitions," *Phys. Rev. B*, vol. 38, pp. 4916–4928, 7 1988. DOI: 10.1103/PhysRevB.38.4916. [Online]. Available: https://link.aps.org/doi/10.1103/PhysRevB.38.4916.

[31] S. A. Antonenko, A. I. Sokolov, and K. B. Varnashev, "Chiral transitions in three-dimensional magnets and higher order ϵ expansion," *Phys. Lett. A*, vol. 208, p. 161, Feb. 1995. DOI: 10.1016/0375-9601(95)00736-M.

[32] A. Pelissetto, P. Rossi, and E. Vicari, "Large-n critical behavior of $O(n)\times O(m)$ spin models," *Nucl. Phys. B*, vol. 607, p. 605, Jul. 2001. DOI: 10.1016/S0550-3213(01)00223-1.

[33] A. Pelissetto, P. Rossi, and E. Vicari, "Critical behavior of frustrated spin models with noncollinear order," *Phys. Rev. B*, vol. 63, p. 140 414, 14 2001. DOI: 10.1103/PhysRevB.63.140414. [Online]. Available: https://link.aps.org/doi/10.1103/PhysRevB.63.140414.

[34] T. Debelhoir and N. Dupuis, "Simulating frustrated magnetism with spinor Bose gases," *Phys. Rev. A*, vol. 93, p. 051 603, 5 2016. DOI: 10.1103/PhysRevA.93.051603. [Online]. Available: https://link.aps.org/doi/10.1103/PhysRevA.93.051603.

[35] N. Dupuis *et al.*, "The nonperturbative functional renormalization group and its applications," *Physics Reports*, vol. 910, 1–114, May 2021, ISSN: 0370-1573. DOI: 10.1016/j.physrep.2021.01.001. [Online]. Available: http://dx.doi.org/10.1016/j.physrep.2021.01.001.

[36] A. Ringwald and C. Wetterich, "Average action for the n-component Φ^4 theory," *Nuclear Physics B*, vol. 334, no. 2, pp. 506–526, 1990, ISSN: 0550-3213. DOI: https://doi.org/10.1016/0550-3213(90)90489-Z. [Online]. Available: https://www.sciencedirect.com/science/article/pii/055032139090489Z.

[37] B. Delamotte, D. Mouhanna, and M. Tissier, "Nonperturbative renormalization-group approach to frustrated magnets," *Phys. Rev. B*, vol. 69, p. 134 413, 13 2004. DOI: 10.1103/PhysRevB.69.134413. [Online]. Available: https://link.aps.org/doi/10.1103/PhysRevB.69.134413.

[38] P. Le Doussal, K. J. Wiese, and P. Chauve, "Functional renormalization group and the field theory of disordered elastic systems," *Phys. Rev. E*, vol. 69, p. 026 112, 2 2004. DOI: 10.1103/PhysRevE.69.026112. [Online]. Available: https://link.aps.org/doi/10.1103/PhysRevE.69.026112.

Appendix A: Path Integrals

A.1 Gaussian Integrals

Path integrals, or functional integrals, are generalizations of integrals which integrate over functionals rather than functions. The path integrals of interest are generalizations of Gaussian integrals, which are the integrations of the exponentiation of second-order polynomials. The simplest example is the one-dimensional case is

$$\int dx \exp\left(-ax^2 + bx\right) = e^{\frac{b^2}{4a}} \sqrt{\frac{\pi}{a}}, \tag{A.1}$$

where $a > 0$. Over one complex dimension, our Gaussian integral is

$$\int d\left(z, \bar{z}\right) \exp\left(-zw\bar{z} + \bar{u}z + \bar{z}v\right) = e^{\frac{uv}{w}} \frac{\pi}{w}, \tag{A.2}$$

where $\mathbf{Re}(w) > 0$. or more generally, we can have a Gaussian integral over $\mathbb{R}^N$ of the form

$$\int d^N v \exp\left(-v^T \mathbf{A} v + b \cdot v^T\right) = (2\pi)^{N/2} \left(\det \mathbf{A}\right)^{-\frac{1}{2}} \exp\left(b^T \mathbf{A}^{-1} b\right), \tag{A.3}$$

where $\det\mathbf{A} > 0$. We can have a Gaussian integral over $\mathbb{C}^N$ of the form

$$\int d^N \left(v, v^\dagger\right) \exp\left(-v^\dagger \mathbf{A} v + wv + v^\dagger w'\right) = \pi^N \left(\det \mathbf{A}\right)^{-1} \exp\left(w\mathbf{A}^{-1} w'\right). \tag{A.4}$$

In Gaussian path integrals, we generalize this to an infinite continuum of variables

$$\begin{aligned} &\int \mathcal{D}\phi \exp\left(-\frac{1}{2} \iint \mathrm{d}x\mathrm{d}y \;\; \phi(x) A(x,y) \phi(y) + \int dx \;\; J(x)\phi(x)\right) \\ &\propto \det(\mathbf{A})^{-\frac{1}{2}} \exp\left(\frac{1}{2} \int dx \int dy \;\; J(x) A^{-1}(x,y) J(y)\right), \end{aligned} \tag{A.5}$$

where

$$\mathcal{D}\phi = \prod_{k\in\mathbb{R}} d\phi_k, \tag{A.6}$$

and ϕ_k is the Fourier transform of $\phi(x)$. $A^{-1}(x,y)$ is defined by

$$\int dy \;\; A(x,y)A^{-1}(y,z) = \delta(y-z) \tag{A.7}$$

A.2 Expectation values

Now, we are interested in proving certain properties of our Gaussian path integral. Our standard path integral is given by

$$Z = \int \mathcal{D}\phi \exp\left(-\frac{1}{2}\iint dxdy \;\; \phi(x)A(x,y)\phi(y)\right). \tag{A.8}$$

We can define the expectation value as

$$\langle H(\phi)\rangle = \frac{1}{Z}\int \mathcal{D}\phi \exp\Big(-\frac{1}{2}\iint dxdy \;\; \phi(x)A(x,y)\phi(y)\Big)H(\phi), \tag{A.9}$$

Now we define a functional that depends on a source J(x) as

$$Z[J] = \int \mathcal{D}\phi \exp\left(-\frac{1}{2}\iint dxdy \;\; \phi(x)A(x,y)\phi(y) + \int dx \;\; J(x)\phi(x)\right). \tag{A.10}$$

We also define $F[J]$ with

$$Z[J] = \int \mathcal{D}\phi \exp\Big(-F[J]\Big). \tag{A.11}$$

Then, we can derive the following

$$\langle\phi(z)\rangle = \int \mathcal{D}\phi \exp\Big(-\frac{1}{2}\iint dxdy \;\; \phi(x)A(x,y)\phi(y)\Big)\phi(x) \tag{A.12}$$

$$= \frac{\delta}{\delta J(x)}\Big|_{J=0}\int \mathcal{D}\phi \exp\left(-\frac{1}{2}\iint dxdy \;\; \phi(x)A(x,y)\phi(y) + \int dx \;\; J(x)\phi(x)\right) \tag{A.13}$$

$$= \frac{1}{Z}\frac{\delta}{\delta J(x)}\Big|_{J=0} Z[J] = \frac{\delta}{\delta J(x)}\Big|_{J=0}\ln Z[J]. \tag{A.14}$$

We can substitute the known expression for Z[J] from eq. (A.5) and find

$$\langle\phi(z)\rangle = \frac{\delta}{\delta J(x)}\Big|_{J=0}\int dx\int dy \;\; J(x)A^{-1}(x,y)J(y) = 0. \tag{A.15}$$

Next, we determine the two-point correlation function

$$\langle \phi(z)\phi(w)\rangle = \frac{1}{Z}\frac{\delta^2}{\delta J(z)\delta J(w)}\Big|_{J=0} Z[J] \tag{A.16}$$

$$= \frac{\delta^2}{\delta J(z)\delta J(w)}\Big|_{J=0} \iint dxdy \;\; J(x)A^{-1}(x,y)J(y) \tag{A.17}$$

$$= A^{-1}(z,w) \tag{A.18}$$

If F is the free energy, then $A(x,y)$ is given by the propagator $G(x,y)$. For higher-order terms, we can apply Wick's theorem.

A.3 Trace-Log Formula

Now we aim to derive the trace-log formula. Some function $\bar{\phi}$ is a critical point of a functional $F[\phi]$ if it satisfies

$$\frac{\delta F[\bar{\phi}]}{\delta \phi} = 0. \tag{A.19}$$

The functional can be approximated locally around this critical point with a Taylor series

$$F[\bar{\phi}+\eta] \approx F[\bar{\phi}] + \frac{1}{2}\iint dtdt'\eta(t')\frac{\delta^2 F[\bar{x}]}{\delta\phi(t)\delta\phi(t')}\eta(t)\dots \tag{A.20}$$

In a path integral given by

$$Z = \int \mathcal{D}\phi \exp\Big(-F[\phi]\Big). \tag{A.21}$$

The first-order approximation is given by minimizing $F[\phi]$ with minimum $\bar{\phi}$ which can be written as

$$Z \approx \exp\Big(-F[\bar{\phi}]\Big), \tag{A.22}$$

where we assume the path integral measure is normalized. This is equivalent to the mean-field approximation; The free energy is given by the order parameter that minimizes it. However, we can improve this by adding the second-order corrections to the functional F

$$Z \approx \int \mathcal{D}\phi \;\; \exp\Big(-F[\bar{\phi}] + \frac{1}{2}\iint dtdt'\eta(t')\frac{\delta^2 F[\bar{\phi}]}{\delta\phi(t)\delta\phi(t')}\eta(t)\dots\Big). \tag{A.23}$$

Now this a Gaussian path integral that can be evaluated to

$$Z \approx \int \mathcal{D}\phi \;\; \exp\Big(-F[\bar{\phi}]\Big) \det\left(\frac{\delta^2 F[\bar{\phi}]}{\delta\phi(t)\delta\phi(t')}\right)^{\frac{1}{2}} \tag{A.24}$$

$$\propto \int \mathcal{D}\phi \;\; \exp\left(-F[\bar{\phi}] + \frac{1}{2}\log\det\left(\frac{\delta^2 F[\bar{\phi}]}{\delta\phi(t)\delta\phi(t')}\right)\right). \tag{A.25}$$

We apply the formula $\det\log A = \mathrm{tr}\log A$ to obtain

$$Z \approx \int \mathcal{D}\phi \;\; \exp\left(-F[\bar{\phi}] + \frac{1}{2}\mathrm{tr}\log\left(\frac{\delta^2 F[\bar{\phi}]}{\delta\phi(t)\delta\phi(t')}\right)\right). \tag{A.26}$$

This is the trace-log formula.

Appendix B: Derivatives of the Trace-Log Formula

B.1 RG

We are interested in taking the fourth derivative of a matrix logarithm. Let ϕ be an arbitrary vector with components ϕ_a. First, we derive the expression for the derivative of a matrix logarithm of the inverse propagator, as shown below

$$\frac{\partial}{\partial \phi_a} \ln \mathcal{G}^{-1}(\phi, q). \tag{B.1}$$

We begin with the identity

$$\frac{\partial}{\partial \phi_a} \exp\left(\log \mathcal{G}^{-1}(\phi, q)\right) = \frac{\partial}{\partial \phi_a} \mathcal{G}^{-1}(\phi, q) \tag{B.2}$$

$$\implies \exp\left(\log \mathcal{G}^{-1}(\phi, q)\right) \frac{\partial}{\partial \phi_a} \log \mathcal{G}^{-1}(\phi, q) = \frac{\partial}{\partial \phi_a} \mathcal{G}^{-1}(\phi, q) \tag{B.3}$$

$$\mathcal{G}^{-1}(\phi, q) \frac{\partial}{\partial \phi_a} \log \mathcal{G}^{-1}(\phi, q) = \frac{\partial}{\partial \phi_a} \mathcal{G}^{-1}(\phi, q) \tag{B.4}$$

$$\implies \frac{\partial}{\partial \phi_a} \log \mathcal{G}^{-1}(\phi, q) = \mathcal{G}(\phi, q) \frac{\partial}{\partial \phi_a} \mathcal{G}^{-1}(\phi, q). \tag{B.5}$$

Next, we will derive the formula for the derivative of the matrix inverse

$$\mathcal{G}(\phi, q) \mathcal{G}^{-1}(\phi, q) = \mathbb{I} \tag{B.6}$$

$$\implies \frac{\partial}{\partial \phi_a} \left(\mathcal{G}(\phi, q) \mathcal{G}^{-1}(\phi, q)\right) = 0 \tag{B.7}$$

$$\frac{\partial \mathcal{G}(\phi, q)}{\partial \phi_a} \mathcal{G}^{-1}(\phi, q) + \mathcal{G}(\phi, q) \frac{\partial}{\partial \phi_a} \mathcal{G}^{-1}(\phi, q) = 0 \tag{B.8}$$

$$\frac{\partial \mathcal{G}(\phi, q)}{\partial \phi_a} = -\mathcal{G}(\phi, q) \left[\frac{\partial}{\partial \phi_a} \mathcal{G}^{-1}(\phi, q)\right] \mathcal{G}(\phi, q). \tag{B.9}$$

Now, we compute our derivatives, only including terms that involve the second derivative of the inverse propagator; all other derivatives are zero at $\phi = 0$, assuming we have a quartic free energy. Let $\mathcal{G}(0, \mathbf{q}) = \mathcal{G}_0$. Then, the fourth derivative of a matrix logarithm is

$$\frac{\partial^4}{\partial\phi_a\partial\phi_b\partial\phi_c\partial\phi_d}\Big|_{\phi=0} \log \mathcal{G}^{-1} = \frac{\partial^3}{\partial\phi_b\partial\phi_c\partial\phi_d}\left(\mathcal{G}\frac{\partial\mathcal{G}^{-1}}{\partial\phi_a}\right)\Bigg|_{\phi=0} \tag{B.10}$$

$$= \frac{\partial^2}{\partial\phi_c\partial\phi_d}\left(-\mathcal{G}\frac{\partial\mathcal{G}^{-1}}{\partial\phi_a}\mathcal{G}\frac{\partial\mathcal{G}^{-1}}{\partial\phi_b} + \mathcal{G}\frac{\partial^2\mathcal{G}^{-1}}{\partial\phi_a\partial\phi_b}\right)\Bigg|_{\phi=0}. \tag{B.11}$$

We repeat this procedure while only having derivatives of second-order.

$$= -\left(\mathcal{G}_0\frac{\partial^2\mathcal{G}^{-1}}{\partial\phi_a\partial\phi_b}\mathcal{G}_0\frac{\partial^2\mathcal{G}^{-1}}{\partial\phi_c\partial\phi_d} + \mathcal{G}_0\frac{\partial^2\mathcal{G}^{-1}}{\partial\phi_a\partial\phi_c}\mathcal{G}_0\frac{\partial^2\mathcal{G}^{-1}}{\partial\phi_b\partial\phi_d} + \mathcal{G}_0\frac{\partial^2\mathcal{G}^{-1}}{\partial\phi_a\partial\phi_d}\mathcal{G}_0\frac{\partial^2\mathcal{G}^{-1}}{\partial\phi_b\partial\phi_c}\right)\Bigg|_{\phi=0}. \tag{B.12}$$

This is specifically relevant to taking derivatives of the trace-log formula for perturbative RG. To take derivatives of the Wetterich equation, we would like to evaluate both the second and fourth derivative of the propagator since we need the flow equation of α and β_i. We also use the condition that only the second derivative of $\mathcal{G}^{-1}$ is non-zero. The second derivative of the propagator with respect to a field is given by

$$\frac{\partial^2}{\partial\phi_a\partial\phi_b}\Bigg|_{\phi=0}\mathcal{G} = -\frac{\partial}{\partial\phi_b}\left(\mathcal{G}\frac{\partial\mathcal{G}^{-1}}{\partial\phi_a}\mathcal{G}\right)\Bigg|_{\phi=0} \tag{B.13}$$

$$= -\mathcal{G}_0\frac{\partial^2\mathcal{G}^{-1}}{\partial\phi_a\partial\phi_b}\Bigg|_{\phi=0}\mathcal{G}_0 \tag{B.14}$$

$$\frac{\partial^4}{\partial\phi_a\partial\phi_b\partial\phi_c\partial\phi_d}\Bigg|_{\phi=0}\mathcal{G} = -\frac{\partial^3}{\partial\phi_b\partial\phi_c\partial\phi_d}\left(\mathcal{G}\frac{\partial\mathcal{G}^{-1}}{\partial\phi_a}\mathcal{G}\right)\Bigg|_{\phi=0} \tag{B.15}$$

$$= \frac{\partial^2}{\partial\phi_c\partial\phi_d}\left(\mathcal{G}\frac{\partial\mathcal{G}^{-1}}{\partial\phi_a}\mathcal{G}\frac{\partial\mathcal{G}^{-1}}{\partial\phi_b}\mathcal{G} - \mathcal{G}\frac{\partial^2\mathcal{G}^{-1}}{\partial\phi_a\partial\phi_b}\mathcal{G} + \mathcal{G}\frac{\partial\mathcal{G}^{-1}}{\partial\phi_b}\mathcal{G}\frac{\partial\mathcal{G}^{-1}}{\partial\phi_a}\mathcal{G}\right)\Bigg|_{\phi=0} \tag{B.16}$$

$$= \left(\mathcal{G}_0\frac{\partial^2\mathcal{G}^{-1}}{\partial\phi_a\partial\phi_b}\mathcal{G}_0\frac{\partial^2\mathcal{G}^{-1}}{\partial\phi_c\partial\phi_d}\mathcal{G}_0 + \mathcal{G}_0\frac{\partial^2\mathcal{G}^{-1}}{\partial\phi_a\partial\phi_c}\mathcal{G}_0\frac{\partial^2\mathcal{G}^{-1}}{\partial\phi_b\partial\phi_d}\mathcal{G}_0 + \mathcal{G}_0\frac{\partial^2\mathcal{G}^{-1}}{\partial\phi_a\partial\phi_d}\mathcal{G}_0\frac{\partial^2\mathcal{G}^{-1}}{\partial\phi_b\partial\phi_c}\mathcal{G}_0\right)\Bigg|_{\phi=0}. \tag{B.17}$$

Appendix C: Flow equations

C.1 Derivation of integrals

Calculating the RG flow of a coupling constant involves taking derivatives of integrals, which allows ur to take advantage of the fundamental theorem of calculus

$$\frac{\mathrm{d}}{\mathrm{d}x}\int_0^x f(k)\mathrm{d}k = f(x). \tag{C.1}$$

We can apply this to our momentum shell integrals

$$\frac{\mathrm{d}}{\mathrm{d}\ln b}\int_{\mathbf{q}}'(\dots) = b\frac{\mathrm{d}}{\mathrm{d}b}\int_{\Lambda/b}^{\Lambda}\mathrm{d}q\int_{S^{d-1}}\mathrm{d}\Omega\Big[q^{d-1}(\dots)\Big] \tag{C.2}$$

$$= \Big[\frac{\Lambda}{b}\Big]^d\Big[\int_{S^{d-1}}\mathrm{d}\Omega(\dots)\Big]\Big|_{q=\Lambda/b}. \tag{C.3}$$

In perturbative RG, the flow of our β_a is determined by calculating the following

$$\frac{\mathrm{d}}{\mathrm{d}\ln b}\int_{\mathbf{q}}'\frac{1}{q^4} = \frac{\mathrm{d}}{\mathrm{d}\ln b}\int_{\Lambda/b}^{\Lambda}\mathrm{d}q\frac{q^{d-1}}{q^4} = b\frac{\mathrm{d}}{\mathrm{d}b}\int_{\Lambda/b}^{\Lambda}\mathrm{d}q\frac{1}{q^{5-d}} \tag{C.4}$$

$$= -b\Big(\frac{1}{q^{5-d}}\Big)\Big|_{q=\Lambda/b}\Big(\frac{\mathrm{d}}{\mathrm{d}b}\frac{\Lambda}{b}\Big) = \Big(\frac{b}{\Lambda}\Big)^{4-d}. \tag{C.5}$$

C.2 Flow of gamma

The flow equation for the parameter γ obtained from ref. [26] does not have the same normalization for their β_a, as our equations in our explorations of perturbative RG and FRG. We denote the quartic coefficients in ref. [26] as $\tilde{\beta}_a$. The flow of $\tilde{\beta}_1$ for d spatial dimensions and 3 spin degrees of freedom reads

$$\frac{\mathrm{d}}{\mathrm{d}\ln b}\tilde{\beta}_1 = 2\tilde{\beta}_1 - \frac{1}{4\pi^2}3d\tilde{\beta}_1^2 + \dots \tag{C.6}$$

$$\tag{C.7}$$

We have a variety of flow equations in both 2D and 3D. When $\gamma = 1$, they have the form

$$\frac{\mathrm{d}}{\mathrm{d}\ln b}\beta_1 = \epsilon\beta_1 - z\beta_1^2 + \ldots, \tag{C.8}$$

where z will vary based on the way we calculate our flow equations. Both schemes must be related via the rescaling

$$\frac{3d}{4\pi^2}\tilde{\beta}_a = z\beta_a \;\Rightarrow\; \beta_a = \frac{3d}{4\pi^2 z}\tilde{\beta}_a. \tag{C.9}$$

The beta function for the kinetic coefficient γ in ref. [26] is given by

$$\dot{\gamma} = \frac{1}{(16\pi^2)^2}\frac{4}{3}(1-\gamma)\Big(\frac{1}{\gamma^2}+3\Big)\tilde{f}_\gamma, \tag{C.10}$$

where $\tilde{f}_\gamma$ is a quadratic form of the quartic couplings. We can now write this in terms of our alternative coupling constants

$$\frac{1}{(16\pi^2)^2}\tilde{f}_\gamma(\tilde{\beta}_a) = \frac{1}{(16\pi^2)^2}\Big(\frac{4\pi^2 z}{3d}\Big)^2 f_\gamma(\beta_a) = \Big(\frac{z}{12d}\Big)^2 f_\gamma(\beta_a). \tag{C.11}$$

We then have

$$\dot{\gamma} = \frac{1}{108}\Big(\frac{z}{d}\Big)^2(1-\gamma)\Big(\frac{1}{\gamma^2}+3\Big)f_\gamma \tag{C.12}$$

with

$$\begin{aligned} f_\gamma = {} & 12\beta_1^2 + 2\beta_1\beta_2 + 8\beta_1\beta_3 + 2\beta_1\beta_4 + 6\beta_1\beta_5 + \frac{13}{2}\beta_2^2 \\ & + 4\beta_2\beta_3 + 7\beta_2\beta_4 + 5\beta_2\beta_5 + 8\beta_3^2 + 4\beta_3\beta_4 \\ & + \frac{13}{2}\beta_4^2 + 5\beta_4\beta_5 + \frac{15}{2}\beta_5^2. \end{aligned} \tag{C.13}$$

C.3 Quasi-2D RG

The FRG flow equations for the quasi 2D regime are defined using $\mathcal{E}_i$, which are given by

$$
\begin{aligned}
\mathcal{E}_1 &= -6\gamma\beta_3^2k_n^4 + 6\beta_3^2k_n^4 - 12\gamma\beta_4^2k_n^4 + 12\beta_4^2k_n^4 - \gamma\beta_5^2k_n^4 + \beta_5^2k_n^4 - 16\gamma\beta_3\beta_4k_n^4 \\
&+ 16\beta_3\beta_4k_n^4 - 10\gamma\beta_3\beta_5k_n^4 + 10\beta_3\beta_5k_n^4 - 10\gamma\beta_4\beta_5k_n^4 + 10\beta_4\beta_5k_n^4 - 16\alpha\beta_3^2k_n^2 \\
&+ 12\gamma\beta_3^2k_n^2 + 4\beta_3^2k_n^2 - 36\alpha\beta_4^2k_n^2 + 24\gamma\beta_4^2k_n^2 + 12\beta_4^2k_n^2 - 6\alpha\beta_5^2k_n^2 + 2\gamma\beta_5^2k_n^2 + 4\beta_5^2k_n^2 \\
&- 40\alpha\beta_3\beta_4k_n^2 + 32\gamma\beta_3\beta_4k_n^2 + 8\beta_3\beta_4k_n^2 - 28\alpha\beta_3\beta_5k_n^2 + 20\gamma\beta_3\beta_5k_n^2 + 8\beta_3\beta_5k_n^2 \\
&- 28\alpha\beta_4\beta_5k_n^2 + 20\gamma\beta_4\beta_5k_n^2 + 8\beta_4\beta_5k_n^2 - 4\Big((\gamma-1)k_n^4 + (6\alpha - 2(\gamma+2))k_n^2 + 3\alpha^2 + 12\alpha + \gamma \\
&- 16\Big)\beta_1^2 - 2\Big(17(\gamma-1)k_n^4 + (54\alpha - 34\gamma - 20)k_n^2 + 3\alpha^2 + 60\alpha + 17\gamma - 80\Big)\beta_2^2 + 2\alpha^2\beta_3^2 - 12\alpha\beta_3^2 \\
&- 6\gamma\beta_3^2 + 16\beta_3^2 - 36\alpha\beta_4^2 - 12\gamma\beta_4^2 + 48\beta_4^2 - 3\alpha^2\beta_5^2 - 12\alpha\beta_5^2 - \gamma\beta_5^2 + 16\beta_5^2 \\
&+ 8\alpha^2\beta_3\beta_4 - 24\alpha\beta_3\beta_4 - 16\gamma\beta_3\beta_4 + 32\beta_3\beta_4 + 2\alpha^2\beta_3\beta_5 - 24\alpha\beta_3\beta_5 \\
&- 10\gamma\beta_3\beta_5 + 32\beta_3\beta_5 + 2\alpha^2\beta_4\beta_5 - 24\alpha\beta_4\beta_5 - 10\gamma\beta_4\beta_5 + 32\beta_4\beta_5 + 4\beta_2\Big(\Big(-9(\gamma-1)k_n^4 \\
&+ (-26\alpha + 18\gamma + 8)k_n^2 + \alpha^2 - 24\alpha - 9\gamma + 32\Big)\beta_3 + \Big(-11(\gamma-1)k_n^4 + (-32\alpha + 22\gamma + 10)k_n^2 \\
&+ \alpha^2 - 30\alpha - 11\gamma + 40\Big)\beta_4 - 6\Big((\gamma-1)k_n^4 + (3\alpha - 2\gamma - 1)k_n^2 + 3\alpha + \gamma - 4\Big)\beta_5\Big) \\
&- 4\beta_1\Big(4\Big((\gamma-1)k_n^4 + (3\alpha - 2\gamma - 1)k_n^2 + 3\alpha + \gamma - 4\Big)\beta_2 - \Big(-\Big((\gamma-1)k_n^4\Big) - 2(\alpha-\gamma)k_n^2 \\
&+ \alpha^2 - \gamma\Big)\Big(\beta_3 + \beta_4 + \beta_5\Big)\Big)
\end{aligned}
\tag{C.14}
$$

$$\mathcal{E}_2 = -14\gamma\beta_3^2k_n^4 + 14\beta_3^2k_n^4 - 4\gamma\beta_4^2k_n^4 + 4\beta_4^2k_n^4 - \gamma\beta_5^2k_n^4 + \beta_5^2k_n^4 - 16\gamma\beta_3\beta_4k_n^4$$
$$+ 16\beta_3\beta_4k_n^4 - 2\gamma\beta_3\beta_5k_n^4 + 2\beta_3\beta_5k_n^4 - 2\gamma\beta_4\beta_5k_n^4 + 2\beta_4\beta_5k_n^4 - 36\alpha\beta_3^2k_n^2$$
$$+ 28\gamma\beta_3^2k_n^2 + 8\beta_3^2k_n^2 - 8\alpha\beta_4^2k_n^2 + 8\gamma\beta_4^2k_n^2 - 2\alpha\beta_5^2k_n^2 + 2\gamma\beta_5^2k_n^2$$
$$- 72\alpha\beta_3\beta_4k_n^2 + 32\gamma\beta_3\beta_4k_n^2 + 40\beta_3\beta_4k_n^2 - 12\alpha\beta_3\beta_5k_n^2 + 4\gamma\beta_3\beta_5k_n^2$$
$$+ 8\beta_3\beta_5k_n^2 - 4\alpha\beta_4\beta_5k_n^2 + 4\gamma\beta_4\beta_5k_n^2 + 4\Big(-\Big((\gamma-1)k_n^4\Big) - 2(\alpha-\gamma)k_n^2$$
$$+ \alpha^2 - \gamma\Big)\beta_1^2 + 2\Big(-\Big((\gamma-1)k_n^4\Big) - 2(\alpha-\gamma)k_n^2 + \alpha^2 - \gamma\Big)\beta_2^2 + 6\alpha^2\beta_3^2$$
$$- 24\alpha\beta_3^2 - 14\gamma\beta_3^2 + 32\beta_3^2 + 4\alpha^2\beta_4^2 - 4\gamma\beta_4^2 + \alpha^2\beta_5^2 - \gamma\beta_5^2 - 24\alpha^2\beta_3\beta_4$$
$$- 120\alpha\beta_3\beta_4 - 16\gamma\beta_3\beta_4 + 160\beta_3\beta_4 - 4\beta_2\Big(3\Big((\gamma-1)k_n^4 + (4\alpha-2\gamma-2)k_n^2 + \alpha^2$$
$$+ 6\alpha + \gamma - 8\Big)\beta_3 + \Big((\gamma-1)k_n^4 + 2(\alpha-\gamma)k_n^2 - \alpha^2 + \gamma\Big)\beta_4\Big) - 6\alpha^2\beta_3\beta_5$$
$$- 24\alpha\beta_3\beta_5 - 2\gamma\beta_3\beta_5 + 32\beta_3\beta_5 + 2\alpha^2\beta_4\beta_5 - 2\gamma\beta_4\beta_5 + 4\beta_1\Big(\Big(-\Big((\gamma-1)k_n^4\Big) - 2(\alpha-\gamma)k_n^2$$
$$+ \alpha^2 - \gamma\Big)\beta_3 - \Big((\gamma-1)k_n^4 + (6\alpha-2\gamma-4)k_n^2 + 3\alpha^2 + 12\alpha + \gamma - 16\Big)\Big(\beta_4 + \beta_5\Big)\Big) \tag{C.15}$$

$$\mathcal{E}_3 = -6\gamma\beta_3^2k_n^4 + 6\beta_3^2k_n^4 - 12\gamma\beta_4^2k_n^4 + 12\beta_4^2k_n^4 - 17\gamma\beta_5^2k_n^4 + 17\beta_5^2k_n^4 - 16\gamma\beta_3\beta_4k_n^4 + 16\beta_3\beta_4k_n^4$$
$$- 2\gamma\beta_3\beta_5k_n^4 + 2\beta_3\beta_5k_n^4 - 2\gamma\beta_4\beta_5k_n^4 + 2\beta_4\beta_5k_n^4 - 32\alpha\beta_3^2k_n^2$$
$$+ 12\gamma\beta_3^2k_n^2 + 20\beta_3^2k_n^2 - 44\alpha\beta_4^2k_n^2 + 24\gamma\beta_4^2k_n^2 + 20\beta_4^2k_n^2 - 50\alpha\beta_5^2k_n^2$$
$$+ 34\gamma\beta_5^2k_n^2 + 16\beta_5^2k_n^2 - 40\alpha\beta_3\beta_4k_n^2 + 32\gamma\beta_3\beta_4k_n^2 + 8\beta_3\beta_4k_n^2$$
$$- 4\alpha\beta_3\beta_5k_n^2 + 4\gamma\beta_3\beta_5k_n^2 - 12\alpha\beta_4\beta_5k_n^2 + 4\gamma\beta_4\beta_5k_n^2 + 8\beta_4\beta_5k_n^2$$
$$+ 4\Big(-\Big((\gamma-1)k_n^4\Big) - 2(\alpha-\gamma)k_n^2 + \alpha^2 - \gamma\Big)\beta_1^2 + 2\Big(-\Big((\gamma-1)k_n^4\Big)$$
$$- 2(\alpha-\gamma)k_n^2 + \alpha^2 - \gamma\Big)\beta_2^2 - 14\alpha^2\beta_3^2 - 60\alpha\beta_3^2 - 6\gamma\beta_3^2 + 80\beta_3^2$$
$$- 8\alpha^2\beta_4^2 - 60\alpha\beta_4^2 - 12\gamma\beta_4^2 + 80\beta_4^2 + \alpha^2\beta_5^2 - 48\alpha\beta_5^2 - 17\gamma\beta_5^2 + 64\beta_5^2$$
$$+ 8\alpha^2\beta_3\beta_4 - 24\alpha\beta_3\beta_4 - 16\gamma\beta_3\beta_4 + 32\beta_3\beta_4 + 4\beta_2\Big(\Big(-\Big((\gamma-1)k_n^4\Big)$$
$$- 2(\alpha-\gamma)k_n^2 + \alpha^2 - \gamma\Big)\beta_3 - 3\Big((\gamma-1)k_n^4 + (4\alpha-2\gamma-2)k_n^2 + \alpha^2 + 6\alpha + \gamma - 8\Big)\beta_4\Big)$$
$$+ 2\alpha^2\beta_3\beta_5 - 2\gamma\beta_3\beta_5 - 6\alpha^2\beta_4\beta_5 - 24\alpha\beta_4\beta_5 - 2\gamma\beta_4\beta_5$$
$$+ 32\beta_4\beta_5 - 4\beta_1\Big(\Big((\gamma-1)k_n^4 + (6\alpha-2\gamma-4)k_n^2 + 3\alpha^2 + 12\alpha + \gamma - 16\Big)\beta_3 + \Big((\gamma-1)k_n^4$$
$$+ 2(\alpha-\gamma)k_n^2 - \alpha^2 + \gamma\Big)\beta_4 - \Big(-5(\gamma-1)k_n^4 + (-14\alpha+10\gamma+4)k_n^2 + \alpha^2 - 12\alpha - 5\gamma + 16\Big)\beta_5\Big) \tag{C.16}$$

$$\mathcal{E}_4 = 8\beta_1\Big(\beta_2\Big(\alpha^2-\gamma-2(\alpha-\gamma)k_n^2-\Big((\gamma-1)k_n^4\Big)\Big)-\beta_3\Big(\alpha^2+6\alpha+\gamma+(4\alpha-2\gamma-2)k_n^2$$
$$+(\gamma-1)k_n^4-8\Big)+2\beta_4\Big(-3\alpha-\gamma+(-3\alpha+2\gamma+1)k_n^2-\Big((\gamma-1)k_n^4\Big)+4\Big)\Big)$$
$$-2\beta_5\Big(2\alpha^2\beta_4+3\alpha^2\beta_5+48\alpha\beta_4+18\alpha\beta_5+14\beta_4\gamma+3\beta_5\gamma-64\beta_4-24\beta_5$$
$$+4\beta_2\Big(\alpha^2+9\alpha+2\gamma+(7\alpha-4\gamma-3)k_n^2+2(\gamma-1)k_n^4-12\Big)-2\beta_3\Big(\alpha^2-6\alpha-3\gamma$$
$$+(-8\alpha+6\gamma+2)k_n^2-3(\gamma-1)k_n^4+8\Big)+44\alpha\beta_4k_n^2+12\alpha\beta_5k_n^2+14\beta_4\gamma k_n^4$$
$$+3\beta_5\gamma k_n^4-28\beta_4\gamma k_n^2-6\beta_5\gamma k_n^2-14\beta_4k_n^4-3\beta_5k_n^4-16\beta_4k_n^2-6\beta_5k_n^2\Big) \tag{C.17}$$
$$3\pi(\gamma-1)\gamma^2\Big(k_n^2-1\Big)^2 \tag{C.18}$$
$$\mathcal{E}_5 = (\alpha-1)^3\Big(24\beta_1^2+4\Big(\beta_2+4\beta_3+\beta_4+3\beta_5\Big)\beta_1+13\beta_2^2+16\beta_3^2+13\beta_4^2$$
$$+15\beta_5^2+8\beta_3\beta_4+10\beta_4\beta_5+2\beta_2\Big(4\beta_3+7\beta_4+5\beta_5\Big)\Big)\Big(3\gamma^2+1\Big)\Big(\alpha-\gamma+(\gamma-1)k_n^2\Big)^3 \tag{C.19}$$

Appendix D: Notation and Conventions

Bold letters like $\mathbf{q}$ denote vector, and q would denote the magnitude of the vector $\mathbf{q}$. We use the following shorthand for integrals

$$\int_{\mathbf{q}} := \int \mathrm{d}^d\mathbf{q}. \tag{D.1}$$

The Kronecker delta is defined as

$$\delta_{ij} := \begin{cases} 0 & i \neq j \\ 1 & i = j \end{cases}. \tag{D.2}$$

We denote functional derivatives as

$$\frac{\delta}{\delta\phi}, \tag{D.3}$$

which act on functionals.

We distinguish between the trace operators tr and Tr. We use tr in the conventional way; to only sum over the diagonal of a matrix or tensor

$$\mathrm{tr}A = \sum_i A_{ii}, \tag{D.4}$$

whereas Tr is used to sum over all degrees of freedom, including the diagonal of a matrix. For example,

$$\mathrm{Tr}A(x) = \int_{\mathbf{x}} \sum_i A_{ii}(x). \tag{D.5}$$

Let $\phi(x)$ be a real function. We define its Fourier transform as

$$\phi(x) = \int \frac{\mathrm{d}^d\mathbf{q}}{(2\pi)^d} \tilde{\phi}(\mathbf{q}) e^{iq\cdot x}. \tag{D.6}$$

Sometimes we will drop the tilde, and it is understood that $\phi(x)$ is the real space function and $\phi(q)$ is its Fourier transform.

For our quartic couplings β_i, we use the convention

$$\beta_{ijk} := \beta_i + \beta_j + \beta_k. \tag{D.7}$$

log refers to the natural logarithm.